

MATERNAL OBESITY EFFECT ON OFFSPRING PANCREATIC
ENDOCRINE CELLS:
INVESTIGATION OF THE CELL TRANSDIFFERENTIATION PROFILE
THAT CAUSES DIABETIC SUSCEPTIBILITY

A THESIS SUBMITTED TO
THE GRADUATE SCHOOL OF NATURAL AND APPLIED SCIENCES
OF
MIDDLE EAST TECHNICAL UNIVERSITY

BY

MEHMET SEDAT FEYAT

IN PARTIAL FULFILLMENT OF THE REQUIREMENTS
FOR
THE DEGREE OF DOCTOR OF PHILOSOPHY
IN
BIOTECHNOLOGY

JUNE 2022

Approval of the thesis:

**MATERNAL OBESITY EFFECT ON OFFSPRING PANCREATIC
ENDOCRINE CELLS: INVESTIGATION OF THE CELL
TRANSDIFFERENTIATION PROFILE THAT CAUSES DIABETIC
SUSCEPTIBILITY**

submitted by **MEHMET SEDAT FEYAT** in partial fulfillment of the requirements
for the degree of **Doctor of Philosophy in Biotechnology Department, Middle
East Technical University** by,

Prof. Dr. Halil Kalipcilar
Dean, Graduate School of **Natural and Applied Sciences** _____

Assoc. Prof. Dr. Yesim Soyer
Head of Department, **Biotechnology, METU** _____

Assoc. Prof. Dr. Tulin Yanik
Supervisor, **Biotechnology, METU** _____

Assoc. Prof. Dr. Salih Ozcubukcu
Co-Supervisor, **Chemistry, METU** _____

Examining Committee Members:

Prof. Dr. Mesut Muyan
Dept. of Biological Sciences/Mol. Biol. and Genetics, METU _____

Assoc. Prof. Dr. Tulin Yanik
Dept. of Biological Sciences/Mol. Biol. and Genetics, METU _____

Prof. Dr. Sreeparna Banerjee
Dept. of Biological Sciences/Mol. Biol. and Genetics, METU _____

Prof. Dr. Oya Topaloglu
Dept. of Endocrinology and Metabolism, Ankara City Hospital,
Ankara Yildirim Beyazit University _____

Assoc. Prof. Dr. Mukerrem Sahin
Energy System Engr., Ankara Yildirim Beyazit University _____

Date: 13/06/2022

I hereby declare that all information in this document has been obtained and presented in accordance with academic rules and ethical conduct. I also declare that, as required by these rules and conduct, I have fully cited and referenced all material and results that are not original to this work.

Name, Surname: Mehmet Sedat Feyat

Signature:

ABSTRACT

MATERNAL OBESITY EFFECT ON OFFSPRING PANCREATIC ENDOCRINE CELLS: INVESTIGATION OF THE CELL TRANSDIFFERENTIATION PROFILE THAT CAUSES DIABETIC SUSCEPTIBILITY

Feyat, Mehmet Sedat
Doctor of Philosophy, Biotechnology
Supervisor: Assoc. Prof. Dr. Tulin Yanik
Co-Supervisor: Assoc. Prof. Dr. Salih Ozcubukcu

June 2022, 147 pages

In general, Type 2 Diabetes (T2D) is a disease characterized by impaired functioning of pancreatic beta cells and progressive insulin hormone deficiency progressively in combination with physiologically ongoing insulin resistance. In the later stages of the disease, beta cell dysfunction is defined as beta cell death and a decrease in functional cell count. It is a common clinical finding in patients with T2D that therapeutic drugs lowering insulin resistance and diet in the course of the disease treatment cause increased levels of insulin secretion in the patients and thus increased functional beta cell population. From the literature view, it has been observed that apoptotic cell death does not occur in adult mouse pancreatic beta cells exposed to obesity-sourced hyperglycemia, and these cells undergo dedifferentiation and transform into progenitor cells or other pancreatic endocrine cell types. However, maternal obesity induced human or animal pancreatic transdifferentiation in young offspring has not been studied up to date. Our proposed hypothesis was that obesity-induced hyperglycemia in the mother may cause dedifferentiation and/or transdifferentiation in offspring pancreatic beta cells.

In this thesis, the effect of predisposition to diabetes pathology on the pancreas of offspring produced by the mother's cafeteria diet (CAF) was investigated via pancreatic beta cell dedifferentiation and transdifferentiation. We have obtained pancreases of 0, 20, 90 days old Wistar rat offspring whose mothers had diet-induced obesity via CAF. Later, the diabetic tendency of juvenile rats was evaluated according to the glucose-stimulated insulin release test using the islet cells isolated from the pancreas tissues of offspring. Viability rates of isolated pancreatic islet cells were analysed by appropriate viability tests (FDA / PI staining) to determine the quality of the cell isolation performed. To examine the morphological change in pancreatic tissues between groups, the frozen pancreatic tissue sections of offspring were histologically examined using hematoxylin-eosine staining. Pancreatic tissue specimens were also stained with glucagon antibodies to determine cell characteristics for dedifferentiation in the mother subjects using immunohistochemistry. Additionally, RT-qPCR analysis was performed so that the transformation profiles of the pancreatic cells were determined at the gene expression level. Examined gene expressions were Neurogenin 3, Pancreatic and duodenal homeobox 1, Insulin, Somatostatin, Glucagon, Forkhead box O1, Chromogranin A, and Vimentin. Alongside the RT-qPCR analysis, full-genome transcriptome analysis was performed to clarify the transformation profile. Using Western blot analysis of insulin protein expression in the pancreas tissues, dedifferentiation was partially presented at the protein level. When the results of all experiments were considered, it was demonstrated that maternal obesity may affect the dedifferentiation of pancreatic beta cells in offspring and had a predisposing effect for diabetes. In conclusion, it was believed that physiological stress caused by a maternal metabolic disorder may cause a predisposition to the same metabolic disease in offspring through cellular transformation mechanisms.

Keywords: Diabetes, Maternal Obesity, Pancreatic beta cell, Transdifferentiation, Dedifferentiation

ÖZ

MATERNAL OBEZİTENİN YAVRU PANKREAS ENDOKRİN HÜCRELERİ ÜZERİNDEKİ ETKİSİ: DİYABETİK YATKINLIĞINA YOL AÇAN HÜCRE TRANSDÖNÜŞÜM PROFİLİNİN ARAŞTIRILMASI

Feyat, Mehmet Sedat
Doktora, Biyoteknoloji Bölümü
Tez yöneticisi: Doç. Dr. Tülin Yanık
Ortak tez yöneticisi: Doç. Dr. Salih Özçubukçu

Haziran 2022, 147 Sayfa

Tip 2 Diyabet (T2D) fizyolojik olarak devam eden insülin direnciyle birlikte progresif bir şekilde pankreatik beta hücrelerindeki fonksiyon bozukluğu ve ilerleyen dönemde insülin hormonu yetersizliği ile karakterize edilir. Hastalığın ilerleyen döneminde beta hücre fonksiyon bozukluğu, beta hücre ölümü ve fonksiyonel hücre sayısındaki düşüş olarak tanımlanmaktadır. Bununla birlikte hastalara uygulanan tedavi sürecinde insülin direncini düşürücü terapötik ilaç, diyet gibi uygulamalarla hastalardaki insülin salınım seviyelerinde normalleşme ve dolayısıyla azalan fonksiyonel beta hücre popülasyonunda artış, T2D vakalarında sık rastlanan klinik bir bulgudur. Literatürde, obeziteden kaynaklı hiperglisemiye maruz kalan yetişkin fare pankreatik beta hücrelerinde apoptotik hücre ölümünün gerçekleşmediği, bu hücrelerin transdönüşüm ve dediferansiyasyona uğrayarak progenitor hücre veya diğer pankreatik endokrin hücre tiplerine dönüştüğü gösterilmiştir. Literatürde maternal obezite kaynaklı yavru dönemine ait pankreatik transdönüşüm ya da dediferansiyasyon çalışmalarına rastlanmamıştır. Önerilen projedeki hipotezimiz, anneye ait obezite kaynaklı hipergliseminin yavru pankreatik beta hücrelerinde transdönüşüm ve dediferansiyasyona neden olmasıdır.

Bu çalışmada, Wistar sıçanlarda anneye ait kafeterya diyetiyle (KAF) oluşturulan obezite kaynaklı hipergliseminin yavru pankreasları üzerinde diyabet patolojisine yatkınlık etkisi pankreatik beta hücrelerinin transdönüşüm ve dediferansiyasyonu üzerinden araştırılmıştır. Öncül deneylerimizle KAF ile obezite oluşturulan annelerden doğan ve süt verme sürecinden sonra normal fare yemiyle beslenen 0, 20, 90 günlük yavruların ve annelerinin pankreasları elde edilmiştir. Daha sonra yavru sıçanların diyabet eğilimi, bu hayvanların pankreas dokularından izole edilen adacık hücreleriyle yapılan glukoz stimülasyonlu insülin salınım testi sonuçlarına göre belirlenmiştir. İzole edilen pankreas adacık hücrelerinin canlılık oranları, gerçekleştirilen hücre izolasyonunun kalitesini belirlemek için uygun canlılık testi (FDA / PI boyama) ile analiz edilmiştir. Gruplar arasında pankreas dokularındaki morfolojik değişimi incelemek için donmuş pankreas dokusu kesitleri hematoksilin-eozin boyama tekniği kullanılarak histolojik olarak incelenmiştir. Anne pankreas doku örnekleri hormonal düzeyde farklılaşma düzeyinin belirlenebilmesi için glucagon spesifik antikor kullanılarak boyanmış ve immünühistokimya ile analiz edilmiştir. Ek olarak, hücrelerin transdönüşüm profillerinin gen ekspresyon seviyesinde belirlenmesi için RT-qPCR analizi uygulanmıştır. İncelenen gen ifadeleri Neurogenin 3, Pankreatik ve duodenal homeobox 1, Insulin, Somatostatin, Glukagon, Forkhead box O1, Chromogranin A ve Vimentin genlerine aittir. RT-qPCR analizinin yanı sıra, dönüşüm profilini netleştirmek için tam genom transkriptom analizi yapılmıştır. Pankreas dokularında insülin protein ekspresyonlarının Western blot analizi ile protein ekspresyon seviyesinde kısmen dediferansiyasyonu işaret etmiştir. Yapılan tüm deneylerin sonuçlarına göre, maternal obezitenin yavrularda pankreas beta hücrelerinin farklılaşmasına neden olduğu ve diyabet yatkınlığına sebep olan bir etkiye sahip olduğu gösterilmiştir. Sonuç olarak, maternal bir metabolik bozukluğun neden olduğu fizyolojik stresin, hücresel dönüşüm mekanizmaları yoluyla yavrularda aynı metabolik hastalığa yatkınlığa neden olabileceğine inanılmaktadır.

Anahtar Kelimeler: Diyabet, Obez anne, Pankreatik beta hücresi, Transdönüşüm, Dediferansiyasyon

Dedicated to my beloved sister...

ACKNOWLEDGEMENTS

I express my deepest gratitude to my supervisor Assoc. Prof. Dr. Tulin Yanik for her encouraging guidance and support throughout my Ph.D.

I would also give my thanks to Assoc. Prof. Dr. Salih Ozcubukcu for being my co-supervisor.

I present my endless thanks to Prof. Dr. Mesut Muyan, Prof. Dr. Sreeparna Banerjee, Prof. Dr. Oya Topaloglu, and Assoc. Prof. Dr. Mukerrem Sahin for taking place on my thesis monitoring committee and for their time and patience.

I am deeply grateful to my friends, excellent scientists, Çagatay Ozan Karabulut, Salih Berkay Berkcan and K. M. Sifatullah for supporting me both technically and as a friend during the most difficult times of my study.

I am also grateful to Dr. Beycan Ayhan, Sefika Karabulut, and Assoc. Prof. Dr. Aynur Albayrak for their support and collaboration during my Ph.D. study.

This study was supported by METU BAP (project numbers: GAP-108-2019-10089 and GAP-108-2021-10709) and I would like to acknowledge METU BAP for their support.

I would like to acknowledge YOK for their support through 100/2000 PhD Scholarship.

Finally, I would like to express my deepest love and thanks to my dear sister Gulseda Feyat for always being with me, guiding, and supporting me with her pure heart. For being an example to me with her unique patience and character to maintain my beliefs and values in good and truth.

TABLE OF CONTENTS

ABSTRACT.....	v
ÖZ	vii
ACKNOWLEDGEMENTS	xi
TABLE OF CONTENTS	xii
LIST OF TABLES	xvi
LIST OF FIGURES.....	xvii
LIST OF ABBREVIATIONS.....	xx
CHAPTERS	
1. INTRODUCTION	1
1.1. Diabetes Mellitus	1
1.1.1. Pathophysiology	1
1.1.2. Complication	2
1.1.3. Types of Diabetes Mellitus	4
1.1.3.1. Type 1 Diabetes	4
1.1.3.2. Type 2 Diabetes	4
1.2. Obesity	5
1.2.1. Childhood Obesity	6
1.2.1.1. Causes of Childhood Obesity	6
1.2.1.2. Consequences of Childhood Obesity.....	7
1.2.2. Cafeteria Diets (CAF)	8
1.3. The link between Obesity and Type II Diabetes Mellitus	9
1.4. Maternal obesity as a risk factor for developing diabetes in offspring	10
1.5. The Endocrine Pancreas	12
1.5.1. Pancreatic Islet Cells	13
1.5.2. Regulation of Blood Glucose Levels	14
1.6. Beta Cell Failure and Diabetes.....	14
1.6.1. Islet Cell Plasticity	16
1.6.1.1. Transdifferentiation of Islet Cells	16

1.6.1.2. Dedifferentiation of Pancreatic Beta Cells	18
1.6.1.2.1. FoxO1 Role in Beta Cell Dedifferentiation	21
1.7. Aim and Novelty of the Study	22
2. MATERIALS AND METHODS	23
2.1. Animal Studies	23
2.2. Glucose Tolerance Test	27
2.3. Isolation of rat pancreatic islet cells	27
2.4. Determination of islet purity and islet number.....	29
2.5. Assessment of the Viability of Islet Cells	30
2.6. Culture of the islets	31
2.7. Determination of functionality by measuring insulin secretion of the islet cells with static glucose stimulation	32
2.8. Sectioning from frozen pancreas tissues and fixation of tissue sections	32
2.9. Hematoxylin-eosin (H&E) staining	34
2.10. Antibodies	35
2.11. Immunohistochemistry (IF) for Frozen Pancreatic Tissues of Mothers	35
2.12. Real-Time quantitative PCR (RT-qPCR): TaqMan® Gene Expression Assay	35
2.12.1. Relative normalized expression analysis	38
2.12.2. Heatmap analysis	38
2.13. Transcriptome analysis - NGS-based RNA sequencing (RNA-Seq)	39
2.13.1. Sample Preparation	39
2.13.2. Library Construction	40
2.13.3. Sequencing	40
2.13.4. Generation of Raw Data	41
2.14. Western Blotting Studies	41
2.14.1. Protein Isolation from Pancreatic Tissues	41
2.14.2. Protein Quantification	42
2.14.3. Samples Preparation for SDS PAGE gels and the blotting protocol	42

2.15. ELISA Assay	43
2.16. Statistical analysis	44
3. RESULTS	45
3.1. Prepregnancy Body Weight	45
3.2. Glucose tolerance test	46
3.3. Immunohistochemical Staining for Glucagon in Mother Pancreas	47
3.4. 20 days and 90 days Offspring Body Weight	48
3.5. Plasma Insulin Levels 20 days and 90 days Offspring	50
3.6. Assessment of Islet Functional Potency by Glucose Stimulated Insulin Secretion	51
3.7. Assessment of Viability of Islet Cells	56
3.8. Morphometric analysis of Islet Cells	65
3.9. Gene Expression Studies Results	74
3.9.1. RT-qPCR results	75
3.10. Transcriptome analysis – NGS-based RNA sequencing (RNA-Seq)	81
3.11. Western Blot Analysis	89
4. DISCUSSION	91
5. CONCLUSIONS	99
6. REFERENCES	101
APPENDICES	
A. PRIMERS, TaqMan™ PROBES, and RT-PCR CURVES	115
B. PROTEIN ASSAY and WESTERN BLOT.....	138
C. TRANSCRIPTOME	141
CURRICULUM VITAE	145

LIST OF TABLES

TABLES

Table 2.1. Cafeteria diet content	25
Table 2.2. Standard (normal) rat diet composition.....	26
Table 2.3. Experimental animal groups and pancreas tissue section numbers	33
Table 2.4 Total RNA concentrations and A260/A280 ratios	37

LIST OF FIGURES

Figure 1.1 Schematic illustration of diabetes development mechanism and complications	3
Figure 1.2 T2D pathophysiology	5
Figure 1.3 Children that are overweight in the world	8
Figure 1.4 Maternal obesity and the developmental origin of health and disease concept	11
Figure 1.5 The anatomical organization of the pancreas	12
Figure 1.6 Models for beta cell failure	16
Figure 1.7 Model of pancreatic islet cell transdifferentiation	17
Figure 1.8 Images of dedifferentiated beta cells	20
Figure 1.9 Beta cell failure mechanism	21
Figure 2.1. Animal studies and average calorie intake for the CAF and control groups	23
Figure 2.2. Isolation of rat pancreatic islet cells	29
Figure 2.3. Isolated islet cells	30
Figure 2.4. Rat islets stained for viability	31
Figure 2.5 Cryosectioning of frozen pancreatic tissue samples	34
Figure 2.6. Overall sequencing experiment steps for RNA-Seq	39
Figure 3.1. Body weights of mother Wistar rats before pregnancy	45
Figure 3.2. Blood glucose levels of mother Wistar rats before pregnancy	46
Figure 3.3. Representative images of immunohistochemistry of beta cells from the mother rats` pancreas	47
Figure 3.4. Quantitative analysis of IHC for anti-glucagon on mothers` pancreatic sections	48
Figure 3.5. Body weights of 20 days offspring	49
Figure 3.6. Body weights of 90 days offspring	49
Figure 3.7. Plasma insulin levels of 20 days offspring.....	50
Figure 3.8. Plasma insulin levels of 90 days offspring	51

Figure 3.9. Static low concentration glucose stimulated insulin secretion of isolated islet cells of 0 days offspring	52
Figure 3.10. Static high glucose stimulated insulin secretion of isolated islet cells of 0 days offspring	52
Figure 3.11. Static low glucose stimulated insulin secretion of isolated islet cells of 20 days offspring	53
Figure 3.12. Static high glucose stimulated insulin secretion of isolated islet cells of 20 days offspring	54
Figure 3.13. Static low glucose stimulated insulin secretion of isolated islet cells of 90 days offspring	55
Figure 3.14. Static high glucose stimulated insulin secretion of isolated islet cells of 90 days offspring	56
Figure 3.15. Cell viability of isolated pancreatic islets of 0 days offspring control group	57
Figure 3.16. Cell viability of isolated pancreatic islets of 0 days offspring CAF group	58
Figure 3.17. The percentage of live pancreatic cells	59
Figure 3.18. Cell viability of isolated pancreatic islets of 20 days offspring control group	60
Figure 3.19. Cell viability of isolated pancreatic islets of 20 days offspring CAF group	61
Figure 3.20. The percentage of live pancreatic cells	62
Figure 3.21. Cell viability of isolated pancreatic islets 90 days offspring control group	63
Figure 3.22. Cell viability of isolated pancreatic islets of 90 days offspring CAF group	64
Figure 3.23. The percentage of live pancreatic cells	65
Figure 3.24. HE stained histopathological sections of 20 days offspring control group pancreas	66
Figure 3.25. HE stained histopathological sections of 20 days offspring CAF group pancreas	67

Figure 3.26. The average area of the islet cells of 20 days offspring Control and CAF groups	68
Figure 3.27. 90 days offspring control group pancreatic islet cells were stained with HE	69
Figure 3.28. 90 days offspring CAF group pancreatic islet cells were stained with HE	70
Figure 3.29. The average area of the islet cells of 90 days offspring Control and CAF groups	71
Figure 3.30. Pancreatic tissue sections of the mother Control group were stained with HE	72
Figure 3.31. Pancreatic tissue sections of the mother Control group were stained with HE	73
Figure 3.32. The average area of the islet cells of mother Control and CAF groups	74
Figure 3.33. Relative normalized gene expression profiles of mothers' control and CAF groups	75
Figure 3.34. The mRNA expression profile of mothers' CAF and control groups ...	76
Figure 3.35. Relative normalized gene expression profiles of 0 days offspring control and CAF groups	77
Figure 3.36. The mRNA expression profile of 0 days offspring CAF and Control groups	77
Figure 3.37. Relative normalized gene expression profiles of 20 days offspring control and CAF groups	78
Figure 3.38. The mRNA expression profile of 20 days offspring CAF and Control groups	79
Figure 3.39. Relative normalized gene expression profiles of 90 days offspring control and CAF groups.....	79
Figure 3.40. The mRNA expression profile of 90 days offspring CAF and Control groups	80
Figure 3.41. Relative gene expression profile of Chga gene	81
Figure 3.42. MDS plot of gene expression profiles of 20 and 90 days old offspring groups tissue sample	83

Figure 3.43. Differentially expressed genes in 20 days old offspring pancreas.....	83
Figure 3.44. Volcano plot of 20 days old offspring pancreatic genes expressions....	84
Figure 3.45. The heat map of 20 and 90 days old offspring	85
Figure 3.46. Differentially expressed genes in 90 days old offspring pancreas	86
Figure 3.47. Volcano plot of 90 days old offspring pancreatic genes expressions	87
Figure 3.48. Gene Ontology enrichment analysis of the differentially expressed genes	88
Figure 3.49. Representative image of Western blot for anti-insulin in 20 days old offspring pancreas	89
Figure 3.50. Representative image of Western blot of the mother and 90 days old offspring for anti-insulin	90

LIST OF ABBREVIATIONS

BCL	Base calls
BMI	Body mass index
BSA	Bovine Serum Albumin
CAF	Cafeteria diet
cal	calorie
cDNA	Complementary DNA
Chga	Chromogranin A
cm	Centimeter
DM	Diabetes mellitus
DNA	Deoxyribonucleic acid
dNTP	Nucleoside triphosphates
DPBS	Dulbecco's Phosphate-Buffered Saline
DTZ	Dithizone
ELISA	Enzyme-Linked Immunosorbent Assay
FC	Fold change
FDA	Fluorescein diacetate
FDR	False discovery rate
Foxo1	Forkhead box O1
Gcg	Glucagon
gDNA	Genomic DNA
GHO	Global Health Observatory
GI	Glycemic index
gr	Gram
h	Hour
HBSS	Hank's Balanced Salt Solution
HCl	Hydrochloric acid
HE	Hematoxylin and eosin
HFD	High fat diets
HTT	Huntington gene
IDF	International Diabetes Foundation
IEQ	Islet equivalent
IHC	Immunohistochemistry
Ins2	Insulin
kg	Kilogram
mg	Milligram
min	Minute

mL	Milliliter
mM	Millimolar
Neurog3	Neurogenin 3
ng	Nanogram
NGS	Next-generation sequencing
OCT	Optimal temperature compound
PBS	Phosphate Buffered Saline
PCR	Polymerase chain reaction
Pdx1	Pancreatic and duodenal homeobox 1
pg	Picogram
PI	Propidium iodide
PP	Pancreatic polypeptide
PVDF	Polyvinylidene fluoride
QC	Quality control
RT	Room temperature
RNA	Ribonucleic acid
RPMI	Roswell Park Memorial Institute
rRNA	Ribosomal RNA
RTA	Real time analysis
RT-qPCR	Real-Time quantitative polymerase chain reaction
SEM	Standard Error of the Mean
Sst	Somatostatin
T1D	Type 1 diabetes
T2D	Type 2 diabetes
TBS	Tris-buffered saline
Vim	Vimentin
WHO	World Health Organization
μg	Microgram
μL	Microliter
μm	Micrometer
μM	Micromolar

CHAPTER 1

1. INTRODUCTION

1.1. Diabetes Mellitus

Diabetes mellitus (DM) commonly named diabetes is caused by insufficient insulin production of pancreatic beta cells and body cell insulin resistance; also both can be defined as a metabolic disorder (Chang-Chen *et al.* 2008). In the long-term period, diabetes is a serious health problem with a high mortality rate, harming different tissues including the heart, kidneys, blood vessels, and nerve tissue in patients (Skyler *et al.* 2017). Particularly, T2DM has a 6.9% prevalence over the world according to the International Diabetes Foundation (IDF) data of 2021 and higher prevalence in more developed regions of the world. With the increasing rate of obesity and aging in all populations, the rate of diabetes population increasing rapidly (Ogurtsova *et al.* 2022).

1.1.1. Pathophysiology

After the consumption of food, carbohydrates are broken down into glucose molecules in the digestive system. Blood glucose levels rise as a result of glucose absorption into the circulation. The rise in glucose levels stimulates the secretion of insulin hormone from the pancreatic beta cells. Body cells need insulin to allow glucose entry. Insulin has specific cell surface receptors and when bound to receptors, it facilitates the entry of glucose into the cell. As a result of this process, blood glucose levels become normal and insulin secretion is decreased (Sato 2014).

Blood glucose dynamics can be changed due to a metabolic disease condition like obesity. When insulin production is decreased, glucose cannot be utilized by the body

cells and blood glucose levels are evaluated, resulting in hyperglycemia. If secreted insulin is not used properly by target body cells the same effect will be seen. If insulin secretion is above the needed level, blood glucose levels may become very low (hypoglycemia) because most of the glucose molecules in the blood enter body tissue cells, and little remains in the bloodstream. There are several hormones responsible for controlling glycemia. Insulin is the only hormone that lowers blood glucose levels. The other hormones are glucagon, thyroid hormone, growth hormone, and glucocorticoids which all act to increase blood glucose levels (Mealey & Oates 2006).

1.1.2. Complications

There are lots of different paths, triggered by different genetic and environmental factors, that cause the progressive loss of pancreatic beta cells (Matveyenko & Butler 2008, Campbell-Thompson *et al.* 2016) and/or function (Ferrannini *et al.* 2005) that clinically called hyperglycemia. After hyperglycemia develops, patients are at risk of developing the same complications (Fig. 1.1.). Diabetic complications are a major cause of reduced quality of life, disability, and death in society. These complications can affect many parts of the body including the feet, the eyes and the skin in different ways (Jay S. Skyler *et al.* 2017).

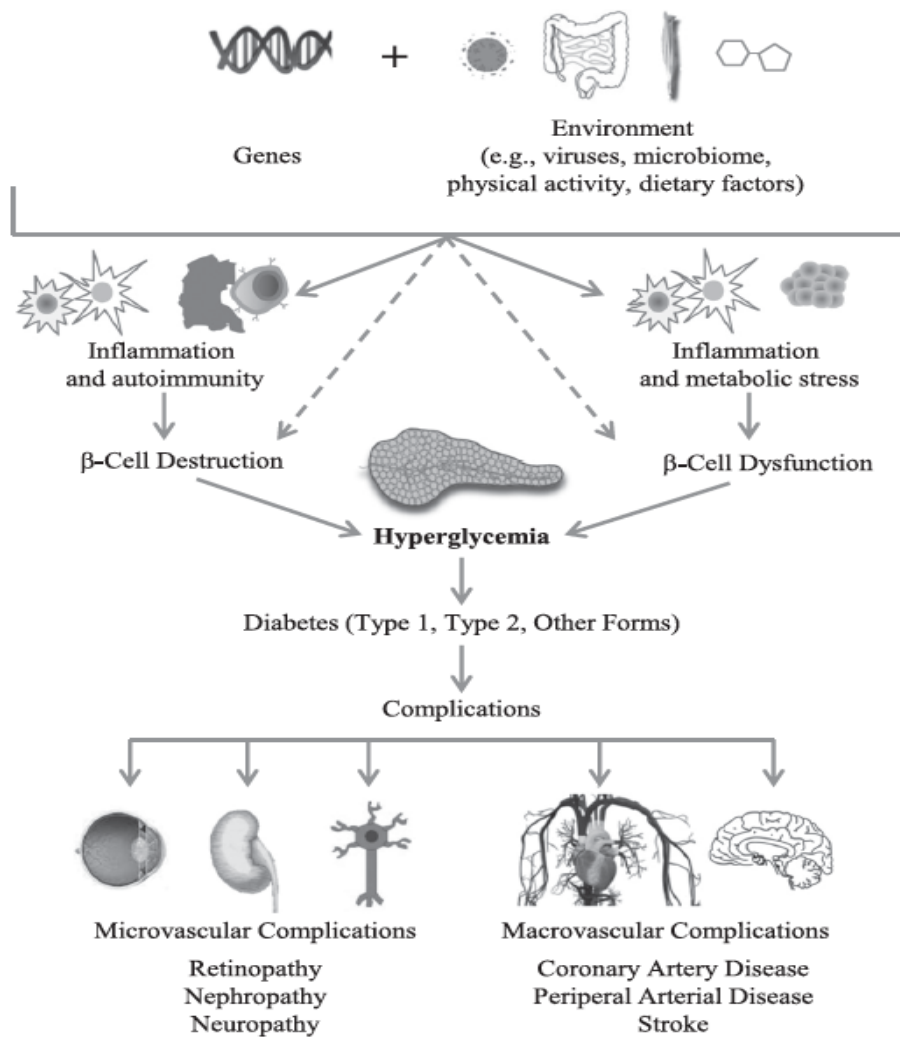


Figure 1.1. Schematic illustration of diabetes development mechanism and complications (Jay S. Skyler *et al.* 2017).

1.1.3. Types of Diabetes Mellitus

1.1.3.1. Type 1 Diabetes

Type 1 diabetes (T1D), or with its previous name juvenile diabetes, is generally diagnosed in children and young adults (Dabelea *et al.* 2014). In T1D, the pancreatic beta cells do not produce enough insulin for glucose metabolism in the body. Beta cells are selectively destroyed by the body's own immune cells as a result of an autoimmune process. Patients need insulin replacement treatment (Afelik & Rovira 2017) and T1D patients comprise approximately five percent of all diabetic patients in the world (Stenström *et al.* 2005).

1.1.3.2. Type 2 Diabetes

Type 2 diabetes (T2D) is a major public health concern, and its prevalence is increasing rapidly with rising obesity rates worldwide. T2D case rates are high in developing countries where 80% of diabetes deaths occur (Misra *et al.* 2019). It is also recently reported that the age of onset has decreased and the number of cases of T2D in adolescents and children start to increase (Wu *et al.* 2022).

In general, T2D is a disease characterized by impaired functioning of pancreatic beta cells and progressive insulin hormone deficiency progressively in combination with physiologically ongoing insulin resistance (Basu *et al.* 2009). It is the most common type of diabetes, affecting almost 95% of diabetic patients, and is also called adult-onset diabetes (Misra *et al.* 2019). T2D usually begins with insulin resistance in peripheral tissues like muscle, liver, and fat tissues and these tissues are not able to use insulin properly. As a result, the body needs more insulin to provide glucose input into body cells for energy metabolism. At the outset, the pancreatic beta cells produce more insulin, though in the progress of time, the insulin secretion is dysregulated, and in the end pancreas loses the ability of

secreting enough amount of insulin to control blood glucose level dynamics (Figure 1.2.) (Van Haeften *et al.* 2000).

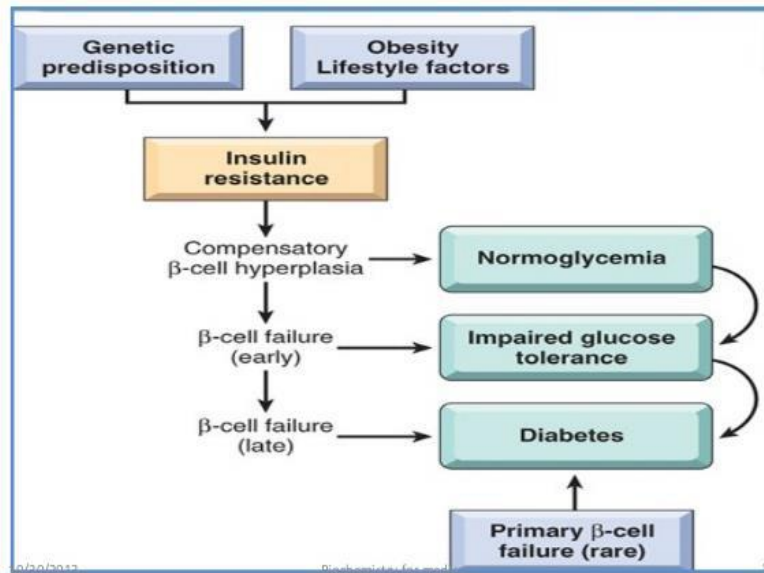


Figure 1.2. T2D pathophysiology. Despite insulin resistance in the early stages of the disease, glucose tolerance remains nearly normal because the pancreatic beta cells meet the increased insulin requirement. By continuing insulin resistance and hyperinsulinemia in a prolonged period, this hyperinsulinemic condition of pancreatic islet cells cannot be maintained and beta cell dysfunction occurs (Gill *et al.* 2013).

1.2. Obesity

Obesity is known as a medical condition that defines when a person carries excess weight or excessive fat accumulation that threatens their health. It is generally suggested that a person has obesity if they have a high body mass index (BMI). BMI is a tool that is used to evaluate if a person is at an appropriate weight for their age, sex, and height (Haslam *et al.* 2006). The measurement combines weight in kg divided by height in m². If BMI is between 25 and 29.9, it means a person is carrying excess weight. If BMI is 30 or above indicates that a person is considered as obese.

Besides, waist circumferences show obesity that waist circumferences >102 cm in men and >88 cm in women (Mitchell *et al.* 2011). According to the World Health Organization (WHO) data, more than 2 billion adults are overweight, of which 650 million are affected by obesity (BMI ≥ 30 kg/m²). It is surmised that 2.7 billion adults will be overweight, and more than 1 billion will be affected by obesity by 2025 (WHO, 2016).

When a person is considered as obese, their risk of developing a number of life-threatening diseases like; T2D, heart disease, high blood pressure, certain cancers (breast, colon, and endometrial), stroke, high cholesterol, arthritis and infertility is high. Considering the increase in the number of obese individuals in the last decade, obesity and related metabolic diseases will be one of the largest public health challenges in this century (World Health Organization WHO 2022).

1.2.1. Childhood Obesity

The number of overweight children under the age of five is approximately 41 million in the world (World Health Organization WHO 2022). About half of all overweight children are under 5 years old. Overweight and obese children are tended to stay obese into adulthood and are more likely to have diseases like diabetes and cardiovascular diseases (de Onis *et al.* 2010).

1.2.1.1. Causes of Childhood Obesity

It is a well-known concept that an imbalance between energy intake and expenditure is the primary cause of obesity and, is related to the lifestyle embraced and the dietary intake preferences. It is emerging convincingly that genetic background has an important role in determining obesity risk. Various studies provide important notions for our understanding of the factors associated with obesity. For example, according to the ecological model, the risk factors for childhood obesity are; dietary intake,

physical activity, and sedentary behavior (Davison & Birch 2001). The factors like age and gender govern the effect of these risk factors. The parenting style and lifestyle of the parents play a role. Environmental factors like milieu and school policies affect eating and activity behaviors (Sahoo *et al.* 2015). Nonetheless, genetics may be the biggest factor studied as a cause of obesity. According to data obtained from some studies body mass index is 25–40% heritable (Patricia M. Anderson & Kristin F. Butcher 2006).

1.2.1.2. Consequences of Childhood Obesity

Childhood obesity could mainly have an impact on the physical health of children, social life, self-reliance, and emotions. It is also related to declining academic performance and quality of life. Unfortunately, there are lots of diseases linked to childhood obesity such as; T2D, asthma, cardiovascular disease, sleep apnea, high cholesterol, insulin resistance, and orthopedic problems (Niehoff 2009).

Besides these medical conditions, one of the conditions that is the least socially acceptable and most stigmatizing to children is obesity (Schwimmer 2003). Children who are overweight or obese are frequently made fun of or ridiculed for their weight. They also experience a variety of additional difficulties, such as unfavorable stereotypes, prejudice, and social exclusion (Sahoo *et al.* 2015). It has also been discovered to have a detrimental impact on academic achievement. According to studies, children who are overweight or obese are four times more likely than classmates who are of a healthy weight to report experiencing issues at school (Schwimmer 2003).

Share of children that are overweight or obese, 2020

Share of children under five years old that are defined as overweight or obese. A child is classified as overweight if their weight-for-height is more than two standard deviations from the median of the World Health Organization (WHO) Child Growth Standards.

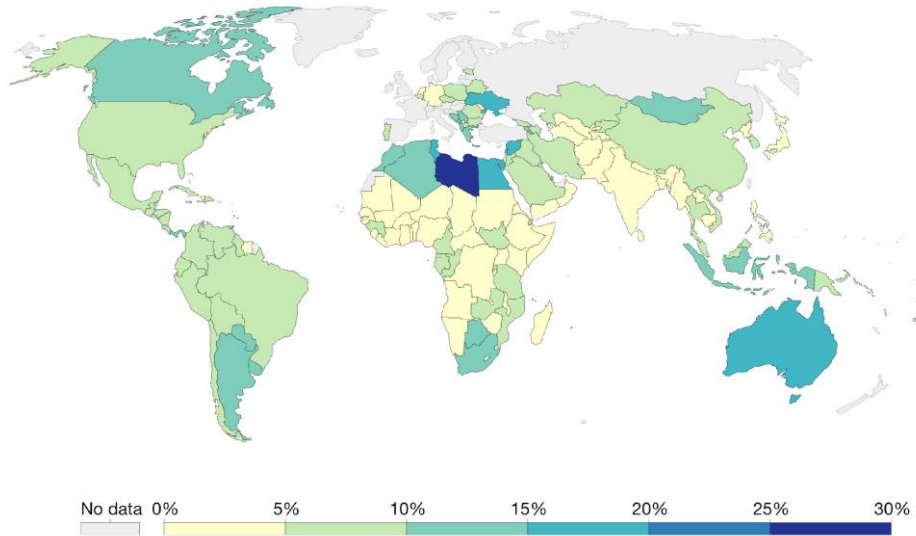


Figure 1.3. Children that are overweight in the world (WHO-Global Health Observatory (GHO), 2020).

1.2.2. Cafeteria Diet (CAF)

The Western diet or cafeteria diet (CAF) comprises a high content of carbohydrates and dietary fat (Cordain *et al.* 2005). It has been shown that CAF administration to obesity prone rodents induces obesity and promotes hyperglycemia and insulin resistance (Buettner *et al.* 2007). Besides, it is also known that the amount and source of dietary fats are contributed to diet induced obesity in humans. Carbohydrates with a high glycemic index (GI) in diet manipulate blood glucose and insulin levels. Especially sucrose has a high GI and is responsible for an instant increase in blood glucose levels (Oakes *et al.* 1997, Malterud & Tonstad 2009).

According to different experiments data with different high fat diets (HFD), omega (6,9) unsaturated and saturated animal fat, can cause obesity and insulin resistance (Buettner *et al.* 2007, Rokling-Andersen *et al.* 2009, Wali *et al.* 2020, Gilbert 2021). Additionally, polyunsaturated fatty acids have an important role in the context of dietary energy efficiency and diet induced obesity (Flachs *et al.* 2005).

1.3. The link between Obesity and Type II Diabetes Mellitus

Obesity has been shown to be a leading factor in the development of T2D with scientific studies using animal subjects and several clinical trials based on statistical observations (Eckel *et al.* 2011, Neeland *et al.* 2012). Given the rapid rate of increase of obesity in all age groups on a global scale, elucidation of the physiological mechanisms associated with diabetes development has particular importance. In recent years, the increase in obesity rates especially seen in childhood has reached a remarkable level (National Clinical Guideline 2014). Therefore, the elucidation of the environmental and physiological factors that trigger childhood obesity from the developmental stage in the mother's womb and the development of alternative treatment modalities have a critical precautionary measure against the rapidly increasing diabetes and obesity cases on a global scale (World Health Organization WHO 2016).

Through the activation of insulin resistance, obesity accelerates the development of T2D. The insufficient knowledge of insulin resistance has limited the therapy of T2D. However, a number of research have discussed the relation between insulin resistance and lipotoxicity, hyperinsulinemia, inflammation, and mitochondrial dysfunction. The etiology of T2D through the development of insulin resistance is also reported to involve endoplasmic reticulum stress, oxidative stress, genetic background, aging, hypoxia, and lipodystrophy. None of those approaches, however, has resulted in the development of T2D medications that work. Lack of clarity about cross-linked mechanisms of insulin resistance in T2D may be the cause (Ota 2014).

There are two main theories explaining how obesity could lead to T2D. First, abdominal fat could cause fat cells to secrete some proinflammatory cytokines. These cytokines may cause a decrease in insulin sensitivity of the body cells and disrupt the function of insulin responsive cells (Al-Goblan *et al.* 2014). Second, obesity may trigger the body's metabolism to change and promote fat tissue to release high amounts of fatty acids, hormones, proinflammatory cytokines, and other factors that cause the development of insulin resistance. After this point, insulin resistance leads to dysfunction of pancreatic beta cells, and blood glucose level control is lost (Makki *et al.* 2013).

1.4. Maternal obesity as a risk factor for developing diabetes in offspring

According to epidemiological and clinical studies, maternal obesity predisposes offspring to metabolic syndrome-related diseases (Figure 1.4). For years, in animal studies it has been confirmed that maternal obesity during gestation and lactation accelerated the growth of neonates predisposing offspring to obesity and T2D. Besides, according to meta-analyses, birth weight is another predictor of obesity and T2D (Zimmermann *et al.* 2015, Ling & Rönn 2019). There is the main question about this concept; what underlies the persistence of a developmental events memory in cells long after the stimulus that first triggered has vanished? (Lecoutre *et al.* 2021).

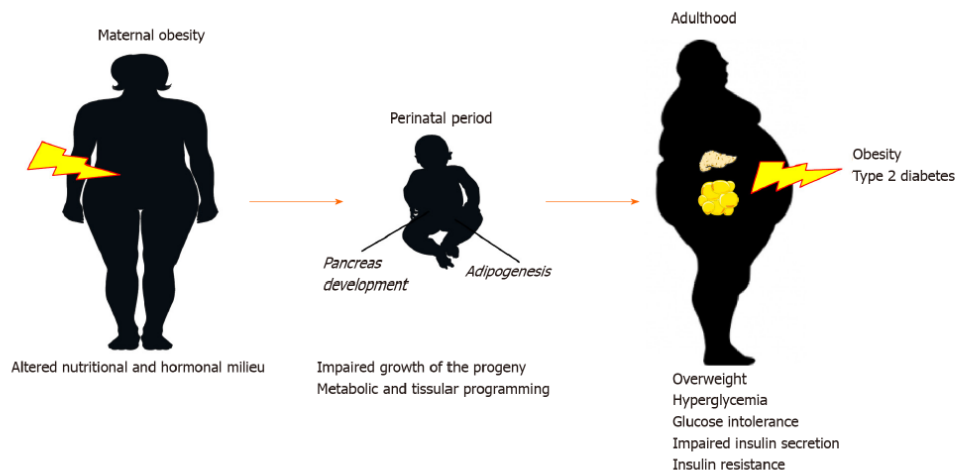


Figure 1.4. Maternal obesity and the developmental origin of health and disease concept. Impaired growth of offspring caused by maternal obesity during the developmental period. Also, maternal obesity impairs the metabolic and tissue programming of offspring. All these developmental changes could give rise to susceptibility to obesity and type 2 diabetes later in life (Lecoutre *et al.* 2021).

The cellular and molecular mechanisms of developmental programming are little known. Epigenetic modifications presumably have a crucial role in the heritability of obesity and T2D (Patricia M Anderson & Kristin F Butcher 2006, Back & Kaufman 2012, Hunter & Stein 2017). In particular, rodent studies showed that epigenetic mechanisms are responsible for linking maternal nutritional imbalances to the risk for T2D in adulthood. According to the concept of epigenetics, somatically heritable states of gene expression refer to modifications in chromatin structure without alterations in DNA's nucleotide sequence (Francesca Cinti, Bouchi, Kim-Muller, Ohmura, Sandoval, Masini, Marselli, Suleiman, Ratner & Marchetti 2016). These alterations can be passed from one generation of cells to the next as well as between generations (Michael G White *et al.* 2013).

The effect of maternal obesity operates during the development in which progenitor cells are plastic (sensible to changes in microenvironment) and where epigenetic remodeling is extremely dynamic and sensitive to the hormonal nutritional environment (Izumi *et al.* 2003, Patricia M Anderson & Kristin F Butcher 2006,

Prentki *et al.* 2013, Swisa *et al.* 2017). Therefore, this diversion of the developmental program may cause dysfunctions in fetal pancreatic beta cells. Inappropriate DNA methylation and chromatin modifications in these precursor cells during gestation and lactation might give rise to deleterious memory of the maternal obesogenic environment. The permanence of these modifications during life and across generations may cause permanent changes in gene expression profiles to result in the inheritance of metabolic diseases (Lecoutre *et al.* 2021).

1.5. The Endocrine Pancreas

The pancreas is a long, slender organ, located in the abdomen (Figure 1.4.). Besides, its exocrine gland function, secreting different types of digestive enzymes, the pancreas is a classical endocrine gland and it is also referred to as a compound gland. As endocrine cells, the islets of langerhans are responsible for secreting various types of hormones like glucagon, insulin, somatostatin, and pancreatic polypeptide (PP) (Da Silva Xavier 2018).

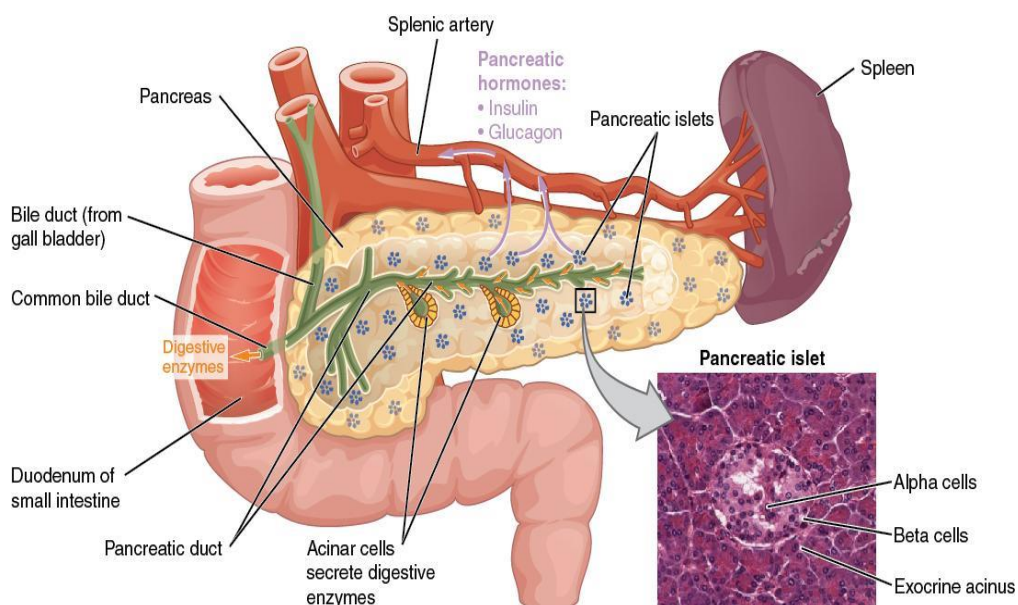


Figure 1.5. The anatomical organization of the human pancreas (Betts *et al.* 2013).

1.5.1. Pancreatic Islet Cells

In the parenchyma of the pancreas, there are islands of mixed populations of endocrine cells called the islets of Langerhans, which were originally identified by their namesake, Paul Langerhans, in 1869. Due to the hormones generated and released by the cells that make up these micro organs, which play a role in the control of glucose homeostasis, islets of Langerhans have received a lot of attention in the context of diabetes.

A human pancreas contains between 3.2 and 14.8 million islets, with a total islet volume ranging from 0.5 to 2.0 cm³ (Ionescu-Tirgoviste *et al.* 2015). The cellular composition and architecture of pancreatic islets differ between and within species (Steiner *et al.* 2010). It has already been shown that the inter-species differences correspond with functional variations (Cabrera *et al.* 2006). Since they have a unique design with a core of beta cells around by other endocrine cell types, rodent islets are commonly utilized in biomedical research (Steiner *et al.* 2010).

There are four types of endocrine cell types in the pancreas. Alpha (α) cells produce glucagon hormone and comprise roughly 20% of islet cells. Glucagon takes an important role in blood glucose regulation together with insulin hormone. When blood glucose level is low its production is stimulated. Beta (β) cells produce insulin hormone and comprise roughly 75% of islet cells (Bakhti *et al.* 2018). The release of insulin is stimulated when the blood glucose level is elevated. Delta (γ) cells produce the peptide hormone somatostatin. As an inhibiting hormone, this hormone inhibits the release of both glucagon and insulin. Pancreatic polypeptide cells (PP cells) secrete the pancreatic polypeptide hormone. PP hormone plays a role in the regulation of pancreatic exocrine and endocrine secretions and appetite.

1.5.2. Regulation of Blood Glucose Levels

Decline in blood glucose levels sensed by the receptors in the pancreas and in response α cells produce glucagon hormone. Glucagon stimulates the liver to convert glycogen into glucose molecules and these glucose molecules are transferred to body cells by blood circulation. It also stimulates the breakdown of stored triglycerides into free fatty acids and glycerol and some of those glycerol molecules go to the liver and convert into glucose. As a result of these actions blood glucose levels are increased. The glucagon secretion mechanism is also controlled by a negative feed-back mechanism further glucagon production is inhibited when the blood glucose levels are high (Röder *et al.* 2016).

The main function of the insulin hormone is to ensure the uptake of glucose molecules into body cells. The primary targets of insulin hormone are skeletal muscle cells and adipose cells. After blood glucose levels increase following digestion, insulin secretion into the blood by the pancreatic beta cells is stimulated. It also stimulates the liver to convert excess glucose in the blood circulation into glycogen in the liver for storage. Eventually, the blood glucose level is reduced. Insulin production is controlled by a negative feedback mechanism as well reacting against low blood glucose levels (Aronoff *et al.* 2004).

1.6. Beta Cell Failure and Diabetes

T2D is defined as a disease associated with progressive functional cell failure resulting from the loss of the number of insulin-secreting functional pancreatic beta cells (Talchai *et al.* 2012). Prospective studies of subjects with a high risk of T2D development suggest that a rapid and sustained decrease in cell function occurs even though insulin resistance remains relatively constant over time (Dunning & Gerich 2007, Wang *et al.* 2014). However, despite its progressive course, functional cell failure can be reversed by dietary or pharmacological interventions (Yoon *et al.* 2003). Interestingly, insulin sensitizers (insulin sensitizing agents) outperform insulin

secretagogues at the expense of cell dysfunction. This functional curative effect of insulin sensitizing agents suggests a positive correlation between increased insulin secretion challenge and cell loss. Cellular pathologies such as apoptosis, autophagia, oxidative stress, and overloading of nutrients ("toxicity") affect cell function and survival negatively (Anna *et al.* 2008, Atkinson *et al.* 2011).

There are three models for beta cell failure (Figure 1.6); *i.* Reduced pancreatic beta cell number due to physiologic and metabolic stress is responsible for the progression of diabetes. When compared to healthy individuals, T2D patients' beta cell mass has decreased by around 50%, according to the histological assessment of autopsies (Butler *et al.* 2003, Yoon *et al.* 2003, Rahier *et al.* 2008). *ii.* A chronic load on beta cells could cause dysfunction and pancreatic beta cells fail to produce insulin properly in response to glucose (Izumi *et al.* 2003, Back & Kaufman 2012, Evans-Molina *et al.* 2013). *iii.* When pancreatic beta cells fail to express the full complement of beta cell specific genes due to chronic physiologic stress phenomenon is called loss of beta cell identity (Guo *et al.* 2013, Michael G. White *et al.* 2013, Spijker *et al.* 2015, Brereton *et al.* 2016, Francesca Cinti, Bouchi, Kim-Muller, Ohmura, Sandoval, Masini, Marselli, Suleiman, Ratner, Marchetti, *et al.* 2016).

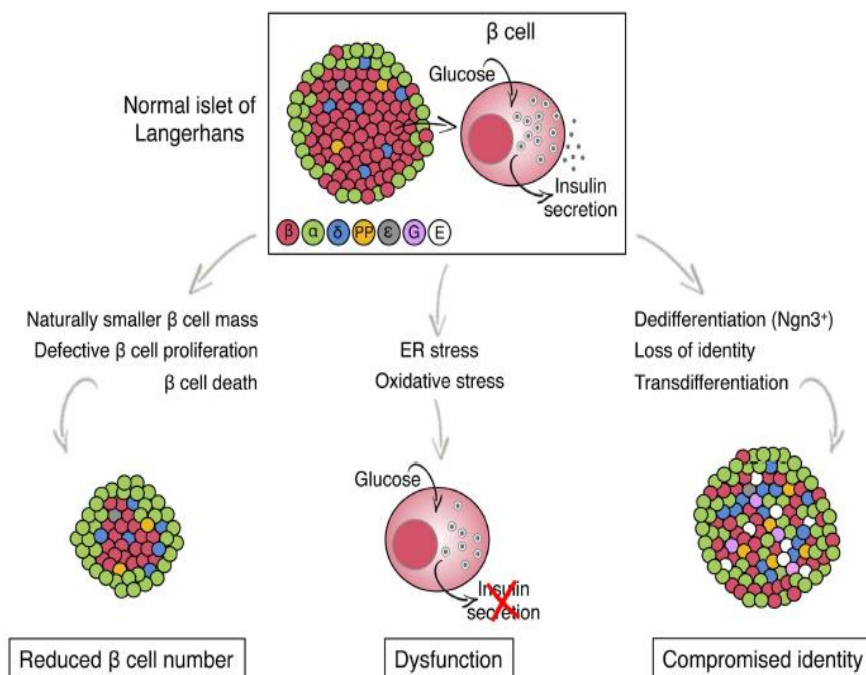


Figure 1.6. Models for beta cell failure. The endocrine cell composition of a pancreatic islet cell (top) and possible changes, differentiated by the beta cell fate, that cause functional beta cell failure in T2D (bottom). Islet cells are illustrated with different colors ϵ , ghrelin; G, gastrin, E, endocrine cell with empty granules (no hormone is produced) (Swisa *et al.* 2017).

1.6.1. Islet Cell Plasticity

1.6.1.1. Transdifferentiation of Islet Cells

Since pancreatic islet cells have a heterogeneous character, it is another research question whether these cell clusters are at a terminally differentiated state or a cellular plasticity exists. Therefore, there is a lot of incoming evidence from different studies in animal models that pancreatic islet cells have the capacity to directly transdifferentiate from a differentiated islet cell type to another islet cell fate or dedifferentiate to a progenitor-like cell type. Especially in studies with numerous

rodent models, it has been shown that different stressors can affect pancreatic cell reprogramming (Figure 1.7.) (Stanger *et al.* 2007, Teta *et al.* 2007, Piran *et al.* 2014).

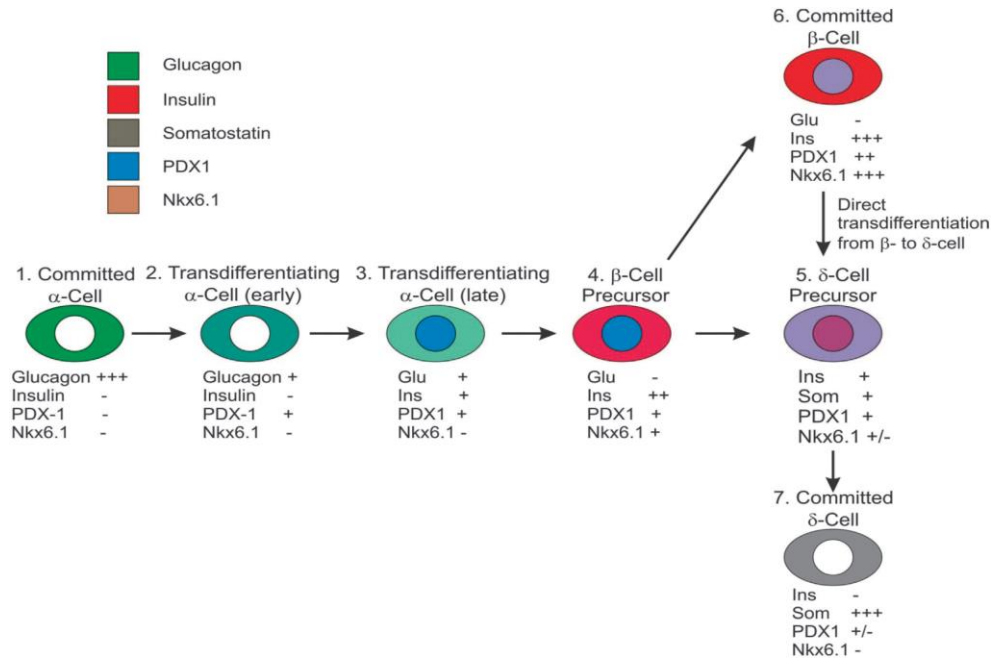


Figure 1.7. Model of pancreatic islet cell transdifferentiation. According to the time course analysis the transdifferentiation sequence was from alpha to beta to delta cells, not directly alpha to delta cells. The transient existence of alpha cells and glucagon–insulin and insulin–somatostatin co-expressing intermediate cells, with the absence of glucagon–somatostatin co-expressing cells, confirms this model of transdifferentiation (Piran *et al.* 2014).

Normally, pancreatic beta cells are defined as insulin expressing and controlled secreting under glucose conditions. Actually, this definition should also include the complete expression of key beta cell transcriptional regulators like, Pdx1, Nkx6.1, and MafA (Guo *et al.* 2013, Schaffer *et al.* 2013, Gao *et al.* 2014). Although they have opposite roles in the maintenance of a dynamic equilibrium of blood glucose levels, alpha and beta cells originate from a common progenitor cell. They have common

expressions of many transcription factors and genes for cell functioning like stimulus–secretion coupling, and hormone exocytosis (Benner *et al.* 2014). Thus, non-beta endocrine cells are the cell types that are most closely related to beta cells and makes them prime targets for conversion into beta cells. Therefore, the transdifferentiation process of islet endocrine cells has a potentially novel strategy for treating diabetes (van der Meulen & Huising 2015, Cito *et al.* 2018, Saleh *et al.* 2021).

1.6.1.2. Dedifferentiation of Pancreatic Beta Cells

Pancreatic beta cell failure or cell death underpin all types of diabetes. Beta cell failure in T2D is a compensatory response to peripheral insulin resistance. As a result, the mature beta cell phenotype is lost but does not necessarily cause beta cell death (Weir and Bonner-Weir, 2004; Weir *et al.*, 2013). Today, the most common T2D medications operate by decreasing the liver's ability to produce glucose (Metformin), by improving peripheral insulin sensitivity (Rosiglitazone and other thiazolidinediones), or by encouraging the release of insulin from beta cells that are already under stress (e.g., sulfonylureas such as Glyburide) (Kahn *et al.* 2006).

During the development of diabetes, and beta cell dysfunction in animal models, depletion in beta cell mass is generally considered as caused by an unbalanced rate of apoptosis versus self-renewal (Rieck *et al.* 2009). Besides, pancreatic beta cell apoptosis in diabetic islets is equable relative to the deterioration of beta cell function (Ferrannini 2010).

Under chronic metabolic stress conditions like during pregnancy or aging, the beta cell function failure (Rieck *et al.* 2009, Rankin & Kushner 2010) has been related to various biological mechanisms. Under the conditions of overnutrition seen in diabetes, autophagy can turn into a disease process (Hur *et al.* 2010). Besides, again under the same metabolic stress conditions, endoplasmic reticulum (ER) stress occurred, and as a result, unfolded protein response affects insulin secretion negatively which causes a

decrease in beta cell mass (Matsuda *et al.* 2010). Beta cells have a low capacity of antioxidant enzymes and limited glycolytic capacity resulting in the generation of reactive oxygen species, and this oxidative stress can disrupt glucose sensing from insulin secretion (Robertson 2004). Oxidative stress suppresses the beta cell specific transcription factors like MafA, Nkx6.1, Pdx1, and insulin gene expression and causes beta cell identity loss (Guo *et al.* 2013). However, the beta cell dysfunction rate seen in diabetic islet cells is much greater than observed the rate of apoptosis and cell death. Thereby, cell death may not be the main cause of marked loss of beta cell mass (Talchai *et al.* 2012, Marselli *et al.* 2014, Costes *et al.* 2021).

Beta cell dedifferentiation to endocrine progenitor-like cells under hyperglycemia induced metabolic stress conditions is an alternative proposed mechanism for diabetic loss of functional beta cell number and insulin content which has recently received attention (Talchai *et al.* 2012). To date, studies using animal experiments have found that pancreas cells of mice exhibit a progenitor cell-like character and undergo dedifferentiation in response to hyperglycemia (Wajchenberg 2007, Prentki *et al.* 2013). Dedifferentiated beta cells reverted to progenitor-like cells expressing Neurogenin3 and Vimentin (Talchai *et al.* 2012).

It has also been shown in these studies that pancreatic endocrine cell subtypes, especially alpha cells, show progenitor cell characteristics with glucagon expression in this transformation process (Talchai *et al.* 2012). This is also an explanatory finding for hyperglucagonemia in diabetes patients (Wang *et al.* 2014, Accili *et al.* 2016). In another study, pancreatic tissue sections of T2D patients showed a 3-fold increase in the number of endocrine cells (Chromogranin A-positive) and stain negative for insulin, glucagon, somatostatin, or pancreatic polypeptide (Figure 1.8). In vitro beta cell dedifferentiation was also observed (Weinberg *et al.* 2007). Dedifferentiation caused by beta cell dysfunction has also been referred from partial pancreatectomy studies (Jonas *et al.* 1999).

Together, these studies demonstrate that beta cell dedifferentiation in diabetic islet cells and conversion into other endocrine cell types could be an under-recognized mechanism of beta cell dysfunction in various types of diabetes. These findings are also a subject of a controversial discussion that transgenic transformation of beta cells due to hyperglycemia may be a cellular mechanism that protects these cells against permanent cell damage. The hypothesis that beta cells, which are truly dedifferentiated, inactivate in terms of insulin production and that they may be redifferentiated to produce insulin if appropriate environmental conditions are established may clarify why restoration of cell function is possible even years after the onset of hyperglycemia (F Cinti *et al.* 2015).

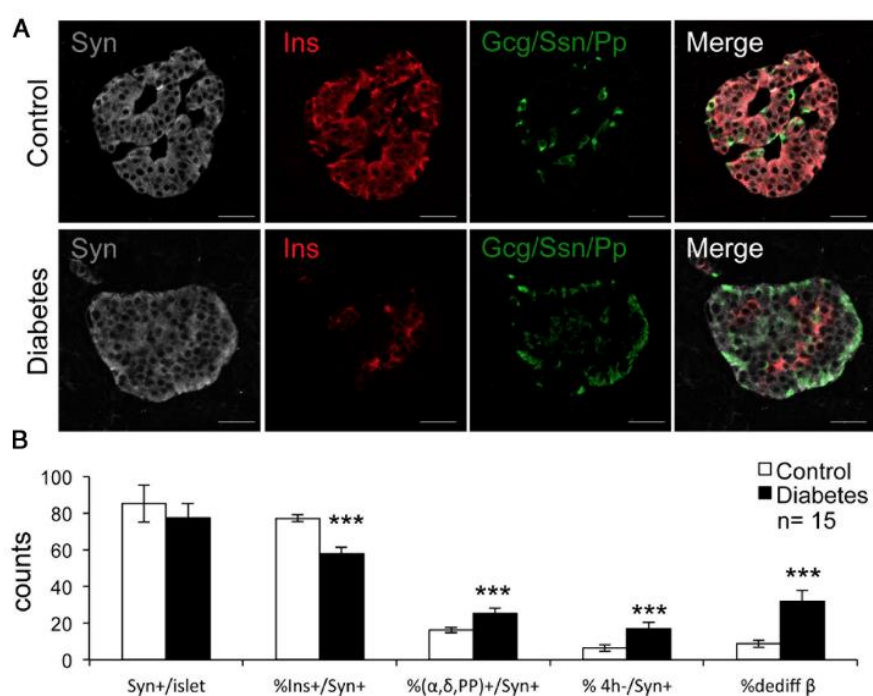


Figure 1.8. Images of dedifferentiated beta cells (A) Immunofluorescent histochemistry on pancreatic section using insulin (Ins, red), combined glucagon (Gcg), somatostatin (Ssn), pancreatic polypeptide (PP) (green) and Synaptophysin (Syn, gray). (B) Quantitative analysis of the data in A (F Cinti *et al.* 2015).

1.6.1.2.1. FoxO1 Role in Beta Cell Dedifferentiation

Transcription factor FoxO1 plays an important role in integrating signals coordinates, functional beta cell mass (Kitamura *et al.* 2005, Okamoto *et al.* 2006), and stress response. In diabetic islet cells, dedifferentiation of beta cells has been shown in vivo with the genetic depredation of key transcription factors, including FoxO1. Insulin is produced in the early stages of metabolic stress, however following prolonged stress, FoxO1 undergoes nuclear translocation to reinforce the beta cell fate and result in beta cell identity loss (Figure 1.9) (Talchai *et al.*, 2012).

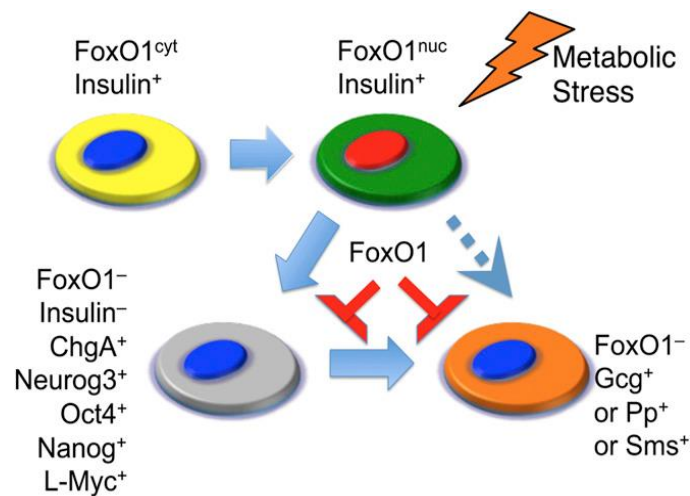


Figure 1.9. Beta cell failure mechanism. Functional beta cells produce insulin and have the cytoplasmic location of FoxO1 (yellow). In the early stages of metabolic stress, insulin production (green) is continued, but FoxO1 goes through nuclear translocation (red). If the stress continues, FoxO1 expression declines (blue nucleus) as Neurog3, Oct4, Nanog, and L-Myc expressions occur as progenitor markers (Talchai *et al.*, 2012).

1.7. Aim and Novelty of the Study

In this study, the objective was to investigate the effect of maternal obesity on T2D diabetic susceptibility on the juvenile pancreas through endocrine cell transduction. In the development of T2D, the literature has clearly shown that cell transduction in the patient's pancreas results in the dedifferentiation of pancreatic beta cells responsible for insulin secretion to progenitor cell types.

Our goal was to investigate whether obesity, which can cause the development of diabetes pathology, has the same effect on obese individuals' offspring pancreas at different age ranges in Wistar rats. It was hypothesized that Wistar rats' offspring, whose mothers were obese and hyperglycemic, pancreases may possess dedifferentiated beta cells even though they were exposed to only mother milk and standard rat chow after weaning.

It was, therefore, aimed to elucidate a better understanding of T2D at the molecular and cellular levels in the early ages of individuals.

CHAPTER 2

MATERIALS AND METHODS

2.1. Animal Studies

In this study, 5 weeks-old 20 female Wistar albino rats were used and before mating, female rats were randomly selected and divided into two groups as 10 rats in each group as the control and the cafeteria diet (CAF) groups. Rats in the CAF group were fed with the human-like CAF given the composition (high fat and sugar) as shown in Table 1.1, in addition to the normal rat chow as shown in Table 2.1 (184 cal/day/rat). Ten Wistar albino rats in the control group were fed with a normal rat chow diet as shown in Table 2.2 (113 cal/day/rat). Approximately 8 months later, the females of the CAF group's body weight of rats increased by 75% compared to the female rats in the control group. Then, the females were mated with normal body weight males, mother rats continued to be fed with the previously selected CAF food type during pregnancy and lactation periods (Figure 2.1).

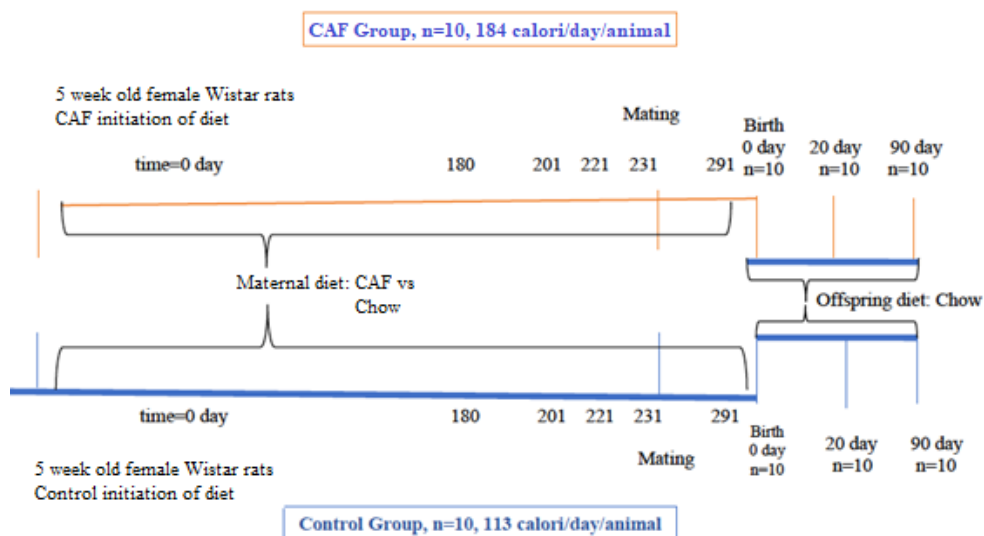


Figure 2.1. Animal studies and average calorie intake for the CAF and control groups. The CAF feeding process had continued for 8 months. From each mother group (n=10 rat/group) n=10 offspring were obtained and sacrificed at different ages (0th, 20th, and 90th days).

The offspring were fed with breast milk until the 20th day of weaning and after the weaning, they were fed with normal rat chow (Table 2.1). Subjects were housed in special rat cages with 3-4 rats in each cage at METU Biological Sciences Department Experimental Animals Unit. A day and night lighting system with automatic photoperiod was used to create a 12 h light and 12 h dark environment. The ambient temperature was set at 20 ± 25 °C and the humidity was set at 50-60%. The Animal Care and Use Committee at METU approved all protocols in accordance with the Turkish Agricultural Department Ministry Guide for the Care and Use of Laboratory Animals (Teker 2014).

Table 2.1. Cafeteria diet (CAF) content.

Energy and Food Ingredients (100 g)	Total (kcal)	Total fat (g)	Total Carbohydrates (g)	Protein (g)	Sugar (g)
Normal Yem: SC 7001	382	4	54	25	0
Çay Keyfi	462	20.4	67.8	5.8	28.5
Hoşbeş	493	24.5	63.9	7.6	28.4
Hanmeller	427	18.1	62.1	3.9	25.0
Doritos	491	24.5	60.5	7.2	2.3
Lays Klasik	529	33	51	7.0	0
Pringles	515	33	51	4.0	3.2
Crunch	486	26	69	6	51
Burçak	450	17.7	71	7.2	20.4
Lays Wavy	536	36	54	7	0
Mısır gevreği	372	4.1	76.1	7.6	30.7
Kombo	481	21.7	68.5	6.2	29.6
Cizi	473	21.4	64.3	5.8	0

Table 2.2. Standard (normal) diet composition.

BIL-FEED (FULL FEED) ENERGY FOOD ITEMS (%) (100 g)	
Dry matter	88
Raw protein	23
Raw lipid	3
Raw cellulose	7
Insoluble raw ash in HCl	8
Macro elements	
Calcium	1-2,5
Phosphorus	0,9
Sodium	0,5-1
Micro elements	
Manga (mg/kg)	10
Zinc (mg/kg)	4
Amino acids	
Lysine	1
Methionine	0,3
Cystine	0,1
Vitamins	
A (iu/kg) 400	400
D3 (iu/kg) 300	300
B2 (mg/kg) 5	5
B12 (mg/kg) 20	20
E (iu/kg) 30	30
K3 (iu/kg) 1	1
Metabolic energy	2600
Raw material used	Corn, Soybean Meal, A.T.K., Razmol, Bonkalite, Alfalfa pellet, Molasses, Meat Bone Meal, Chicken Meal, Sepiolite, D.C.P. (Inorganic) Marble Powder, Vitamins and Minerals

2.2. Glucose Tolerance Test

The animals were taken out of their cages and placed overnight in new cages with tap water but no food (approximately 12-18 h). Then, blood samples were collected from the tail vein, and the glucometer was used to assess the initial fasting glucose levels (time 0) (Roche Diagnostics, USA). Following this procedure, rats received 2 grams of 30% Dextrose solution per kilogram of body weight. After that, glucose levels were checked once again using a portable glucometer 5, 10, 15, 30, 60, and 120 minutes after the injection (Tekler, 2014).

2.3. Isolation of rat pancreatic islet cells

Pancreatic islet cell isolation was performed according to a reference study (Carter *et al.* 2009, Morgan *et al.* 2009) on the premise of rats in order to comparatively analyze the insulin release functions of pancreatic islet cells of the subjects (Figure 2.1). The hairs in the abdomen of rats were cleaned and cleared with betadine. Rats were anesthetized using (75 mg/kg) ketamine hydrochloride (Pfizer, New York, USA), (10 mg/kg) xylazine (Alfasan, Woerden, Holland) as anesthetic agents that were applied through the abdomen. After cutting the abdominal cavity, the liver was removed by applying pressure to the chest. To hinder the bleeding in the liver, the liver was wrapped up with a gauze bandage, the ductus was made apparent and the ampulla vater was clamped. Depending on the thickness of the ductus channels, we used a 26-G or 22-G catheter to perfuse 7 mL of 1 mg/mL cold collagenase type V enzyme (Sigma, Missouri, USA) into the pancreas. Rats were sacrificed by cutting their aorta. This prevents the flushing of the pancreas. The pancreas was collected in a 50 mL falcon tube and embedded into ice. The pancreas was incubated for 18 min in a 37°C water bath. At the end of the incubation period, the pancreas was homogenized by shaking. Next, 25 mL of cold Hanks Balanced Salt Solution (HBSS) (Lonza, Basel, Switzerland) (+) was added and inverted strongly. The digested pancreas was centrifuged at 4°C for 3 min at 310 x g. Slow acceleration and braking of the centrifuge prevents the dispersion of the pellet. After the digested pancreas was centrifuged, the

supernatant was thrown away gently. The pellet was shaken to break it up. Next, 25 mL of cold HBSS (+) was added and inverted strongly. The digested pancreas was centrifuged at 4°C for 3 min at 310 x g 3 accelerations and 1 break. The pellet was inverted to break it up. Next, 50 mL of cold HBSS (+) was added and inverted strongly. The digested pancreas was filtered by a 425-µm steel sieve into a new 50 mL falcon tube, and the undigested pancreas was removed. The filtered pancreas was centrifuged at 4°C for 3 min at 310 x g, 3 accelerations, and 1 break. The supernatant was thrown away gently. The islet cells were purified by a discontinuous gradient method. Firstly, the pellet of the filtered pancreas was shaken to break it up. Next, 5 mL Biocoll 1100 (Biochrom, Berlin, Germany) was added to the pellet. The pellet was shaken to homogenize it. Secondly, a 10 mL Biocoll 1077 (Biochrom, Berlin, Germany) solution was added to Biocoll 1100; the pellet was mixed slowly. Finally, 10 mL Roswell Park Memorial Institute 1640 (RPMI 1640) (-) solution was added to the Biocoll 1077 solution. The discontinuous gradient was centrifuged at 4°C for 20 min at 1300 x g, acceleration 1 break 0. The slow acceleration and stopping without brakes prevent the intermingling of the intensity. The islet cells between Biocoll 1077 density and RPMI 1640 (-) layer were collected into the RPMI 1640 (+) solution manually. The islet cells were washed with RPMI 1640 (Lonza, Basel, Switzerland) (+) solution by centrifugation two times at 310 x g for 3 min 3 acceleration 1 break at 4°C to obtain islet cells.

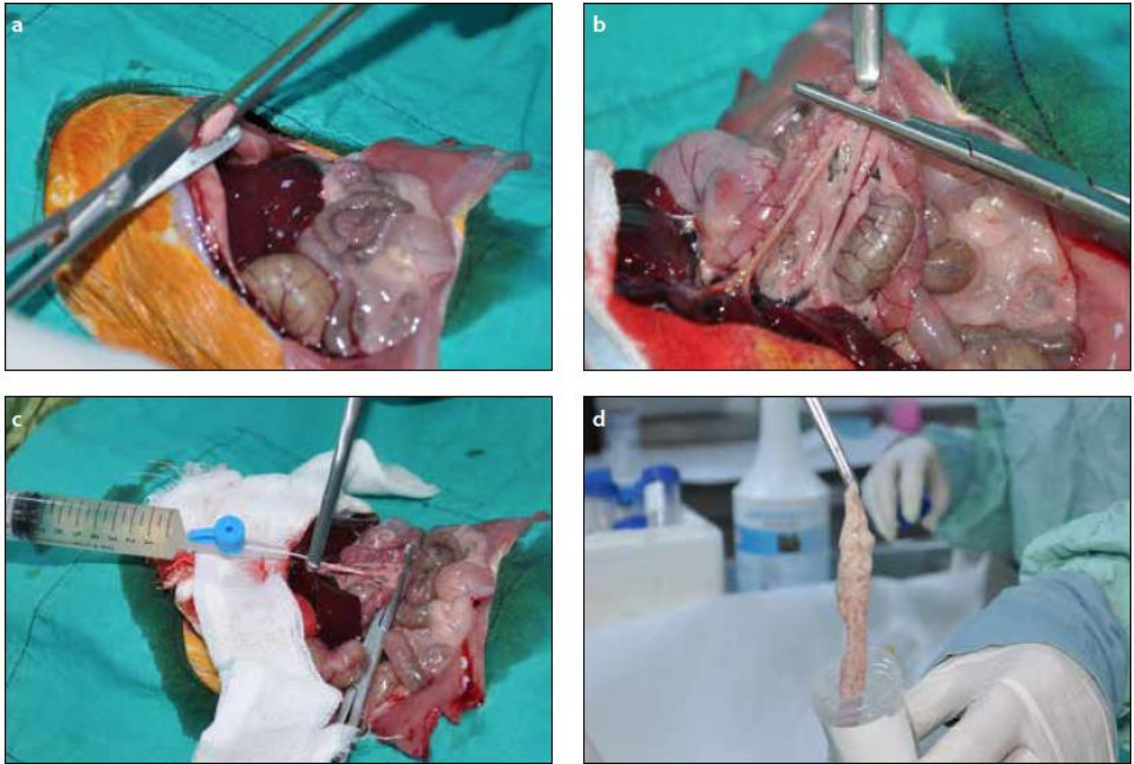


Figure 2.2. Isolation of rat pancreatic islet cells. (a) Dissection of the rat abdomen and removal of the sternum (b) Making pancreatic duct (Wirsung's canal) apparent and clamping of the duodenum branch of the canal (c) Collagenase enzyme solution was injected into the pancreas through the pancreatic duct (d) Bloated pancreas was dissected from its tissue connections.

2.4. Determination of islet purity and islet number

The islet cell sample (100 μ L) was added to a 10 \AA ~35 mm petri dish. A few drops of dithizone (DTZ) (Sigma, Missouri, USA) solution, a stain specific for the Zn²⁺ granules in islet beta cells (8), were added to it. Approximately 1 min is allowed for the dye to penetrate the cells. Stained islets appear red (Figure 2.3). The islet sample was examined using an inverted microscope. The percentage of islet purity was determined by estimating the proportion of islets, stained red with DTZ, to the exocrine tissue, unstained (appears light brown) (Figure 2.3). The total islet number was determined as islet equivalent (IEQ). According to the IEQ calculation, an islet was standardized to an average of 150 μ m in diameter. Islets of different diameters (sizes)

were normalized to an IEQ of 150 μm in diameter by mathematically compensating for their volumes (Lehmann *et al.* 2007).

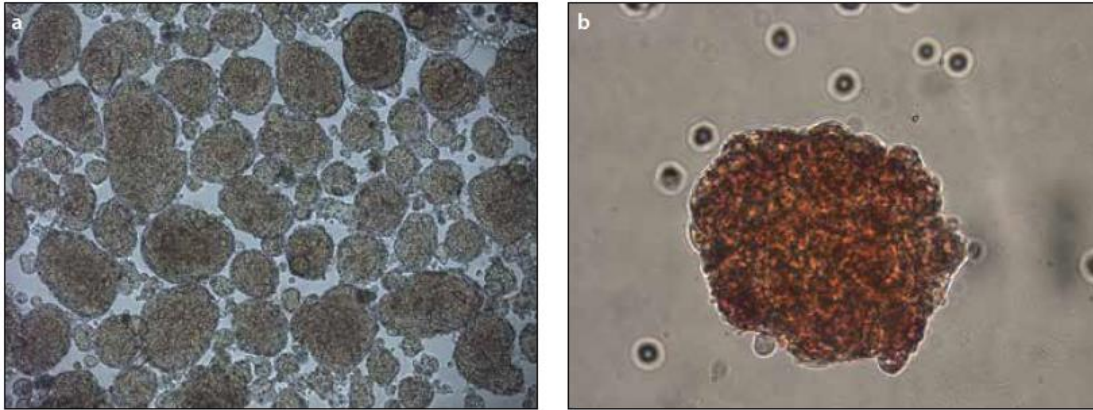


Figure 2.3. Isolated islet cells. (a) Light microscope view of the rat islet cells (b) Insulin-producing rat islet cells were red when stained with dithizone (DTZ) and viewed under the light microscope.

2.5. Assessment of the Viability of Islet Cells

Viability rates of isolated pancreatic islet cells were analyzed by an appropriate viability test (FDA/PI staining) to determine the quality of the cell isolation performed. Dulbecco's Phosphate-Buffered Saline (DPBS) (910 μL) (Life Technologies, Massachusetts, USA) (pH 7.4) solution was added into a 10 \AA ~35 mm petri dish. In total, 90 μL of the islets simply was added on it. After adding 20 μL of the fluorescein diacetate (FDA) (Sigma, Missouri, USA) stock solution and 20 μL of propidium iodide (PI) (Sigma, Missouri, USA) stock solution to it, they were stored in darkness for 5 min, and the viability at 40X magnification was determined using a fluorescent microscope (Leica, Wetzlar, Germany). New concentrations of the used fluorescent dye were 0.46 μM FDA and 14.34 μM PI.

FDA penetrates the membrane of living cells in the islet cells and changes to fluorescein by the action of esterase enzymes in the cytoplasm and produces bright green fluorescence under blue excitation light; thus, viable cells can be determined. Because the PI cannot penetrate the membrane of living cells, it binds to the nucleic acids of dead or dying cells in the islet cells and causes them to fluoresce bright red under green excitation light and dead cells can be identified (Figure 2.4) (Bank *et al.*, 1987). The photography of the cells under both fluorescent conditions was taken. They were merged using the MAT-LAB program. The percentage of viability for each islet was estimated by the number of viable (green fluorescence) vs. nonviable (red fluorescence) cells and by calculating their viability.

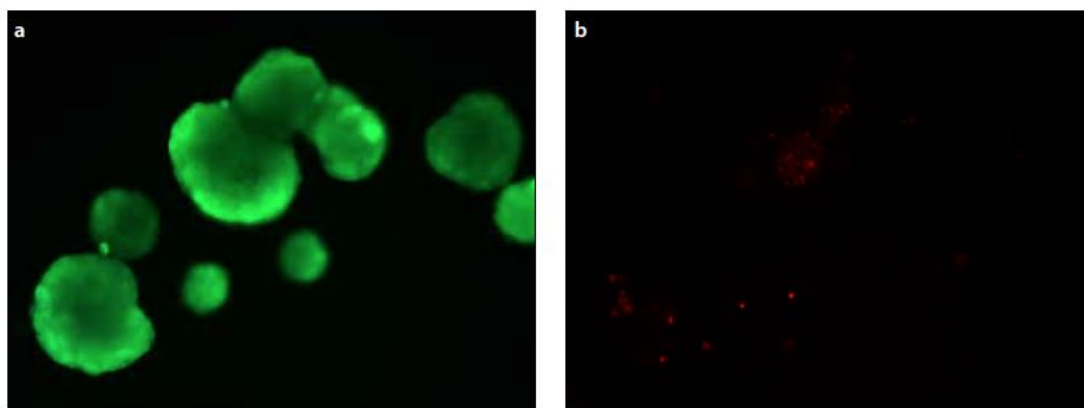


Figure 2.4. Rat islets were stained for viability. (a) Viable rat islet cells were green when stained with Fluorescein diacetate (FDA)/propidium iodide (PI) and viewed under a fluorescence microscope, (b) Dead or non-viable islets were red.

2.6. Culture of the islets

The islet cells, whose purity and viability had been specified, were cultured in a 5% CO₂ incubator (Panasonic, Osaka, Japan) at 37°C in T25 culture flasks (Corning, New York, USA) with a density of 30 islets/cm² with 5 mL RPMI 1640 (+) solution (Johnson *et al.*, 2011).

2.7. Determination of functionality by measuring insulin secretion of the islet cells with static glucose stimulation

A glucose-stimulated insulin release test was performed on isolated islet cells to determine the effect of maternal obesity conditioning on the functioning of juvenile pancreatic beta cells. RPMI 1640 solution (1 mL) containing 3.3 mM glucose for a basal glucose level was added to the first and second wells of 24-well plates (Corning, New York, USA), and 1 mL of RPMI 1640 solution containing 16.7 mM glucose for a high glucose level was added to the third well. An 8- μ m pore diameter insert (Merck, Darmstadt, Germany) was placed in the first well, and 25 islets of approximately 150 μ m in diameter were placed into the insert. The islets were incubated in a 5% CO₂ incubator at 37°C for 30 min. Then, the insert was placed in the second well. The islets were incubated in a 5% CO₂ incubator at 37°C for 1 h. When the incubation period was finished, the insulin sample was collected from the second well. Then, the insert was placed in the third well and incubated in a 5% CO₂ incubator at 37°C for 1 h. When the incubation period was finished, the insulin sample was collected from the third well. The received insulin samples were measured using a rat/mouse insulin ELISA kit (Merck, Darmstadt, Germany), according to manufacturer's instructions. The stimulation index, a measure of the ability of the purified rat islets product to produce insulin when stimulated by an increase in the concentration of glucose, was calculated as the amount of insulin derived from the 16.7 mM glucose concentrations divided by the amount of insulin derived from the 3.3 mM glucose concentrations (Sakata *et al.*, 2008).

2.8. Sectioning from frozen pancreas tissues and fixation of the tissue sections

In accordance with the reference study (Cinti *et al.*, 2016), the optimum tissue thickness for immunofluorescence staining was determined as 10 μ m in the previous preliminary study from preserved tissue samples at -80°C. Samples from the animal groups (Table 2.3) were collected and sections were taken using a cryotome (Shandon-Thermo Scientific, UK) sectioning device (Figure 2.5).

Tissue sections were placed in cold acetone, which was previously cooled to -20° C for at least 30 min, and then incubated at 4°C for 5 min, then at RT for another 5 min. The tissue sections were then washed 3 times in PBS for 5 min (3X5). The fine-tipped Pap Pen (Abcam, USA) was drawn around the tissues to form hydrophobic tissue boundaries. Hundred µL of protein blocks (Abcam, USA) were added to each tissue section and incubated at RT for at least 1 h. The sections were washed by immersion in PBS several times and removed.

Table 2.3. Experimental animal groups and pancreas tissue section numbers

	Age (days)	Number of Rats		Number of Pancreas Tissue Sections
		CAF group	Control group	
RAT	0	5	5	100
	20	5	5	100
	90	5	5	100
	TOTAL	30		300

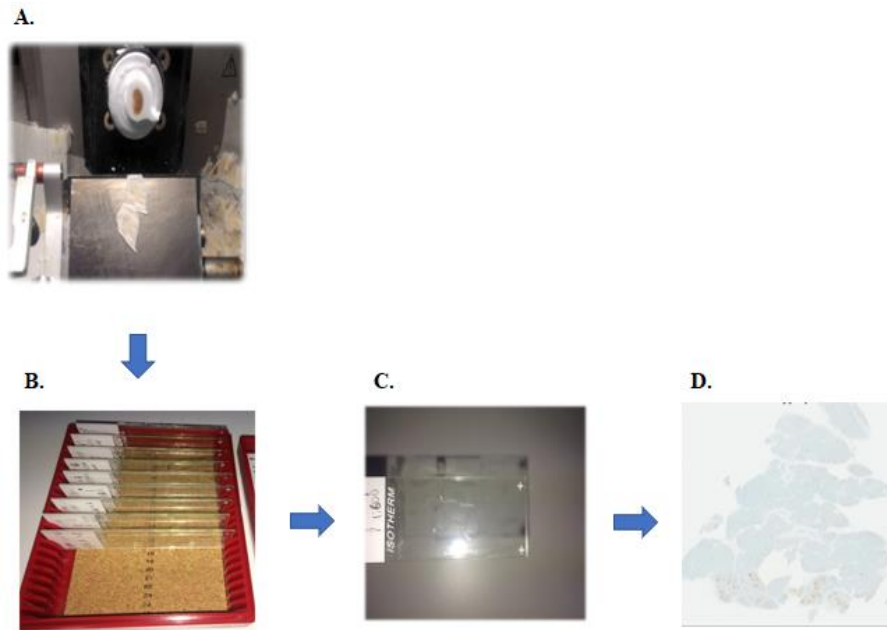


Figure 2.5 Cryosectioning of frozen pancreatic tissue samples; A. The tissue sample was placed on a metal tissue disc which is frozen rapidly to about -20 to -30°C . The tissue sample was embedded in an optimal temperature compound (OCT) medium. B. It was cut frozen with the microtome portion of the cryostat. C. The section was picked up on a glass slide. D. Tissue section view of the pancreas.

2.9. Hematoxylin & eosin (H&E) staining

The frozen pancreatic tissue sections were histologically examined using H&E staining. Sections were stained using an autostainer (Sakura 6188-E, Japan) and according to the instructions (The Tissue-Tek H&E Staining Kit, Sakura, JAPAN). The morphometric study was done using an image analyzer computer system. Data were obtained using Leica Aperio Imagescope Pathology Slide Viewing Software (USA) at Pathology Department, Ministry of Health Ankara City Hospital. Pancreatic tissue sections were stained with H&E and islet sizes and percentage % of the islet areas per field area were measured with ImageJ software v.1.8.0 (Rasband, W.S. 2018).

2.10. Antibodies

Pancreatic tissue specimens were stained with anti-proglucagon D16G10 (Cell signaling, USA) (1:300 dilution) and Alexa Fluor 555 (Thermo Fisher, USA) (1:600 dilution) secondary Abs were used in immunohistochemistry experiments.

In Western blotting studies rabbit polyclonal anti-insulin (Abcam, USA) (1:2000 dilution) as primary and goat anti-rabbit IgG (Abcam, USA) (1:5000 dilution) as secondary Ab were used.

2.11. Immunofluorescence (IF) for Frozen Pancreatic Tissues

After the washing step above, 100 μ L primary antibody was loaded onto tissues and incubated overnight at 4°C. The next day, slides were washed for 5 min 3X in TBS and incubated with 100 μ L secondary Ab for 45 min in RT. After slides were washed with PBS 5 min 3X, they were mounted with flouro-shield mounting medium (Abcam, USA). The slides were evaluated by a laser scanning confocal microscope (Zeiss LSM 510, Germany) and images were generated for anti-glucagon (objective, 40X).

2.12. Real Time quantitative PCR (RT-qPCR): TaqMan® Gene Expression Assays

RT-qPCR analyses were performed so that the transdifferentiation profiles of the cells can be determined at the gene expression level (Xiaowei Wang and Brian Seed, 2003). The general steps performed during RT-qPCR experiments were correlated with the MIQE rules (Alvarez *et al.* 2014). Total RNA was isolated from the pancreatic tissues to be used as a template for the synthesis of single-stranded cDNA. The RNA isolation from a single maximum 10 μ m thick section of tissue was carried out in accordance with the instructions (High Pure FFPE RNA Isolation Kit, Roche, Germany). RNA sample concentrations were determined using the NanoDrop 2000 (Thermo Scientific, US). The NanoDrop 2000 software performed the concentration and A260/A280

measurements by adding 2 μ l of the samples to the device. (Table 2.4). The cDNA synthesis from isolated total RNA samples were carried out according to the manufacturer's instructions (Transcriptor First Strand cDNA Synthesis Kit, Roche, Germany). The final concentrations of RNA samples were adjusted as equal for RT-qPCR studies.

Hydrolysis probes were used which were sequence-specific, double-labeled probes; commonly called “TaqMan” probes (Roche Diagnostic, Turkey). We had designed 12 assays for the quantification of several *Rattus norvegicus* gene products as Neurogenin 3 (Neurog3) (Appendix Figure A. 6.), Pancreatic and duodenal homeobox 1 (Pdx1) (Appendix Figure A. 7.), Insulin (Ins2) (Appendix Figure A. 5.), Somatostatin (Sst) (Appendix Figure A. 8.), Glucagon (Gcg) (Appendix Figure A. 4.), Forkhead box O1 (Foxo1) (Appendix Figure A. 3.), Chromogranin A (Chga), Vimentin (Vim) and 18s rRNA (Appendix Figure A. 2.). Four primers (two direct and indirect) for a gene and a probe using gene identification on NCBI (Appendix FigureA. 1.) were designed. It was planned to test the four possible combinations in an initial assay together with the probe. The assays were designed to work at an annealing temperature of 60°C. Whenever possible, the assays were designed to be specific only for cDNA. The assays were specific for cDNA and a specificity check for the targeted sequence was performed by primer Blast analysis. At this end, the primers were either overlapping the exon-exon borders or they lie in adjacent exons separated by an intron of at least 2 kb.

Table 2.4 Total RNA concentrations and A260/A280 ratios.

Sample	Concentration (ng/ μ l)	A ₂₆₀ /A ₂₈₀ ratio
0 Cont. (3 samples combined)	12	1.87
0 CAF (3 samples combined)	4.8	2.0
20 Cont. 1	35.2	2.176
20 Cont. 2	249.6	2.156
20 Cont. 3	156.8	2.197
20 CAF 1	275.2	2.154
20 CAF 2	172.8	2.160
20 CAF 3	168	2.1
90 Cont. 1	172.8	2.01
90 Cont. 2	231.2	2.06
90 Cont. 3	196	2.03
90 CAF 1	166.4	2.0
90 CAF 2	187.2	2.01
90 CAF 3	222.40	2.04
Mother Cont. 1	164	2.09
Mother Cont. 2	104.8	2.07
Mother Cont. 3	105.6	2.03
Mother CAF 1	264	2.1
Mother CAF 2	612	2.16
Mother CAF 3	117	2.08

In addition to the TaqMan assay, the SYBR Green Quantitative RT-qPCR experiments were carried out using an SYBR Green kit (Roche, Germany) for Chromogranin A gene expression, its primers synthesized according to their NCBI accession (NM_021655) (Roche, Germany).

2.12.1. Relative normalized expression analysis

The $\Delta\Delta C_t$ method was used in the relative normalized expression analysis. The $\Delta\Delta C_t$ method uses the RT-qPCR output C_t value to calculate relative gene expression in experimental and control samples, using a reference gene as the normalizer. $\Delta\Delta C_t$ calculation as below (Rao, X. et al. 2013).

$$\Delta C_t = C_t (\text{Target Gene}) - \Delta C_t (\text{Reference Gene})$$

$$\Delta\Delta C_t = \Delta C_t (\text{Experimental Group}) - \Delta C_t (\text{Control Group})$$

Gene expression studies were performed with the Bio-Rad CFX96 Touch RT-qPCR detection system device. Relative normalized expression analysis was performed with CFX Maestro v.1.1 software (Bio-Rad Laboratories 2017).

2.12.2. Heatmap analysis

The heatmap analysis is a map of the gene expression results of the experimental and the control groups, with dendrograms showing upregulated genes between groups or individual samples. It shows the expression levels (high expression or low expression) of genes using various clustering algorithms (Alvarez & Doné 2014, Oyelade *et al.* 2016). Heatmap analysis was performed with CFX Maestro v.1.1 (Bio-Rad Laboratories 2017) software.

2.13. Transcriptome analysis - NGS-based RNA sequencing (RNA-Seq)

Total RNA and wet tissue samples of two different individuals from all age groups except 0 days offspring individuals were used for transcriptome analysis. Zero days of offspring samples total RNA amount was not enough to run the experiment. Selected samples were sent to Macrogen Inc., South Korea, and the service was purchased. The transcriptome raw data was courtesy of Macrogen Inc. which was sent via e-mail. Raw data were analyzed by Gen-Era Diagnostic, Inc, Turkey as a service provider. Overall steps of RNA-Seq were described in Figure 2.6.



Figure 2.6. Overall sequencing experiment steps for RNA-Seq. A. Sample preparation. B. Library construction C. Sequencing D. Generation of raw data.

2.13.1. Sample Preparation

DNA/RNA was isolated from a sample and used to generate a library. Qualified samples move on to library construction once quality control (QC) has been performed. (Macrogen Inc., South Korea).

The targeted DNA was fragmented into several short segments, usually 100–300 bp in length, using nucleic acid fragmentation. This can be accomplished in a variety of ways. Several combinations of primers were employed in PCR to amplify the desired DNA segments. The PCR products were small pieces of DNA that were targeted. The amplicon assay was the common name for this procedure. After that, the DNA segments were used to make libraries (Qin 2019).

2.13.2. Library Construction

The sequencing library was generated after random fragmentation of the DNA or cDNA sample and 5' and 3' adapter ligation. As an alternative, "tagmentation" improves the library preparation process by combining the fragmentation and ligation processes into a single step. Following PCR amplification, adapter-ligated fragments were gel purified (Macrogen Inc., South Korea).

The process of library preparation involved changing DNA segments so that each DNA sample could have a unique index, such as sample identification, that could be used to determine the patient whose DNA was sequenced. During this phase, the sequencing adaptors can also be added to the DNA segments. Due to this modification, sequencing primers may now attach to all DNA segments, enabling future massive parallel sequencing. (Qin, D. 2019).

2.13.3. Sequencing

The library was introduced into a flow cell for cluster production, where fragments were caught on a lawn of surface-bound oligos that were complementary to the library adapters. Then, using bridge amplification, each fragment was amplified into unique, clonal clusters. The templates might be sequenced when cluster formation was finished (Macrogen Inc., South Korea).

Massively parallel sequencing was carried out using an NGS sequencer. The library was loaded into a sequencing matrix in a particular sequencer. Depending on the sequencer, sequencing matrices vary. For instance, the Ion Torrent NGS sequencer utilizes sequencing chips while the Illumina NGS sequencer uses flow cells. However, it serves the same objective, which is to enable massive parallel sequencing of all DNA segments simultaneously. The sequence data produced by massive parallel sequencing was evaluated using bioinformatics tools (Qin 2019).

The Illumina SBS (USA) technology makes use of a unique, terminator-based reversible technique to identify single bases as they are added to DNA template strands. Natural competition reduces incorporation bias and significantly lowers raw error rates in comparison to other methods since all four reversible, terminator-bound dNTPs were present throughout each sequencing cycle. As a result, homopolymers and repeated sequence sections may be sequenced with extremely high base-by-base accuracy, completely eliminating context-specific mistakes.

2.13.4. Generation of Raw Data

Utilizing sequencing control software for system control and base calling through an integrated primary analysis program called RTA, the Illumina sequencer (USA) creates raw images (Real Time Analysis). Using the Illumina software bcl2fastq, the BCL (base calls) binary was transformed into FASTQ. No adapters were removed from the readings (Macrogen Inc., South Korea).

2.14. Western Blotting Studies

2.14.1. Protein Isolation from Pancreatic Tissues

Empty tubes of 1.5 mL were weighed, tared, and labeled. The tissue was divided into small pieces as much as possible with the help of a scalpel. These parts were taken into the tube and washed with PBS. The tissue pieces purified from blood were pulverized in a mortar with the help of liquid nitrogen. The powdered extract was taken into the tube and weighed beforehand. A volume of approximately 2.5X the weight of tissue (gram-mL, mg- μ L) lysis buffer was added to the tube. Water bath sonication was used for homogenization. The homogenized extract was centrifuged for 45 min. at maximum speed. The supernatant with the protein mixture was taken into a separate tube and was stored at -20°C if it was not used immediately. Before starting the

Western blot application, the centrifuge step was applied again to make the mixture cleaner. The protein mixture was taken into special low-binding tubes.

2.14.2. Protein Quantification

The total amount of protein in the protein mix was determined by the Bradford assay (Thermo 1X Reagent, USA) based on the manufacturer's instruction and, μg of protein per μL were determined using the ELISA reader device (Tecan, Switzerland). BSA (Bovine Serum Albumin) standards were used to determine the amount of protein in the samples. The following steps were applied to determine the amount of protein:

For blank, 5 μL of distilled water was loaded into ELISA plate wells in 3 replicates.

BSA Standards were prepared as 250, 500, 750, and 1000 $\mu\text{g}/\mu\text{L}$ and loaded in 3 replicates of 5 μL of the 96-well plates. Protein mixtures were diluted and 5 μL were loaded in 3 repetitions. Then, 245 μL of Bradford solution was put on all samples. It was incubated at RT for 15 min. The plate was placed on the ELISA reader and the amount of protein was determined by measuring it at 595 nm wavelength.

OD values and total protein amounts ($\mu\text{g}/\mu\text{L}$ protein) were determined by using the reader device with the Bradford method (Appendix Table B.1.).

2.14.3. Samples Preparation for SDS PAGE gels and the blotting protocol

Protein samples of each group were mixed with the loading buffer (4X Laemmli Buffer). For each group, there were $n=3$, technical replicates. Thirty μg protein was used for each sample then heated at 95°C for 5 min. and loaded into the wells. 10-well BIO-RAD Mini-PROTEAN TGX Precast Polyacrylamide Gels were used. Thermo Fisher (PageRuler™ Plus Prestained Protein Ladder, 10 to 250 kDa- USA) protein standard was used as the protein standard (Appendix Figure B.2). Execution started with 100 V. then it was continued with 150 V. The gels were taken into containers

with 1X transfer buffer (Towbin transfer buffer). PVDF membrane was cut to size of the gel and incubated for 3 minutes with 100% methanol on the shaker. The membrane and gel were washed in a shaker with 1X TBS. It was flattened with a cylinder to avoid any air bubbles. Then, the membrane and the gel were loaded into a Western blot transfer device (BIO-RAD Trans-Blot Turbo Transfer) by the sandwich method.

When the system was ready, the device was transferred in accordance with BIO-RAD Mini-PROTEAN TGX Precast Gel user manual for 7 min. at 25V, 2.5A. Membranes to which proteins were transferred were blocked in TBST with 5% BSA (blocking buffer) for 1.5 hours at RT on a shaker. Blocking buffer was poured out and the membrane was washed once with 1X TBST on the shaker for 5 min. The insulin primary Ab was diluted 1: 2000 with a blocking buffer and the membranes were incubated at 4°C overnight. After the incubation, the membranes were washed 4X for 5 min. with 1X TBST on a shaker at RT. Anti-Rabbit secondary antibody was diluted 1: 5000 in the blocking buffer and the membranes were incubated for 1h at RT on a shaker. After the incubation, the membranes were washed 4X for 5 min. with 1X TBST on a shaker at RT. Membranes were incubated with HRP conjugated ECL (Bio-Rad, USA) for 30 sec and were imaged on ChemiDOC Imaging System (Bio-Rad, USA). The imaged membrane was placed in 1X TBST for anti-beta actin as an internal control for the protein study. Images analyzed with ImageJ software v.1.8.0 (Rasband, W.S. 2018).

2.15. ELISA Assay

Rats` plasma insulin level analyzes were performed with the Enzyme-Linked Immunosorbent Assay (ELISA) kit (Mouse/Rat Insulin ELISA kit, Millipore, USA) according to the manufacturer's instructions.

2.16. Statistical analysis

Independent Samples t-test for data analysis and the customary threshold of $*p < 0.05$ to declare a statistically significant difference with IBM SPSS Statistic 26 software (IBM Corp. 2019) was used in all experiments otherwise indicated. The values are mean \pm SEM) unless indicated.

CHAPTER 3

RESULTS

3.1. Prepregnancy Body Weight

There was a statistically significant difference in body weights between prepregnancy the control and CAF group mothers (Figure 3.1). The mean weight of the CAF group was 570g and the mean weight of the control group was 310g ($****p < 0.0001$). As a result, the CAF group was considered as obese after 8 months of cafeteria diet.

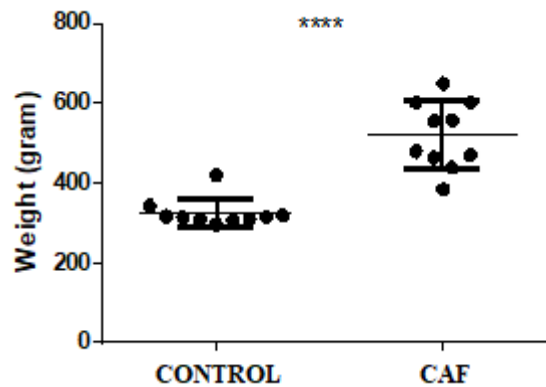


Figure 3.1. Body weights of mother Wistar rats before pregnancy (Control group, n = 10, CAF group, n = 10). Mother rats fed with CAF were statistically obese compared to the control group ($****p < 0.0001$) (Teker 2014).

3.2. Glucose tolerance test

According to the 2-h blood glucose measurement results obtained in the glucose tolerance test performed, it was observed that the blood glucose level in the CAF group did not fall below 200 (mg/dL) at the end of 2 h, and the blood glucose level in the control group was normalized. After the cafeteria diet were provided to the CAF group, it was determined that individuals in the CAF group may have developed insulin resistance, which is an important marker of T2D (Figure 3.2) (**** $p < 0.0001$, $n = 10$ rats/group).

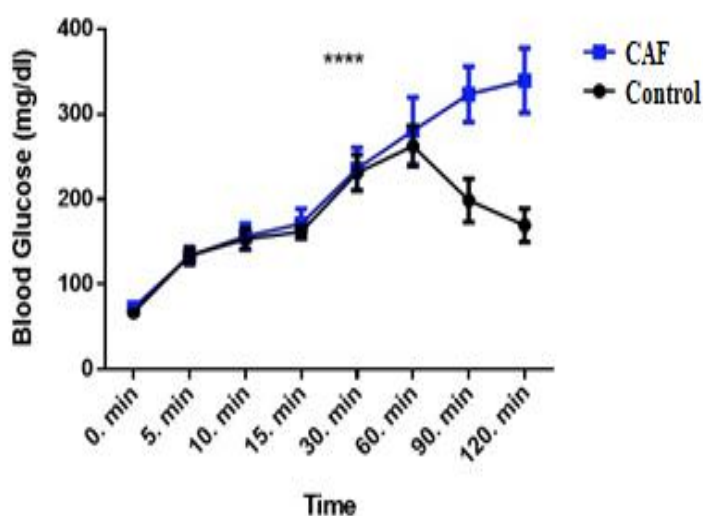


Figure 3.2. Blood glucose levels of mother Wistar rats before pregnancy (Control group $n = 10$, CAF group $n = 10$). CAF fed mother rats showed statistically significant hyperglycemia (**** $p < 0.0001$) (Tekler 2014).

3.3. Immunohistochemical Staining for anti-Glucagon in Mother Pancreas

The immunohistochemistry (IHC) was performed using anti-glucagon for pancreatic tissues of the mother group (Figure 3.3). The unit of area for the CAF group was $4200 \pm 1000 \text{ mm}^2$ and the control group was $800 \pm 100 \text{ mm}^2$ for the expression of glucagon hormone. As shown in Figure 3.4 the statistical analysis of the IHC data for anti-glucagon ($n=3$) was statically significant (** $p < 0.01$).

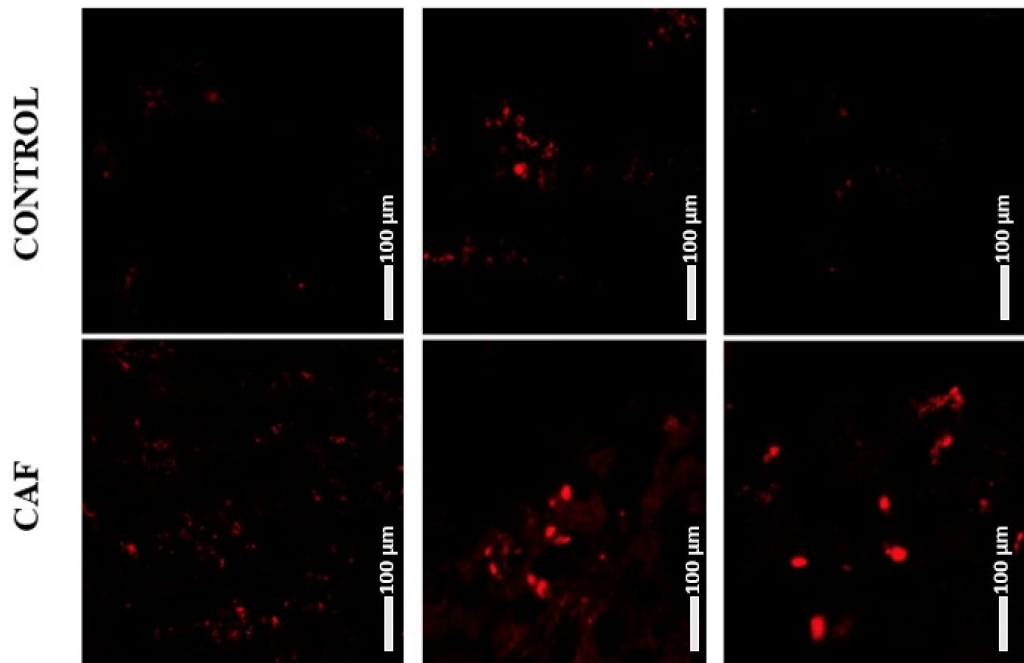


Figure 3.3. Images of immunohistochemistry of beta cells from the mother rats' pancreas using anti-glucagon (anti-Glucagon: red). (Scale bars = 100 μm , 40X objective). ($n=3$, each panel represents $n=1$).

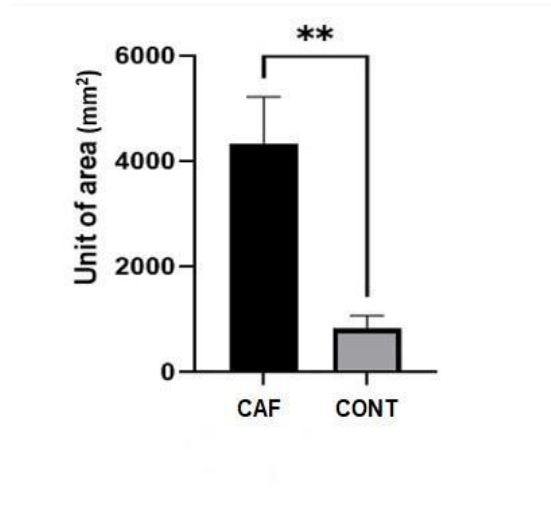


Figure 3.4. Quantitative analysis of IHC for anti-glucagon on mothers' pancreatic sections. The stained area was acquired by using the ImageJ program. The CAF group had $4200 \pm 1000 \text{ mm}^2$ (SEM) and the control group $800 \pm 100 \text{ mm}^2$ (SEM). (** $p < 0.01$).

3.4. 20 days and 90 days Offspring Body Weight

When the body weight of 20 days of offspring were measured it was found to be $45 \pm 3 \text{ g}$ ($n=6$) for the control group vs. the CAF group body weight of 20 days old offspring was $30 \pm 2 \text{ g}$ ($n=6$). The weight difference between the groups was statistically significant (** $p < 0.0001$) (Figure 3.5).

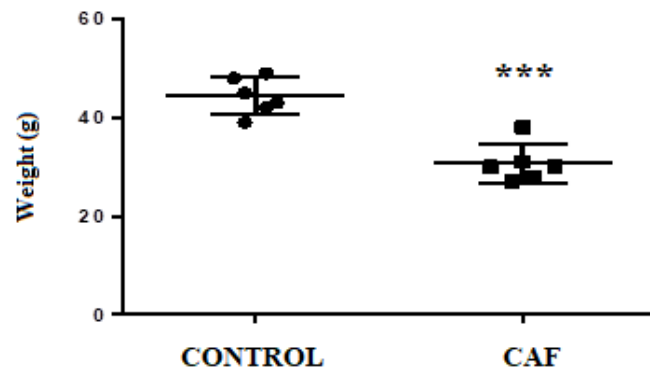


Figure 3.5. Body weights of 20 days of offspring. The control group weight was 45 ± 3 g (SEM) and the CAF group was 30 ± 2 g (SEM). In both groups (n=6). (***) $p < 0.0001$.

When the average body weights of the 90 days offspring were examined (Figure 3.6), the average body weight of the control group was 360 ± 3 g (SEM) and the average body weight of the CAF group was 370 ± 2 g (SEM) with no statistically significant difference between the groups.

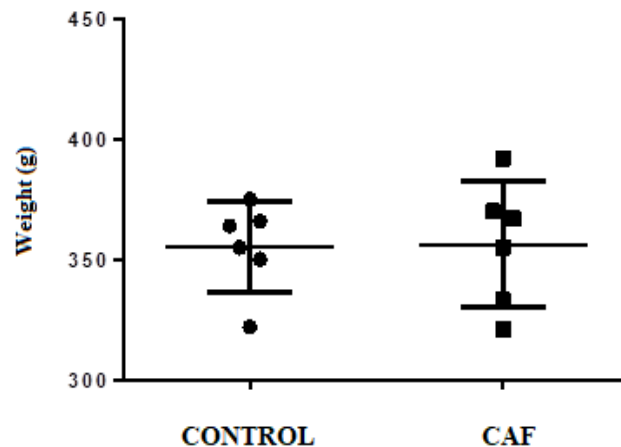


Figure 3.6. Body weights of 90 days of offspring. The control group weight was 360 ± 3 g (SEM) and the CAF group was 370 ± 2 g (SEM). (Control group, n = 6, CAF group, n = 6).

3.5. Plasma Insulin Levels of Offspring

Insulin levels were obtained from plasma samples of 20 days and 90 days old offspring and measured with ELISA assay. The results showed that the control group insulin levels were higher; 2.2 ± 0.6 pg/mL than the CAF group insulin levels 0.98 ± 0.2 pg/mL in 20 days offspring which showed a statistically significant change between the groups (Figure 3.7) ($*p < 0.05$). There was no significant difference between the control vs. the CAF groups of 90 days offspring plasma insulin levels as the results indicated that the control group had 1.98 ± 0.5 pg/mL vs. the CAF group had 2.3 ± 1 pg/mL ($n = 6$) (Figure 3.8).

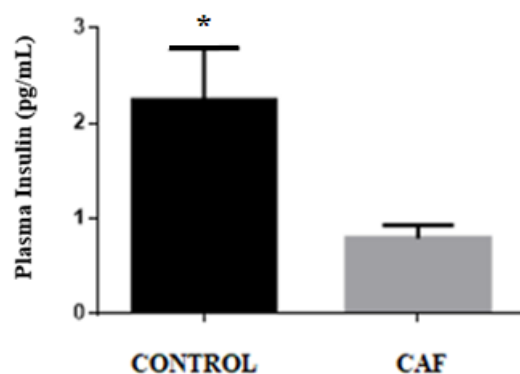


Figure 3.7. Plasma insulin levels of 20 days offspring. Plasma insulin levels of the control group was 2.2 ± 0.6 pg/mL (SEM), CAF group was 0.98 ± 0.2 pg/mL (SEM) (Control group, $n = 6$, CAF group, $n = 6$) ($*p < 0.05$).

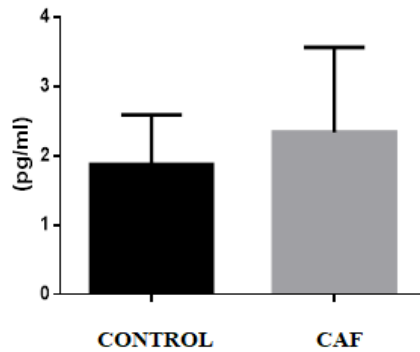


Figure 3.8. Plasma insulin levels of 90 days offspring. Plasma insulin levels of the control group was 1.98 ± 0.5 pg/mL (SEM), CAF group was 2.3 ± 1 pg/mL (SEM) (n = 6). No statistically significant values were detected between the groups.

3.6. Assessment of Islet Functional Potency by Glucose Stimulated Insulin Secretion

After determining pancreatic cell viability tests, isolated islet cells of all offspring (0, 20, 90 days) control and CAF groups were exposed to both low (3,3 mM) and high (16,7 mM) glucose concentrations for 48 h. Results of the ELISA assay showed that there was no significant difference in insulin secretion from the islet cells between the control and the CAF groups of 0 days offspring (Figure 3.9 and Figure 3.10) and 90 days offspring (Figure 3.13 and Figure 3.14). The values are mean \pm SEM). The control group 0 days offspring secreted levels of insulin at low glucose were 12.9 ± 0.96 ng/mL at 0th h, 5.05 ± 0.30 ng/mL at 24th h, 12.5 ± 0.92 ng/mL at 48th h. For this group, insulin secretion levels from the islet cells were not statistically significant compared to the control group ($p > 0.05$). The CAF group 0 days offspring levels of insulin secretion from the islet cells at high glucose were 6.15 ± 0.34 ng/mL at 0th hour, 2.29 ± 0.04 ng/mL at 24th hour, 5.38 ± 1 ng/mL at 48th h. However, the CAF group islet cells of 20 days offspring CAF group secreted more insulin vs. the control group (Figure 3.11 and Figure 3.12).

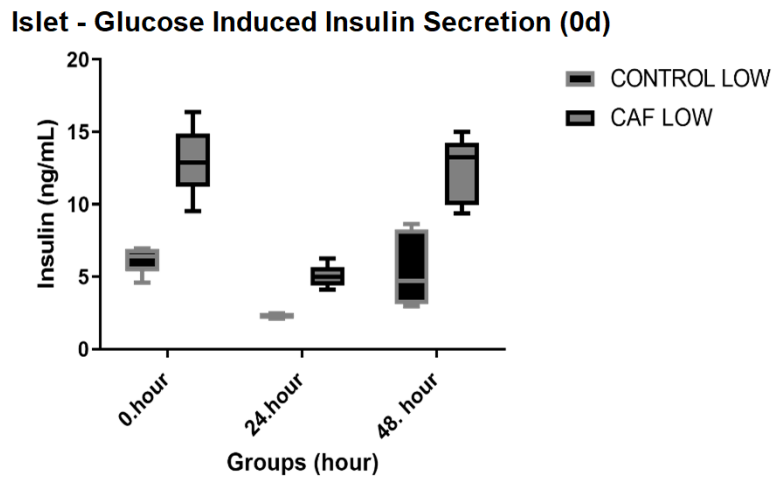


Figure 3.9. Static low concentration glucose stimulated insulin secretion of isolated islet cells of 0 days of offspring. The values are mean \pm SEM). The CAF group 0 days' offspring levels of insulin were 6.15 ± 0.34 ng/mL at 0th h, 2.29 ± 0.04 ng/mL at 24th h, 5.38 ± 1 ng/mL at 48th h. The control group 0 days' offspring levels of insulin were 12.9 ± 0.96 ng/mL at 0th h, 5.05 ± 0.30 ng/mL at 24th h, 12.5 ± 0.92 ng/mL at 48th h. Insulin secretion levels from the islet cells were not statistically significant between the groups ($p > 0.05$).

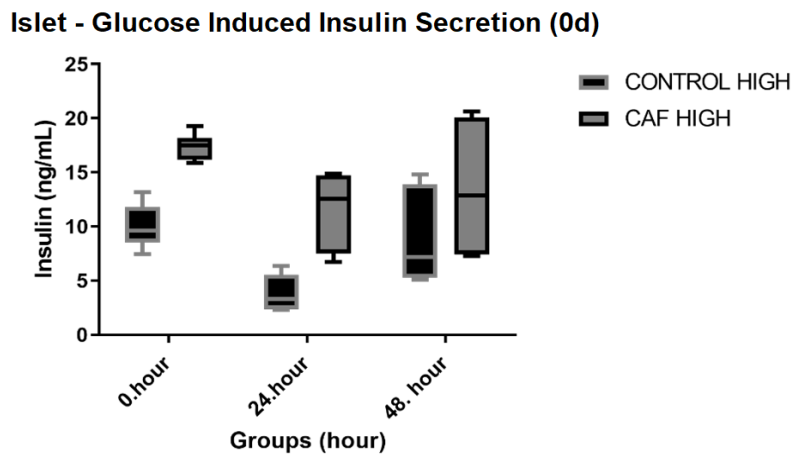


Figure 3.10. Static high glucose stimulated insulin secretion of isolated islet cells of 0 days offspring. Values are mean \pm SEM. CAF group 0 days offspring levels of insulin were 17.3 ± 0.49 ng/mL at 0th hour, 11.5 ± 1.50 ng/mL at 24th hour, 13.4 ± 2.36 ng/mL at 48th hour. Control group 0 days offspring levels of insulin were 10.1 ± 0.98 ng/mL at 0th h., 5.05 ± 0.30 ng/mL at 24th h., 3.92 ± 0.81 ng/mL at 48th h.

Figure 3.11 showed that the low concentration of glucose (3.3 mM) in the control and the CAF group 20 days offspring levels of insulin were 7.43 ± 0.14 ng/mL at 0th h, 1.41 ± 0.18 ng/mL at 24th h, 5.34 ± 0.27 ng/mL at 48th h. ($*p < 0.05$). The control group 20 days offspring levels of insulin from the islet cells were 4.11 ± 0.27 ng/mL at 0th h, 1.44 ± 0.27 ng/mL at 24th h, 1.23 ± 0.07 ng/mL at 48th h. In this category, the insulin levels were statistically significant higher in the CAF group vs. the control ($*p < 0.05$).

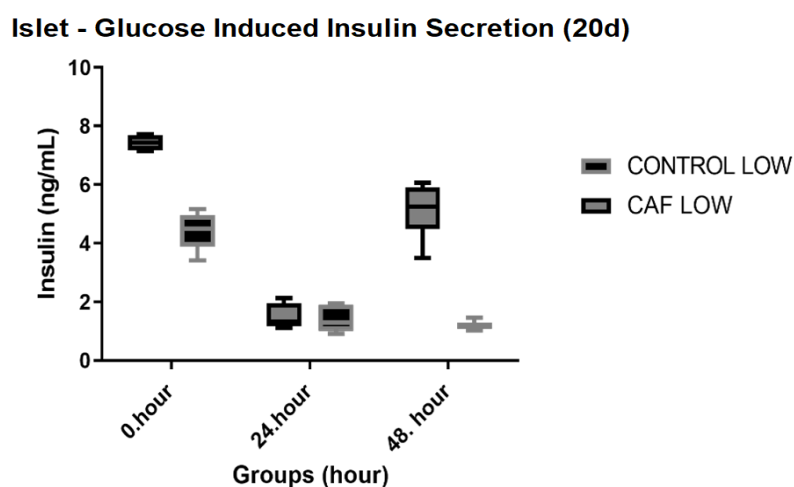


Figure 3.11. Static low glucose stimulated insulin secretion of isolated islet cells of 20 days offspring Values are mean \pm SEM. The CAF group 20 days' offspring levels of insulin were 7.43 ± 0.14 ng/mL at 0th h, 1.41 ± 0.18 ng/mL at 24th h, 5.34 ± 0.27 ng/mL at 48th h. The control group 20 days offspring levels of insulin were 4.11 ± 0.27 ng/mL at 0th h, 1.44 ± 0.27 ng/mL at 24th h, 1.23 ± 0.07 ng/mL at 48th h. The insulin levels were statistically significant between the groups $*p < 0.05$.

Figure 3.12 showed high concentration of glucose (16.7 mM) in the control and the CAF group 20 days of offspring levels of insulin from the islet cells. It was 9.99 ± 0.64 ng/mL at 0th h, 6.27 ± 0.35 ng/mL at 24th h, 5.38 ng/mL at 48th h. The control group 20 days offspring levels of insulin of the islet cells were 4.11 ± 0.27 ng/mL at 0th h, 1.44

± 0.27 ng/mL at 24th h, 1.23 ± 0.07 ng/mL at 48th h. Insulin levels were higher in the CAF group vs. the control at the high concentrations of the glucose ($*p < 0.05$).

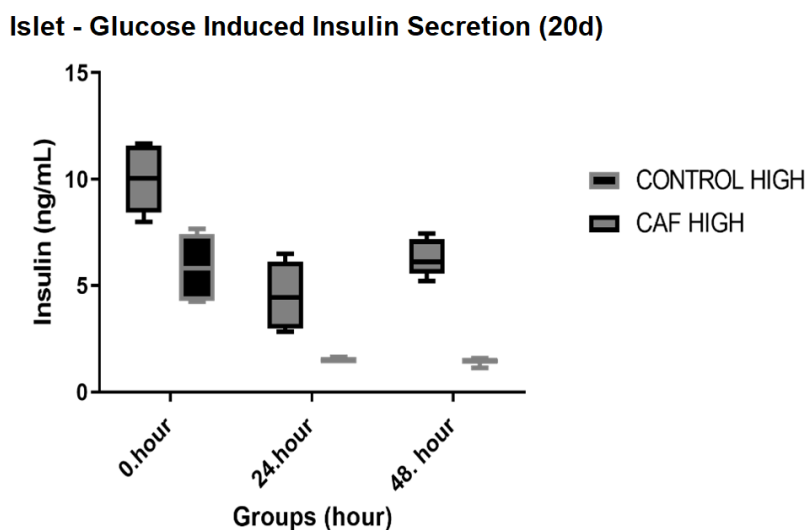


Figure 3.12. Static high glucose stimulated insulin secretion of isolated islet cells of 20 days offspring. Values are mean \pm SEM. The control and CAF groups at 0th, 24th and 48th hours. The CAF group 20 days offspring levels of insulin were 9.99 ± 0.64 ng/mL at 0th hour, 4.54 ± 0.61 ng/mL at 24th h, 6.27 ± 0.35 ng/mL at 48th h. The control group 20 days offspring levels of insulin were 4.11 ± 0.27 ng/mL at 0th h, 1.44 ± 0.27 ng/mL at 24th h, 1.23 ± 0.07 ng/mL at 48th h ($*p < 0.05$)

Figure 3.13 showed that low concentration of glucose (3.3 mM) on the control and the CAF group 90 days offspring levels of insulin were 17.01 ± 2.71 ng/mL at 0th h, 20.45 ± 2.67 ng/mL at 24th h, 9.33 ± 1.16 ng/mL at 48th h. The control group 90 days offspring levels of insulin of the islets were 20.44 ± 1.45 ng/mL at 0th h, 18.19 ± 2.69 ng/mL at 24th h, 4.37 ± 0.36 ng/mL at 48th h. No statistically significant difference was detected between the groups ($p > 0.05$).

Islet - Glucose Induces Insulin Secretion (90d)

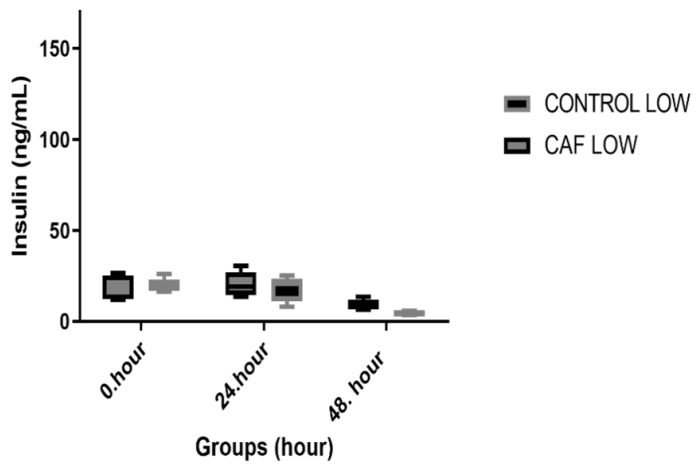


Figure 3.13. Static low glucose stimulated insulin secretion of isolated islet cells of 90 days offspring. Values are mean \pm SEM. The CAF group 90 days offspring levels of insulin of islet cells were 17.01 ± 2.71 ng/mL at 0th h, 20.45 ± 2.67 ng/mL at 24th h, 9.33 ± 1.16 ng/mL at 48th h. The control group 90 days offspring levels of insulin of the islets were 20.44 ± 1.45 ng/mL at 0th h, 18.19 ± 2.69 ng/mL at 24th h, 4.37 ± 0.36 ng/mL at 48th h. There was no statistical significant difference between the groups ($p > 0.05$).

Figure 3.14 showed that high concentration of glucose (16.7 mM) on the control and the CAF group 90 days offspring levels of insulin were 141.30 ± 6.61 ng/mL at 0th hour, 46.56 ± 3.82 ng/mL at 24th hour, 15.13 ± 1.68 ng/mL at 48th hour. The control group 90 days offspring levels of insulin were 132.84 ± 6.30 ng/mL at 0th hour, 49.61 ± 8.04 ng/mL at 24th h, 9.44 ± 0.27 ng/mL at 48th h. There was no statistically significant difference between the groups.

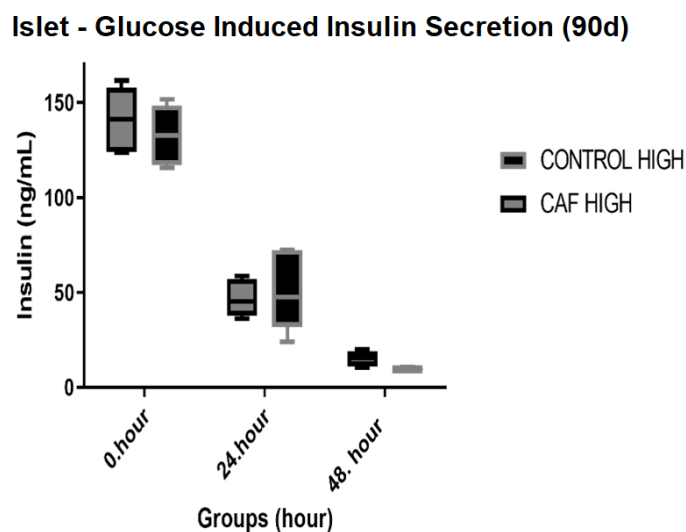


Figure 3.14. Static high glucose stimulated insulin secretion of isolated islet cells of 90 days offspring Values are mean ± SEM. The CAF group's 90 days offspring levels of insulin were 141.30± 6.61 ng/mL at 0th hour, 46.56 ± 3.82 ng/mL at 24th h, 15.13 ± 1.68 ng/mL at 48th h. The control group 90 days offspring levels of insulin were 132.84± 6.30 ng/mL at the 0th hour, 49.61± 8.04 ng/mL at the 24th h, and 9.44 ± 0.27 ng/mL at the 48th h. No statistical significance between the groups ($p>0.05$).

3.7. Assessment of Viability of Islet Cells

Islet cell viability studies were performed on 0 days, 20 days, and 90 days offspring pancreases. For 0 days offspring samples were analyzed 0th, 24th, and 48th h. but for 20 days and 90 days offspring samples were analyzed on the 0th, 24th, 48th, and 72nd h. The images of bright-field of islet cells appear in the left panel, images of live cells stained with fluorescein diacetate (FDA) in the middle panel, and dead cells stained with propidium iodide (PI) in the right panel (Figures 3.15, 3.16, 3.18, 3.19, 3.21, and 3.22).

The results of cell viability of pancreatic islets for the 0 days old offspring of the control group were shown in Figure 3.15. In the observed results, the viable cell rate for the 0th h was 93.92%, 88.69% for the 24th h, and 96.52% for the 48th h.

Dead cell rates were determined as 6.08% for the 0th hour, 11.31% for the 24th h., and 3.48% for the 48th h.

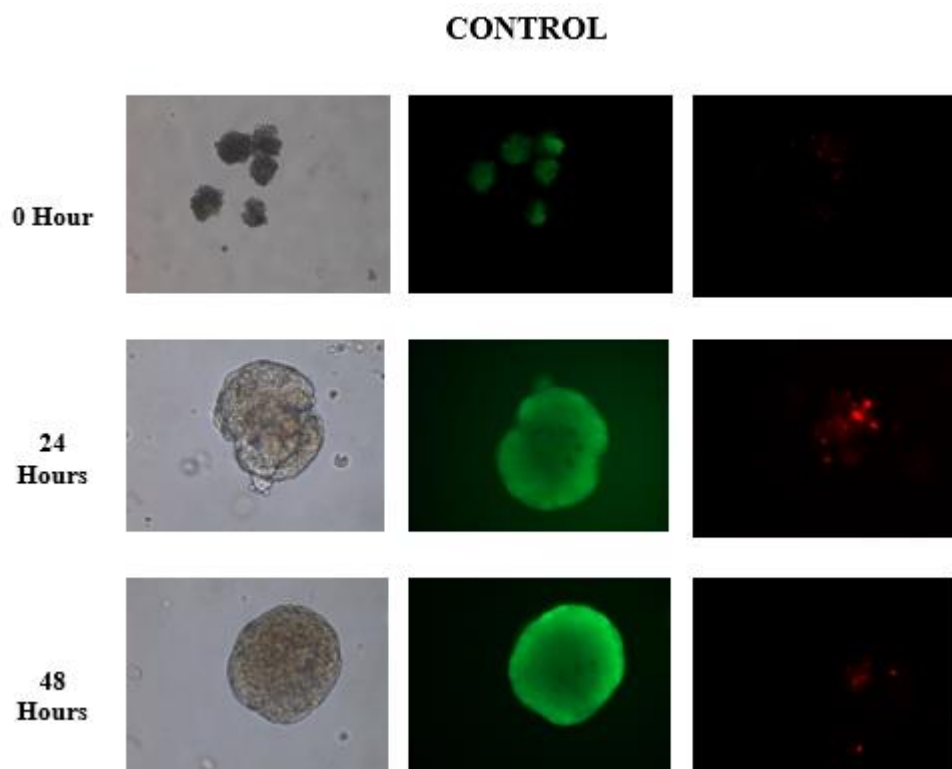


Figure 3.15. Cell viability of isolated pancreatic islets of 0 days offspring control group. Propidium iodide (PI)–fluorescein diacetate (FDA) staining was performed on isolated islet cells at 0th, 24th, 48th h. Bright-field (left panel), FDA-stained (middle panel) green; live cells, and PI-stained (right panel) red; dead islets were shown by fluorescence microscopy (Magnification top lane 200X, bottom lane 400X).

Figure 3.16 showed the cell viability of pancreatic islets for the 0 days old offspring of the CAF group. As results showed, the viable cell rate for the 0th h was 88.38%, 89.90% for the 24th h, and 92.57% for the 48th h. Dead cell rates were determined as 11.62% for 0th h, 10.1% for 24th h, and 7.43% for 48th h.

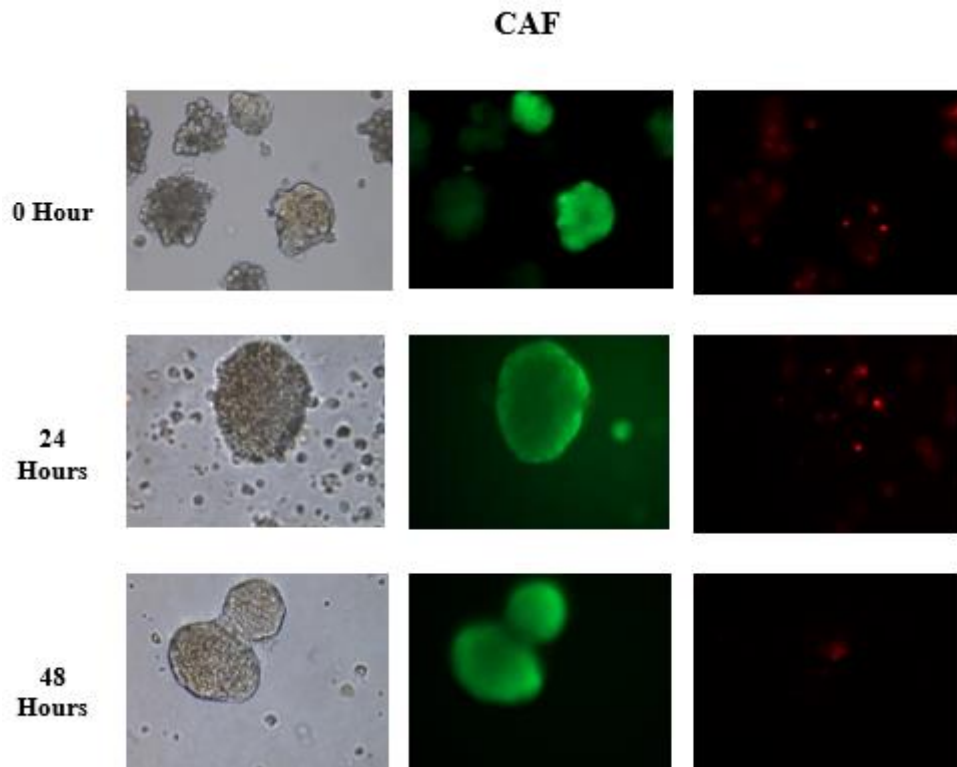


Figure 3.16. Cell viability of isolated pancreatic islets of 0 days offspring CAF group. Propidium iodide (PI)–fluorescein diacetate (FDA) staining was performed on isolated islet cells at 24th, 48th h. Bright-field (left panel), FDA-stained (middle panel) green; live cells, and PI-stained (right panel) red; dead cells islets were shown by fluorescence microscopy (Magnification 400X).

When 0 days old offspring isolated islet cells of the control and CAF groups were compared with each other a significant difference was detected in the viability rates between the groups at the 48th h samples (** $p < 0.01$) (Figure 3.17) that there was lower % of viable cells in the CAF group vs. the control group.

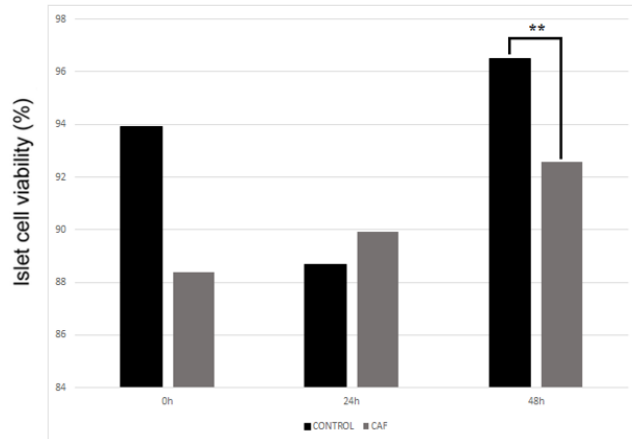


Figure 3.17. The percentage of live pancreatic cells of 0 day old offspring. At 48 h, the CAF group had lower viable islet cells vs. the control islet cells (** $p < 0.01$).

The results of cell viability of pancreatic islets for the 20 days old offspring of the control group were shown in Figure 3.18. As observed, the viable cell rate for 0th h was 64.98%, 93.71% for 24th h, 91.45% for 48th h, and 91.03% for 72nd h. Dead cell rates were determined as 35.02% for 0th h, 6.29% for 24th h, 8.55% for 48th h, and 8.97% for 72nd h.

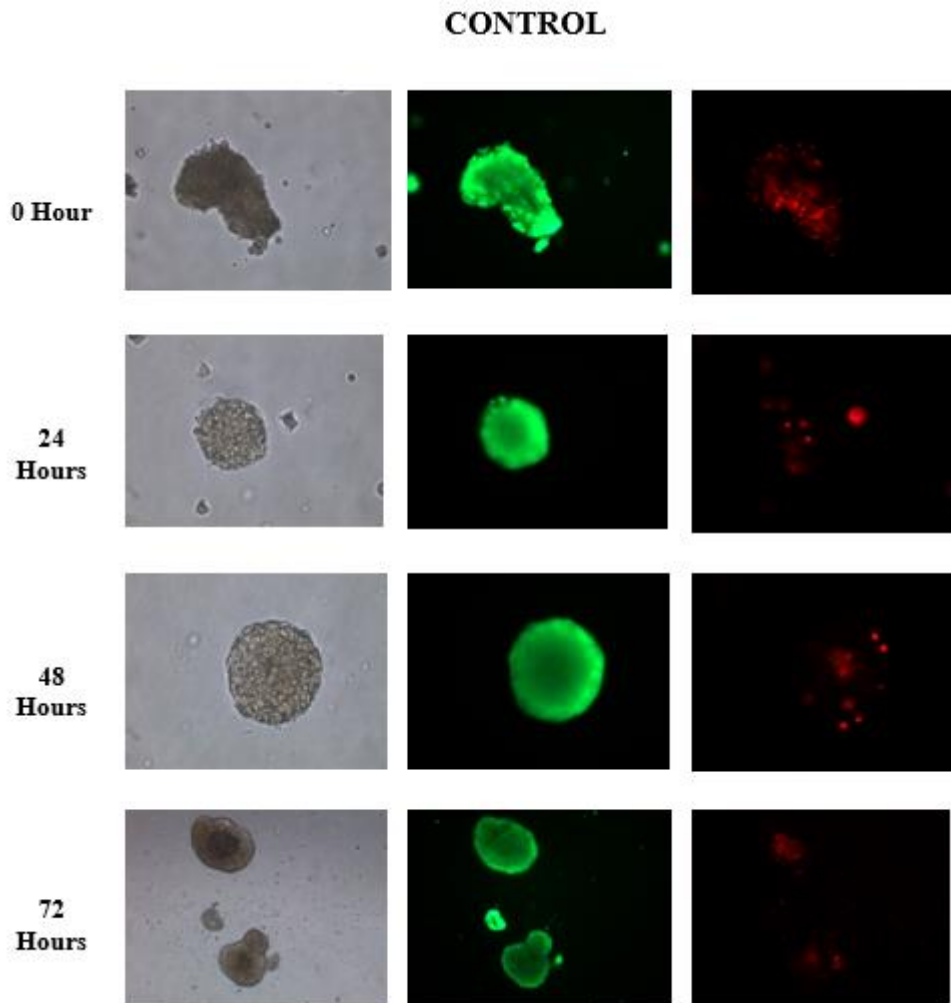


Figure 3.18. Cell viability of isolated pancreatic islets of 20 days offspring control group. Propidium iodide (PI)–fluorescein diacetate (FDA) staining was performed on isolated islet cells at the 24th, 48th, and 72nd h. Bright-field (left panel), FDA-stained (middle panel) green; live cells, and PI-stained (right panel) red; dead islets were shown by fluorescence microscopy (Magnification top lane 200X, bottom lane 400X).

Figure 3.19 showed the cell viability of pancreatic islets for the 20 days old offspring of the CAF group. In the results observed, the viable cell rate for 0th h was 73.19%, 75.39% for 24th h, 77.65% for 48th h, and 75.91% for 72th h. Dead cell rates were determined as 26.81% for 0th h, 24.61% for 24th h, 22.35% for 48th h, and 24.09% for 72th h.

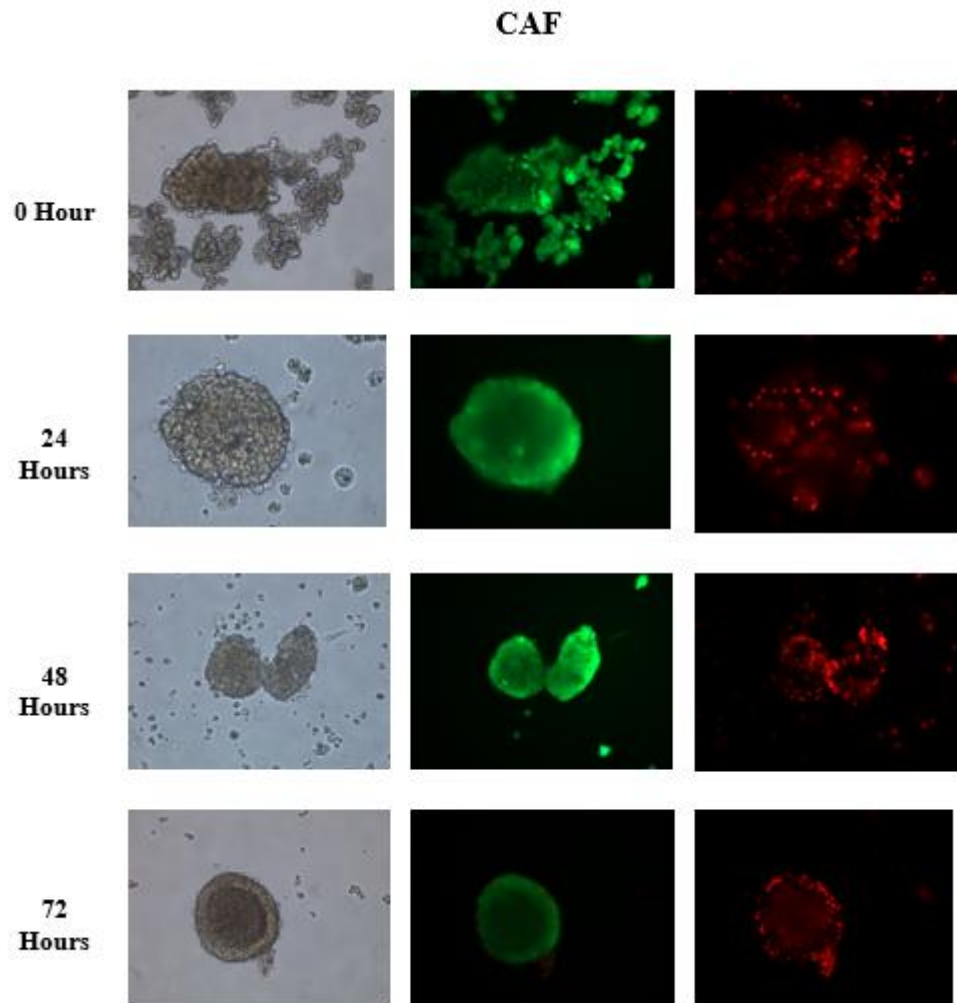


Figure 3.19. Cell viability of isolated pancreatic islets of 20 days offspring CAF group. Propidium iodide (PI)–fluorescein diacetate (FDA) staining was performed on isolated islet cells at the 24th, 48th, and 72th h. Bright-field (left panel), FDA-stained (middle panel) green; live cells, and PI-stained (right panel) red; dead islets were shown by fluorescence microscopy (Magnification top lane 200X, bottom lane 400X).

20 days old offspring control and CAF groups were compared with each other and statistical analyzes were performed a significant difference was obtained in the viability rates between the 24th h (**** $p < 0.0001$), 48th h (***) $p < 0.001$, and 72th h samples (* $p < 0.023$) (Figure 3.20) accordingly.

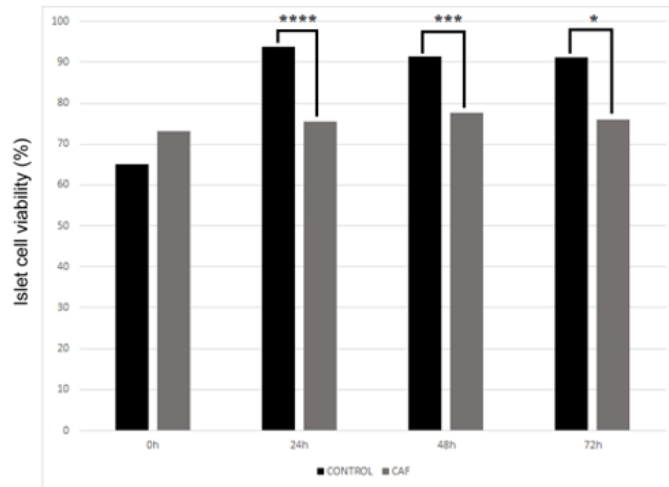


Figure 3.20. The percentage of live pancreatic cells of 20 days old offspring. At 20th, 48th and 72th h, the viable cells % were lower in the CAF group vs. the control (* $p < 0.05$, *** $p < 0.001$, **** $p < 0.0001$).

Lastly, results of cell viability of pancreatic islets for the 90 days old offspring control group were shown in Figure 3.21. As determined, the viable cell rate for 0th h was 94.19%, 95.36% for 24th h, 90.83% for 48th h, and 84.04% for 72th h. Dead cell rates were determined as 5.81% for 0th h, 4.64% for 24th h, 9.17% for 48th h, and 15.96% for 72nd h.

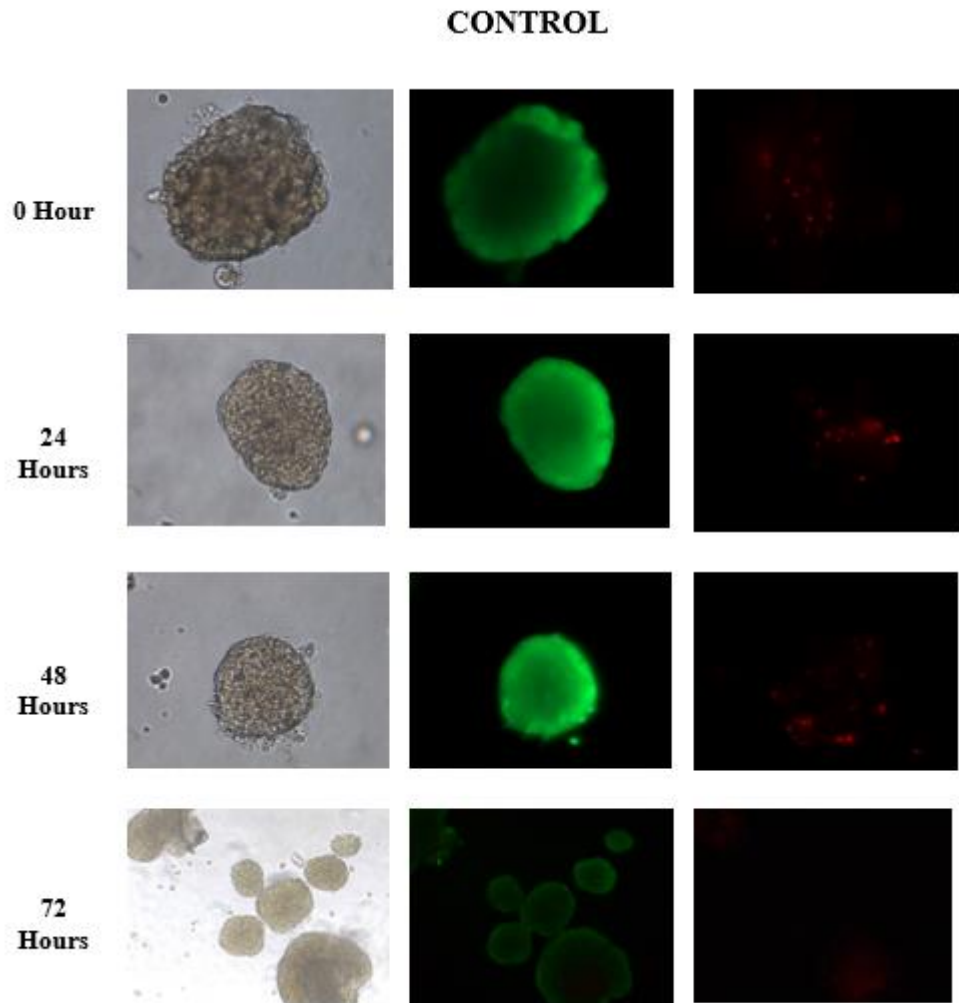


Figure 3.21. Cell viability of isolated pancreatic islets 90 days offspring control group. Propidium iodide (PI)–fluorescein diacetate (FDA) staining was performed on isolated islet cells at the 24th, 48th, and 72nd h. Bright-field (left panel), FDA-stained (middle panel) green; live cells, and PI-stained (right panel) red; dead islets were shown by fluorescence microscopy (Magnification 400X).

Figure 3.22 showed the cell viability of pancreatic islets for the 90 days old offspring CAF group. In the results observed, the viable cell rate for 0th h was 94.79%, 91.70% for 24th h, 93.82% for 48th h, and 85.46% for 72th h. Dead cell rates were determined as 5.21% for 0th h, 8.3% for 24th h, 6.18% for 48th h, and 14.54% for 72nd h.

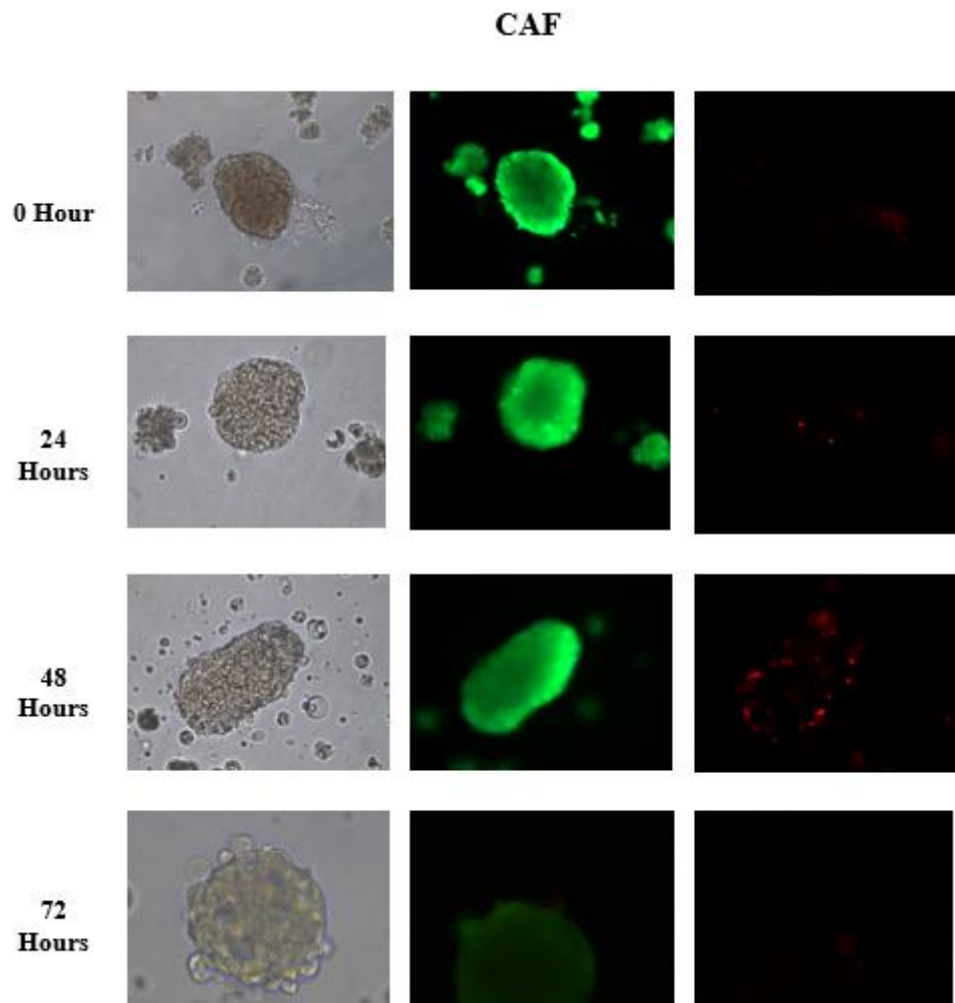


Figure 3.22. Cell viability of isolated pancreatic islets of 90 days offspring CAF group. Propidium iodide (PI)–fluorescein diacetate (FDA) staining was performed on isolated islet cells at the 24th, 48th, and 72nd h. Bright-field (left panel), FDA-stained (middle panel) green; live cells, and PI-stained (right panel) red; dead islets were shown by fluorescence microscopy (Magnification 200X).

90 days old offspring the control and CAF groups were compared with each other according to the analysis results, there is no significant difference between any groups (Figure 3.23) ($p>0.05$).

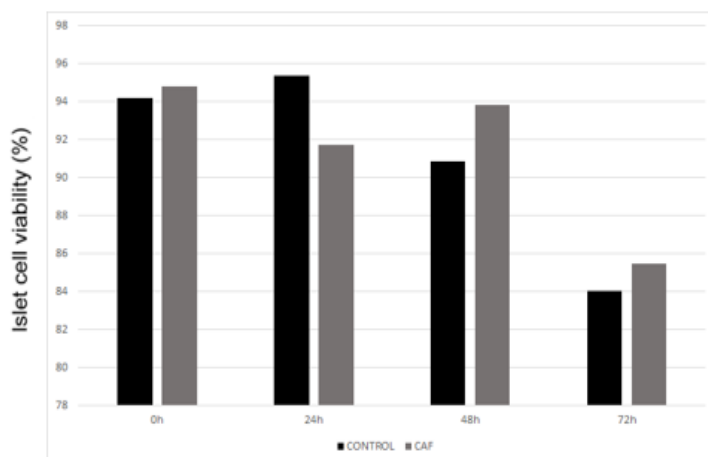


Figure 3.23. The percentage of live pancreatic cells of 90 days old offspring. There was no statistically significant difference between groups ($p>0.05$).

3.8. Morphometric analysis of Islet Cells

The following Figure 3.24 and Figure 3.25 were the results of HE staining images of sections of 20 days offspring rats' pancreatic tissues. As seen in the images, there was a significant decrease in Langerhans islet cell size in the 20 days offspring CAF group (Figure 3.25) compared to the 20 days old offspring control group (Figure 3.24). Based on the statistical analysis results of HE staining in Figure 3.26, islet cell area (mm^2) was higher in the 20 days offspring control group vs. the CAF group ($n=4/\text{rat}$). Twenty sections were evaluated for each group of animals.

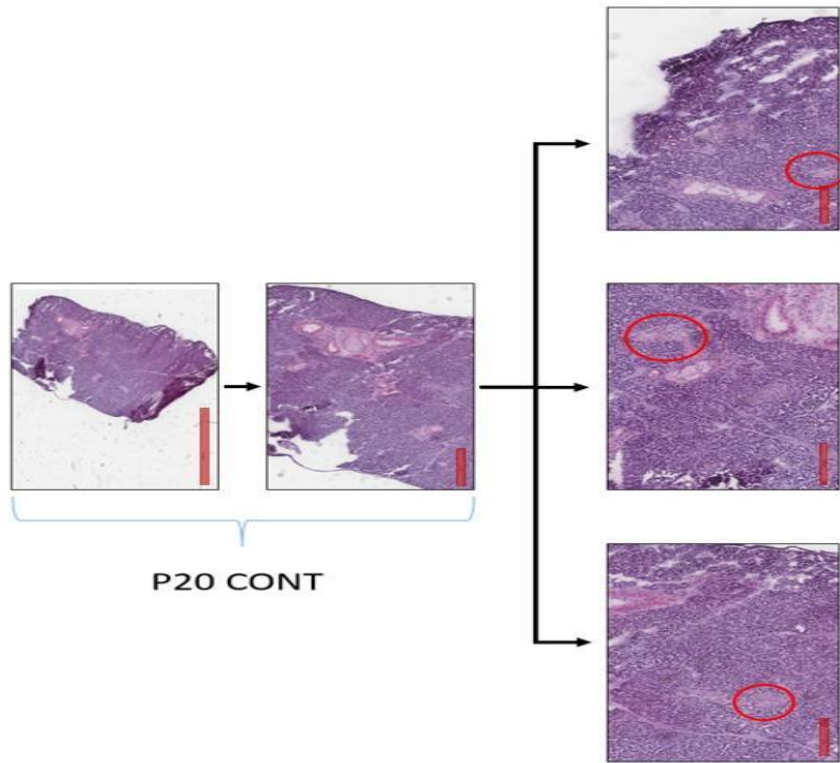


Figure 3.24. HE stained histopathological sections of 20 days offspring control group pancreas. Red circles indicate islet cells (n=4/rat) Scale bar; left 2mm, middle 600 μm, right 100 μm.

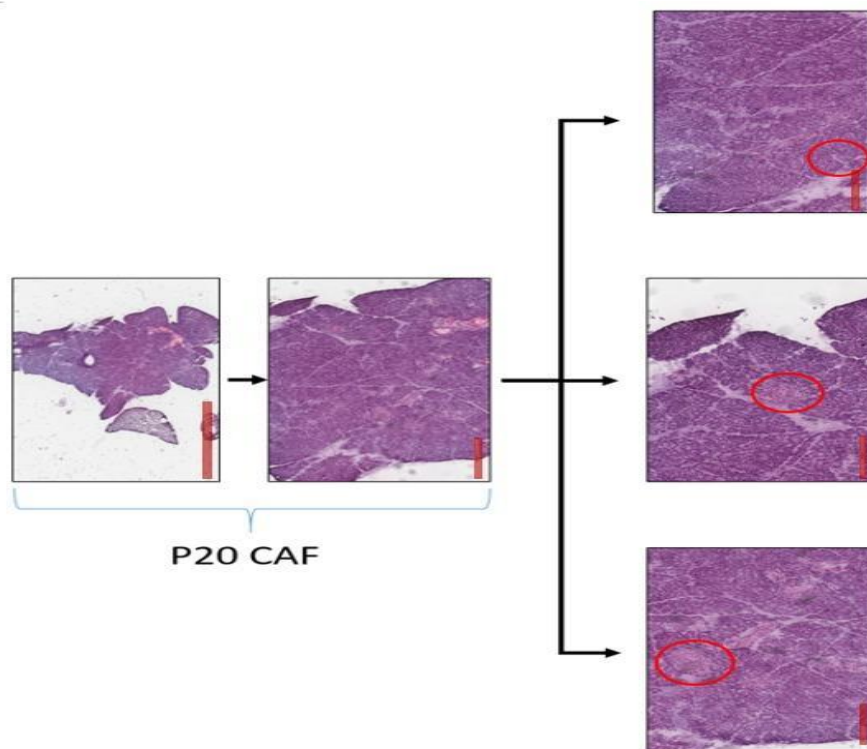


Figure 3.25. HE stained histopathological sections of 20 days offspring CAF group pancreas. Red circles indicate islet cells (n=4/rat) Scale bar; left 2mm, middle 600 μm , right 100 μm .

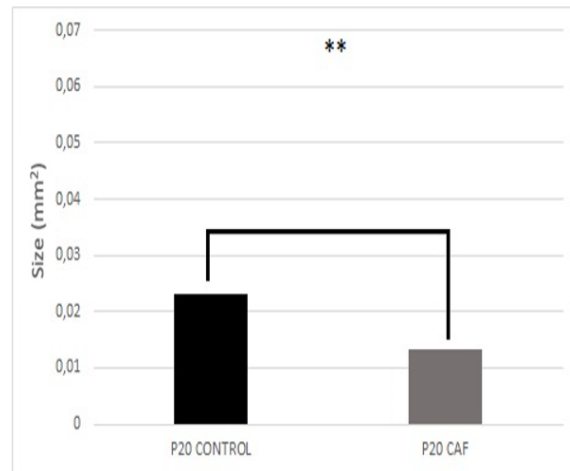


Figure 3.26. The average area of the islet cells of 20 days offspring control vs CAF groups. It was determined that the mean islet cell area was higher in the 20 days offspring control group vs. the 20 days offspring CAF group. Twenty tissue section images were evaluated for each group. The data were expressed as mean \pm SEM. *P* values were calculated by independent sample t-test (n=4) (** $p < 0.001$).

Results of images of Langerhans Islands of 90 days old offspring control (Figure 3.27) and 90 days old offspring CAF groups (Figure 3.28.) for the islet cell size were shown that islet cells of Langerhans appear to be shrunken 3 times in the 90-day old offspring CAF group (Figure 3.28) compared to the 90-day old offspring control group (Figure 3.27). Statistical analysis results of HE staining of the sections indicated in Figure 3.29, that the CAF group average islet cells area was lower (0.02 mm²) than the control group islet cells area (0.06 mm²) (** $p < 0.001$).

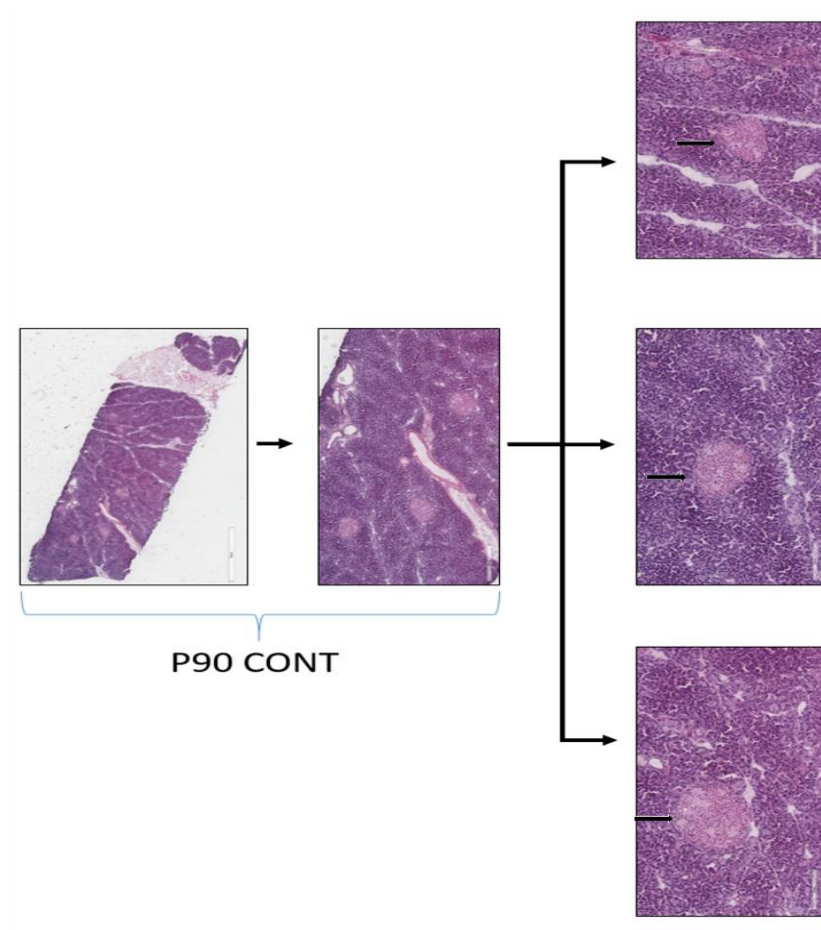


Figure 3.27. 90 days offspring control group pancreatic islet cells were stained with HE. Red circles indicate islet cells. (n=4/rat) Scale bar; left 2mm, middle 600 μm, right 100 μm.

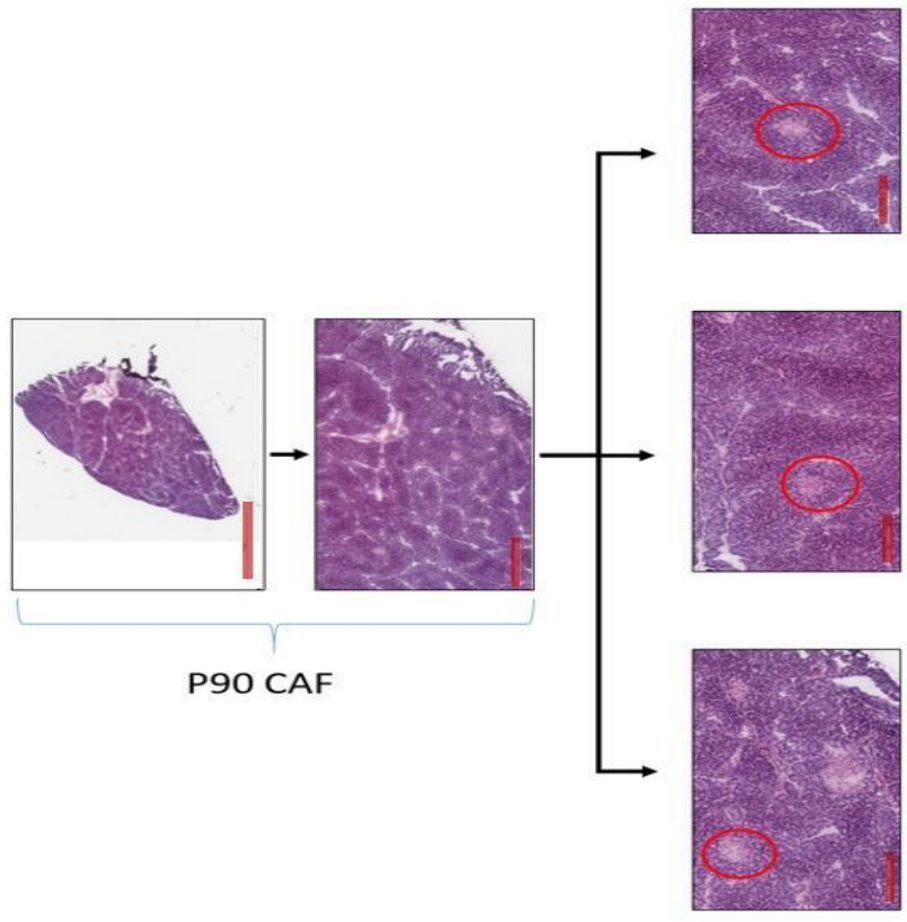


Figure 3.28. 90 days offspring CAF group pancreatic islet cells were stained with HE. Red circles indicate islet cells. (n=4/rat) Scale bar; left 2mm, middle 600 μ m, right 100 μ m.

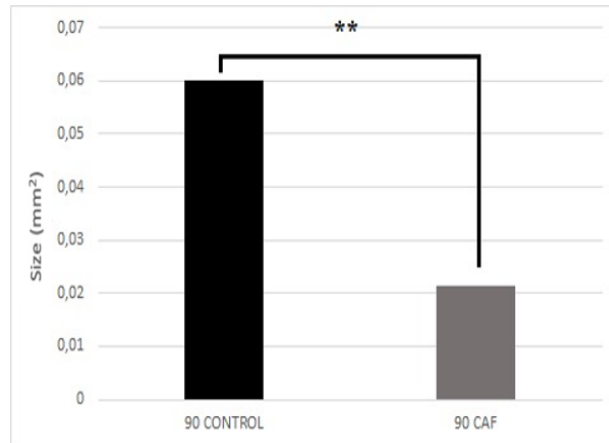


Figure 3.29. The average area of the islet cells of 90 days old offspring control vs. CAF groups. It was observed that the mean islet cell area was higher in the 90 days offspring control group compared to the 20 days offspring CAF group. 20 tissue section images were evaluated for each experimental group. The data were expressed as mean \pm SEM. *P* values were calculated by independent sample t-test (n=4/rat) ** $p < 0.001$.

HE stained islet cells in pancreatic tissue sections were shown in the mother control (Figure 3.30) and the mother CAF group (Figure 3.31). Langerhans islet cell size was not significantly different between the mother control and CAF groups. Statistical analyses of the results of staining of the groups were shown in Figure 3.29 that there was no statistically significant difference between the groups ($p > 0.05$).

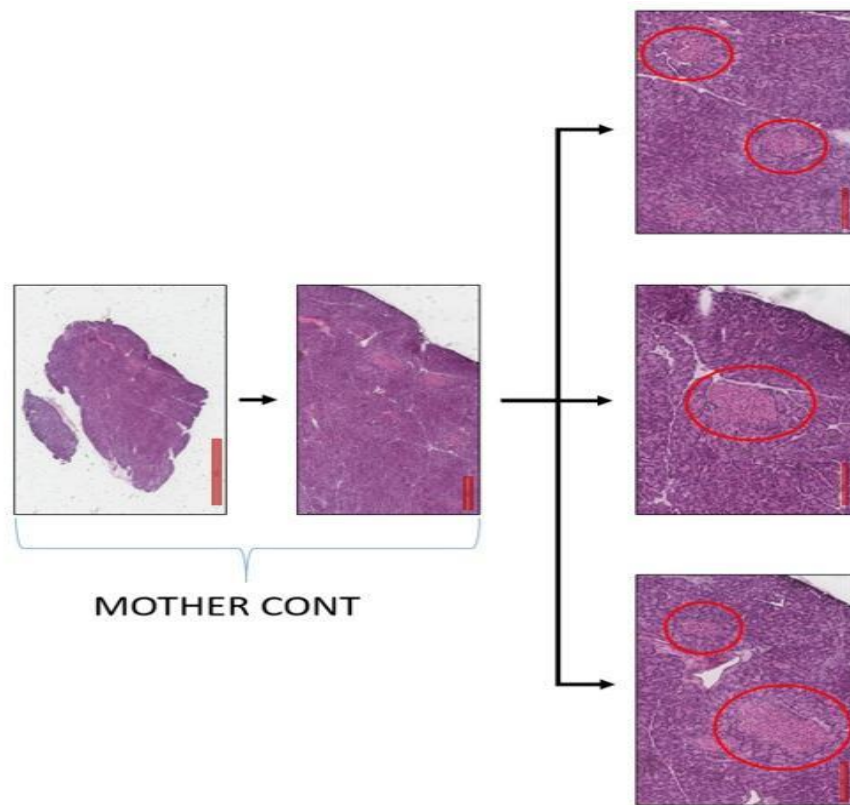


Figure 3.30. Pancreatic tissue sections of the mother control group were stained with HE. Red circles indicate islet cells (n=4/rat) Scale bar; left 2mm, middle 600 μm, right 100 μm.

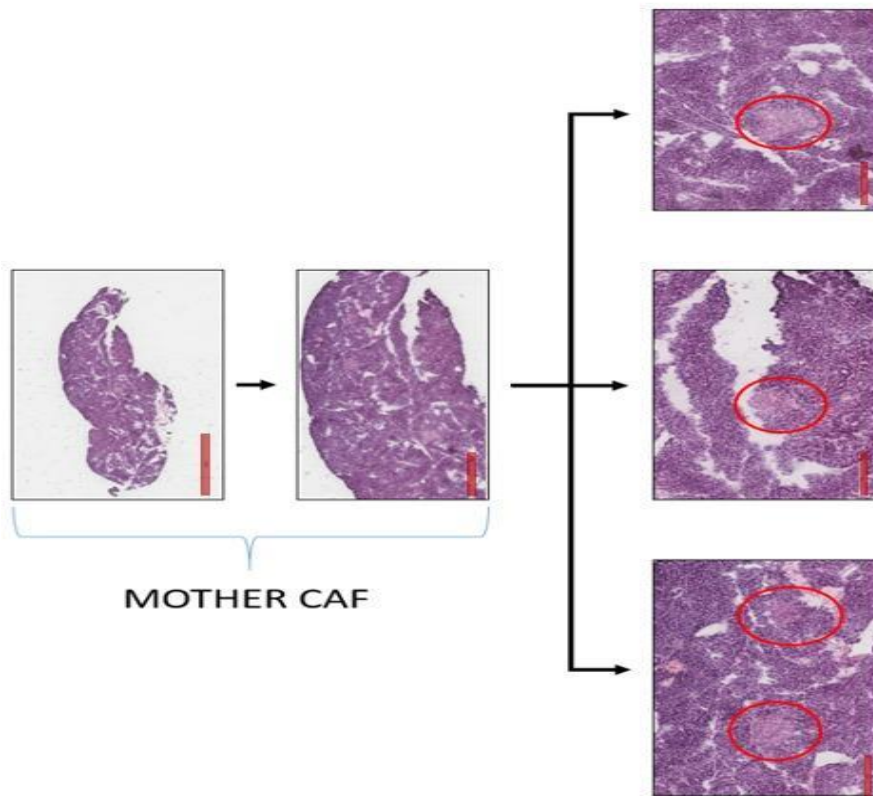


Figure 3.31. Pancreatic tissue sections of the mother control group. Sections were stained with HE. Red circles indicate islet cells. (n=4) Scale bar; left 2mm, middle 600 μm , right 100 μm .

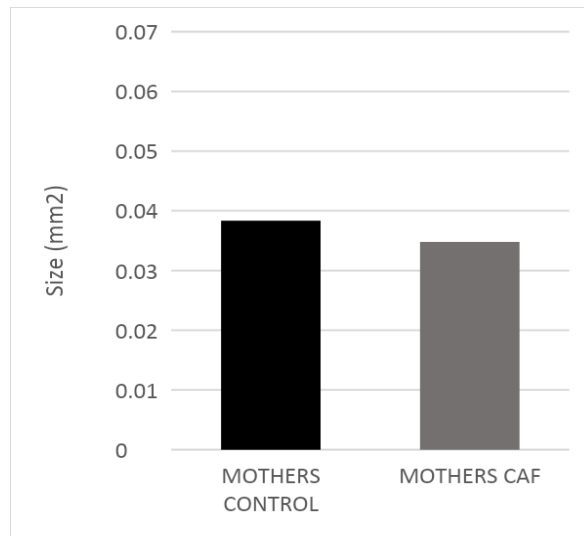


Figure 3.32. The average area of the islet cells of mother control and CAF groups. No statistical significant difference was observed between the control and CAF groups. 20 tissue section images were evaluated for each group. The data were expressed as mean \pm SEM. (n=4/rat).

3.9. Gene Expression Studies

Expression levels of differentiation marker genes for Neurog3, Pdx1, Ins2, Sst, Gcg, FoxO1, Chga, Vim were studied by RT-qPCR from frozen pancreatic tissue samples of control and CAF groups. The results were grouped according to the age of the individuals. The expression levels of the genes belonged to n=3/rat in each age group of offspring and the mother group. These gene expressions were studied for the control and CAF experimental groups and comparative analyzes were applied. RNA sample nucleic acid concentrations and absorbance ratios were noted as shown in Table 2.4. All RNA samples` 260/280 and 260/230 absorbance ratios indicated that the samples were pure and free of contaminants including gDNA or proteins, phenols or other contaminants.

3.1.1. RT-qPCR results

According to relative gene expression profiles; Neurog3, Gcg, and Vim gene expressions were upregulated in the mothers' CAF group compared to the mothers' control group. While Pdx1, Ins2, and FoxO1 gene expressions were upregulated in the mother control group compared to the mothers' CAF group (n=4/rat). Fold change analysis of the expression differences between the groups was compared and presented in Figure 3.33. As it was shown in Figure 3.33 Neurog3 (1fold), Pdx1 (2 fold), Ins2 (2 fold), FoxO1 (2 fold), Vim (0.5 fold) expressions were significantly upregulated (**** $p < 0.0001$), and Gcg (0.5 fold) gene expressions were also upregulated (** $p < 0.01$) in the mother CAF group.

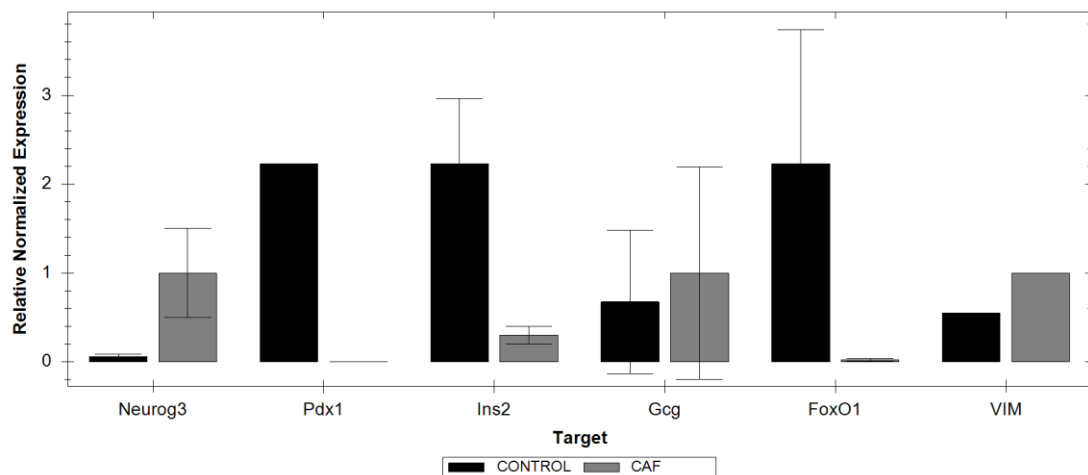


Figure 3.33. Relative normalized gene expression profiles of the mother control and CAF groups.

The values are mean \pm SEM (** $p < 0.01$, **** $p < 0.0001$) (n=3/rat).

The heatmap graph of gene expression data for the mother CAF and control groups showed that FoxO1, Ins2 and Pdx1 genes were significantly up-regulated (upper red colored blocks); while Gcg, Vim, and Neurog3 genes were down-regulated (upper green colored blocks) in the mother control group. For the mother CAF group, Gcg, Vim and Neurog3 genes were significantly up regulated (bottom red colored blocks);

while FoxO1, Ins2, and Pdx1 genes were significantly down-regulated (bottom green blocks) (Figure 3.34).

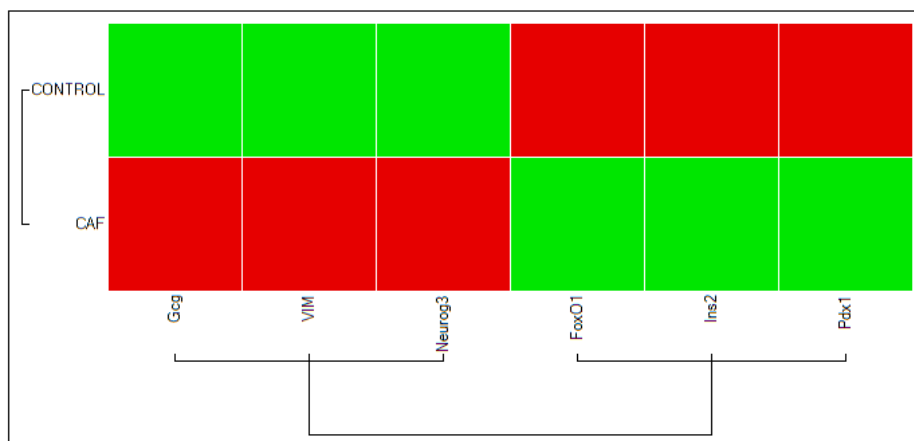


Figure 3.34. The mRNA expression profile of mothers CAF and Control groups. Genes clustered according to their expression patterns. Green: down-regulated, Red: up-regulated.

According to relative gene expression profiles, Neurog3 and Gcg gene expressions were significantly upregulated in the 0 days old offspring CAF group compared to 0 days old offspring control group. While Ins2 and FoxO1 gene expressions were up-regulated in the 0 days old offspring control group compared to the 0 days old offspring CAF group. Fold change analysis of the expression differences between the groups were compared and the heatmap (Figure 3.36) also showed that significant differences were found in Neurog3 (1.5 fold), Ins2 (0.5 fold), FoxO1 (2 fold) and Gcg (5 fold) genes between the groups (**** $p < 0.0001$) (Figure 3.35).

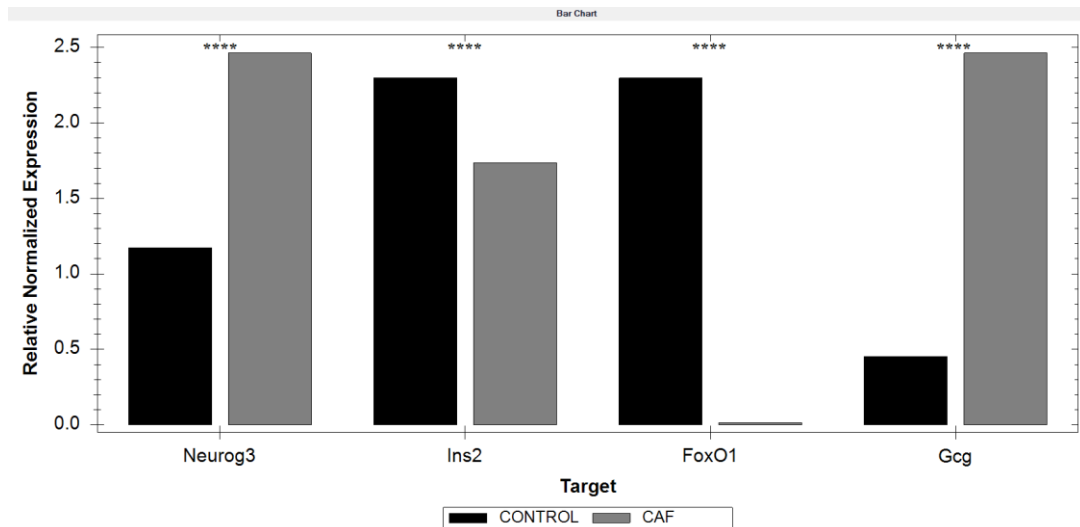


Figure 3.35. Relative normalized gene expression profiles of 0 days old offspring control and CAF groups. The values are mean \pm SEM (**** p <0.0001) (n=3/rat).

Heatmap graph of gene expression data for the 0 days offspring CAF and control groups were shown in Figure 3.36. For the CAF group, Gcg and Neurog3 genes were up regulated (upper red colored blocks); and Ins2 and FoxO1 genes were down regulated (upper green colored blocks). For the control group, Ins2 and FoxO1 genes were up regulated (bottom red colored blocks); but Gcg and Neurog3 genes were down regulated (bottom green blocks) (Figure 3.36).

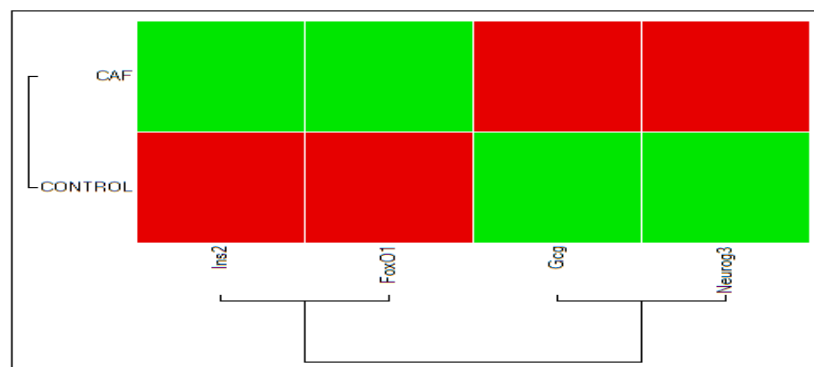


Figure 3.36. The mRNA expression profile of 0 days old offspring CAF and Control groups. Genes clustered according to their expression patterns. Green: down regulated, Red: up regulated.

According to relative gene expression profiles, Neurog3, Gcg, and Vim gene expressions were significantly upregulated in the 20 days old offspring CAF group compared to the 20 days old offspring control group. Whereas, Ins2 and FoxO1 gene expressions were down regulated in the 20 days offspring CAF group compared to the 20 days offspring control group. When those genes expression differences between the groups were compared there were statistically significant in Neurog3 (1 fold), Ins2 (2 fold), Gcg (1 fold), FoxO1 (1 fold), and Vim (0.5 fold) genes (**** $p < 0.0001$) (Figure 3.37).

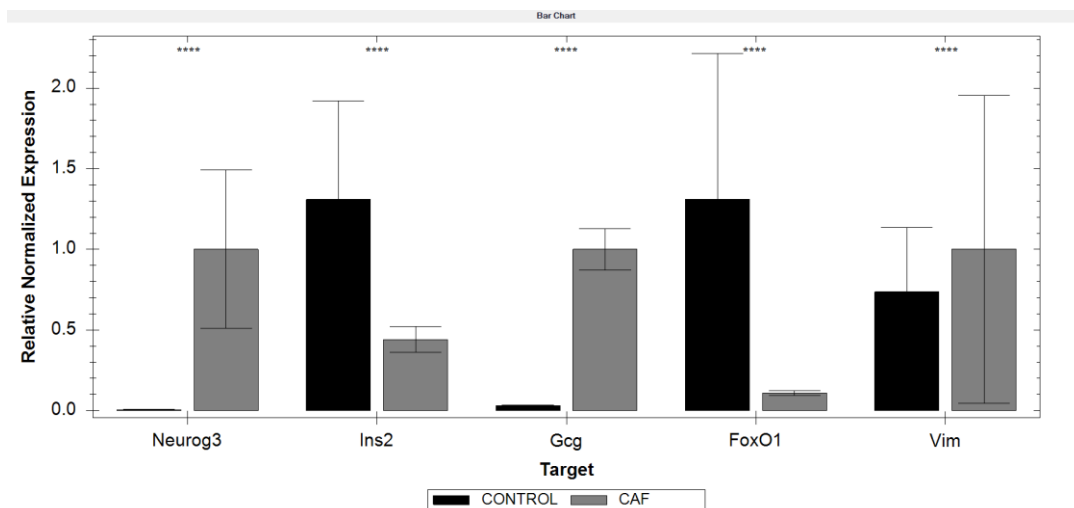


Figure 3.37. Relative normalized gene expression profiles of 20 days old offspring control and CAF groups. The values are mean \pm SEM (**** $p < 0.0001$) (n=3/rat).

A Heatmap graph of gene expression data for the 20 days old offspring CAF and control groups were shown in Figure 3.38. For the CAF group, Vim, Gcg and Neurog3 genes were up-regulated (upper red colored blocks); but Ins2 and FoxO1 genes were down-regulated (upper green colored blocks). For the control group, Ins2 and FoxO1 genes were up-regulated (bottom red colored blocks); while Vim, Gcg and Neurog3 genes were down-regulated (bottom green blocks) (Figure 3.38).

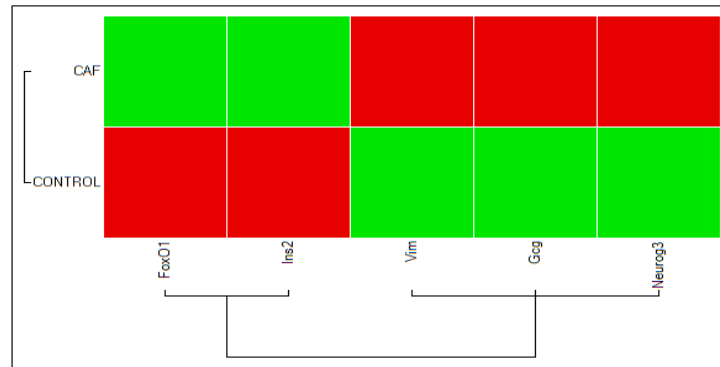


Figure 3.38 The mRNA expression profile of 20 days old offspring CAF and control groups. Genes clustered according to their expression patterns. Green: down regulated, Red: up-regulated.

According to relative gene expression profiles, Neurog3, Gcg, and Vim gene expressions were up-regulated in the 90 days old offspring CAF group compared to the 90 days old offspring control group. Ins2, Sst, and FoxO1 gene expressions were up-regulated in the 90 days offspring control group vs. 90 days old offspring CAF group. When the expression differences between the groups were compared statistically significant differences were determined in Neurog3 (1 fold) and FoxO1 (~5 fold) (**** $p < 0.0001$), Ins2 (~4 fold), Sst (~0.2 fold), and Vim (~0.2 fold) genes (* $p < 0.05$) (Figure 3.39) as indicated in the heatmap (Figure 3.40).

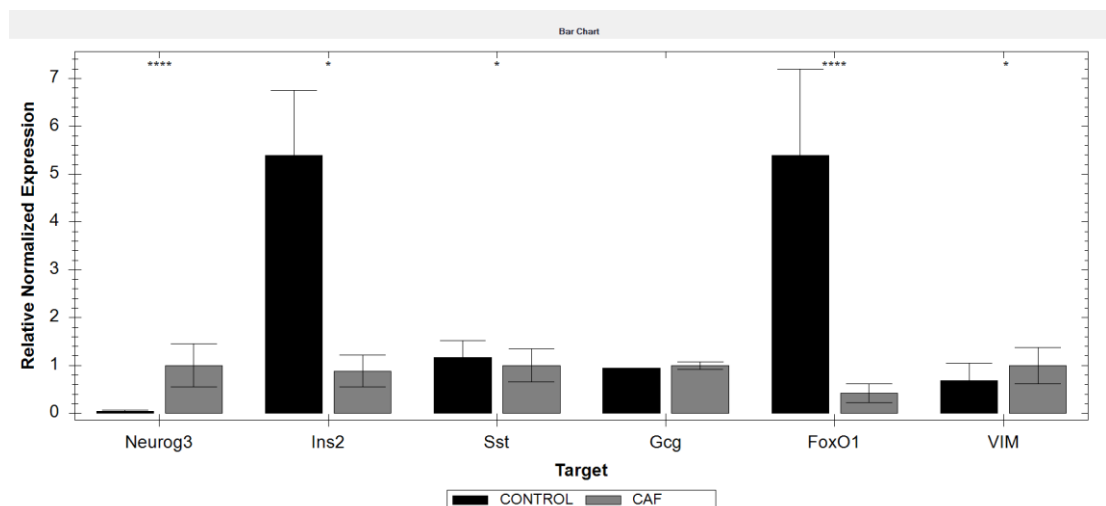


Figure 3.39. Relative normalized gene expression profiles of 90 days old offspring control and CAF groups. The values are mean \pm SEM (ns $p > 0.05$, * $p < 0.05$, **** $p < 0.0001$) (n=3/rat).

Heatmap graph of gene expression data for the 90 days old offspring CAF and control groups were shown in Figure 3.40. For the CAF group, Vim, Gcg and Neurog3 genes were up-regulated significantly (upper red colored blocks); while Ins2, FoxO1 and Sst genes were down regulated (upper green colored blocks). For the control group, Ins2, FoxO1 and Sst genes were up regulated (bottom red colored blocks) but Vim, Gcg and Neurog3 genes were down regulated (bottom green blocks) (Figure 3.40).

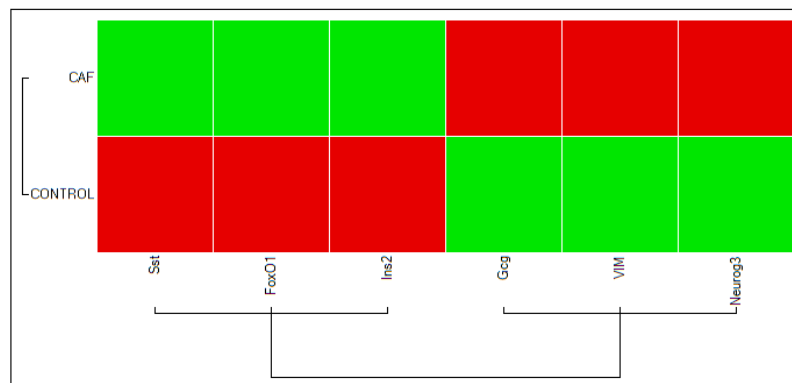


Figure 3.40. The mRNA expression profile of 90 days old offspring CAF and control groups. Genes clustered according to their expression patterns. Green: down regulated, Red: up regulated.

According to the relative gene expression profile of Chga, Chga expression was statistically significantly higher in the CAF groups of all offspring age groups compared to the control groups (**** $p < 0.0001$) (Figure 3.41).

Since Chga is an important progenitor endocrine cell marker for dedifferentiation of pancreatic beta cells in rodent diabetes (Amo-Shiinoki *et al.* 2021) it has been shown separately for all experimental groups.

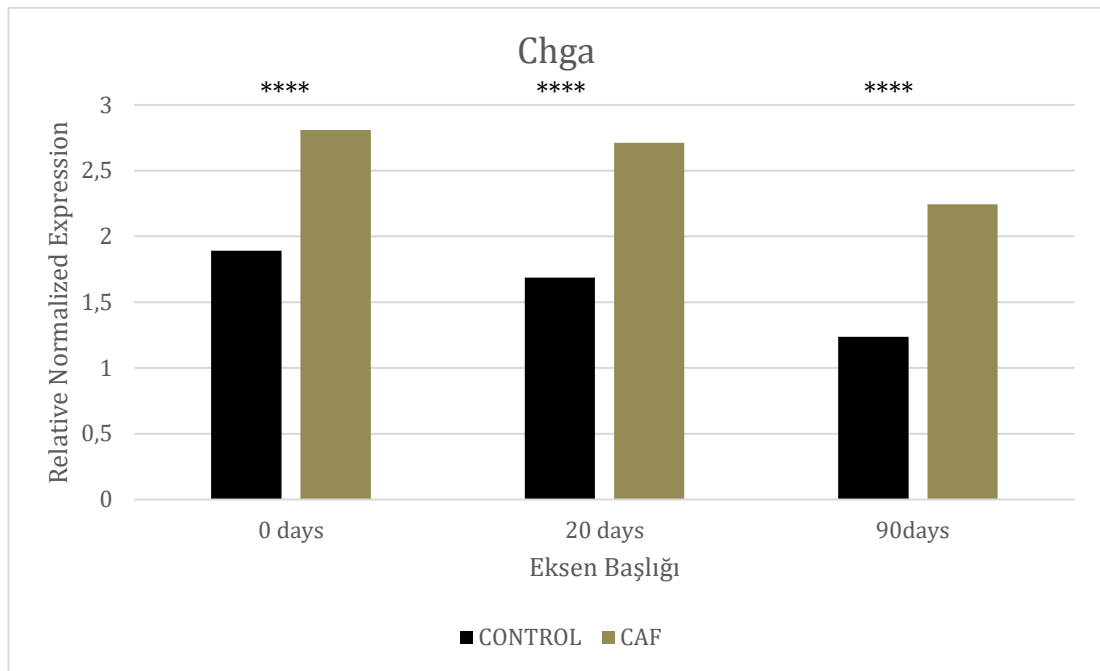


Figure 3.41. Relative gene expression profile of Chga gene. 0, 20, and 90 days old offspring control CAF groups. The values are mean \pm SEM Chga gene expression was significantly up regulated in all groups (**** $p < 0.0001$) (n=3/rat).

3.10. Transcriptome analysis - NGS-based RNA sequencing (RNA-Seq)

A comprehensive comparison of RNA-Seq-based transcriptome analysis was employed to compare 20 days and 90 days old offspring control groups vs. 20 days and 90 days old offspring CAF group pancreatic tissues. Multidimensional scaling (MDS) or Principal Component Analysis (PCA) was performed to best understand profile similarities between samples for gene expression analysis. The graph enables visualization of unsupervised similarities and differences between samples (3.42). The results indicated that there were nearly 938 genes quantitatively differing in expressions within the 20 days old two offspring groups (Figure 3.43) while there were 390 genes quantitatively differing in expressions within the 90 days old two offspring groups (Figure 3.46). Later, a volcano plot was used to define the genes in how differently

they were expressed. It showed the distribution of all genes according to their logFC and FDR (False Discovery Rate) values (Figure 3.44, Figure 3.47). The genes shown in red represent statistically significant differentially expressed genes between the two groups (Figure 3.44).

Using heat map, it was plotted that the expressions of the 50 genes that show the most differences in terms of expression between 20 and 90 days old control and CAF offspring groups (Figure 3.45).

Data on read counts were normalized, and differential expression analysis was utilized to find quantitative differences in expression levels across the experimental groups. (Figure 3.43, Figure 3.46). Depending on the functional properties of the genes for expression analysis, they were assigned to predefined terms or groups. It has been interpreted using the Gene Ontology classification system (Figure 3.49).

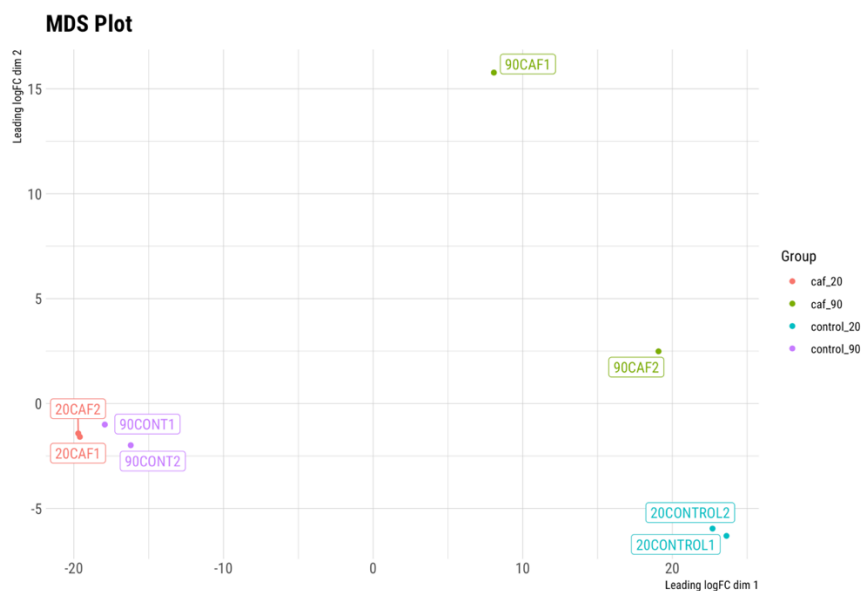


Figure 3.42 MDS plot of gene expression profiles of 20 and 90 days old offspring groups tissue samples. Samples were clustered together according to their main groups, control and CAF groups.

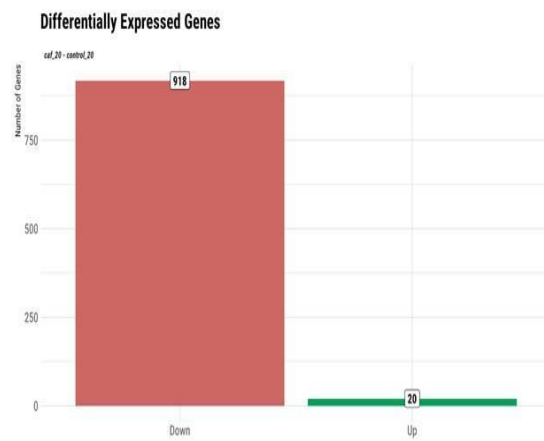


Figure 3.43 Differentially expressed genes in 20 days old offspring pancreas. The numbers of genes showing a significant increase or decrease in expression after the comparison between the groups. According to the analysis between 20 CAF and 20 control groups, expression increased in only 20 genes; but expression decreased in 918 genes in the CAF group respect to the control group.

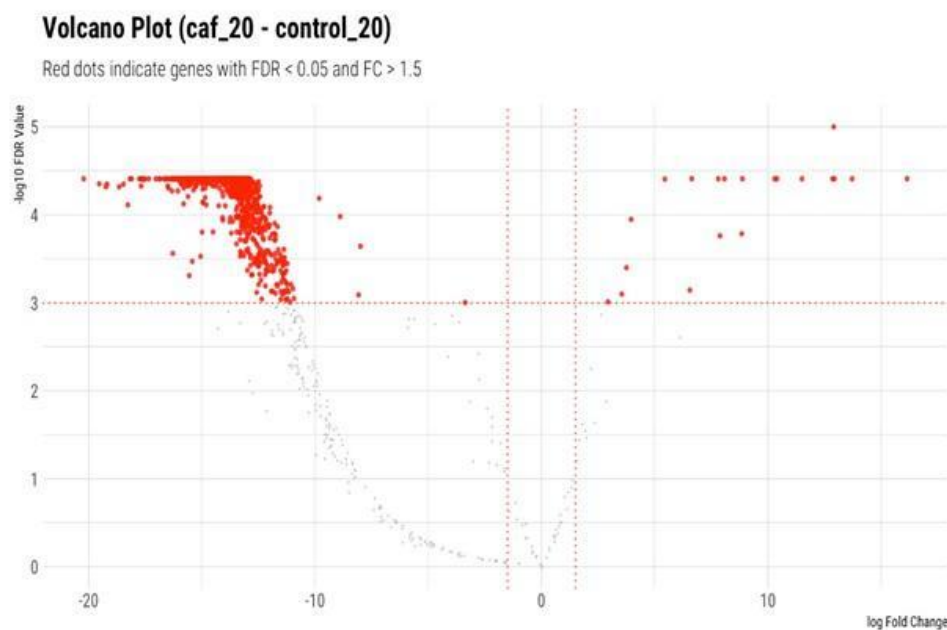


Figure 3.44 Volcano plot of 20 days old offspring pancreatic genes expressions. The graph showed the distribution of all genes according to their logFC and FDR values. Genes shown in red represent statistically significant genes between the two groups. The genes with statistically significant differences as a result of group comparison were listed according to their FDR values. The logFC value in the table shows how many folds change the gene has in the second group compared to the first group; P Value refers to the P value after the statistical analysis, and FDR refers to the False Discovery Rate value. P and FDR values were rounded up to the 5th digit.

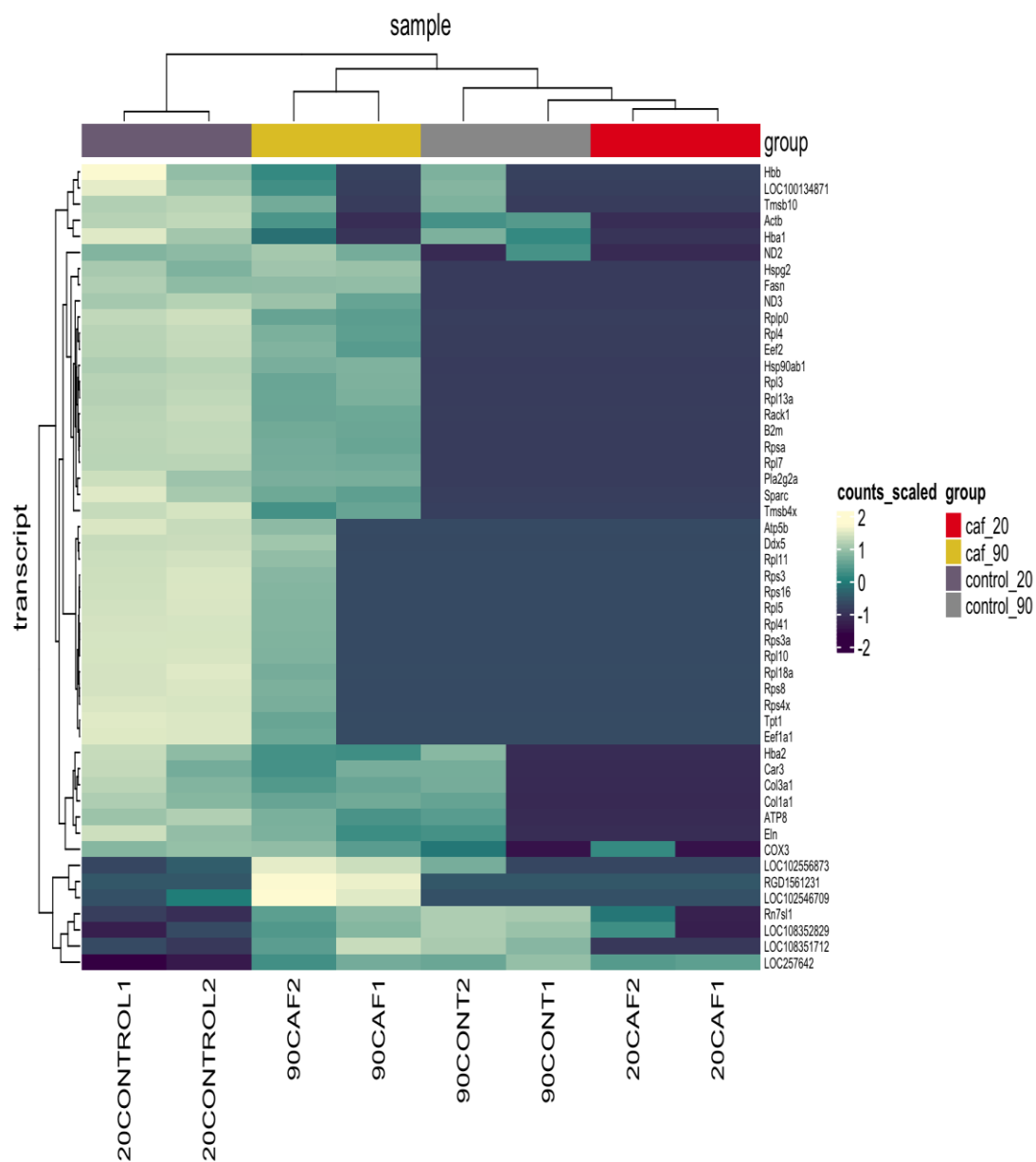


Figure 3.45 The heat map of 20 and 90 days old offspring. Shows the expressions of the 50 genes that show the most differences in terms of expression in the groups compared.

In Figure 3.48 gene ontology interpretation method used as a classification system, in which genes were assigned to predefined terms or groups depending on their functional properties. It was used to take a functional profile of these gene groups to better understand the underlying biological processes.

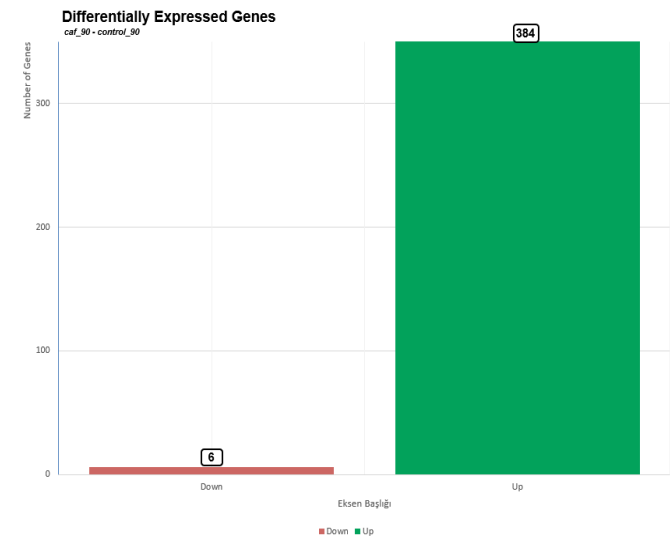


Figure 3.46 Differentially expressed genes in 90 days old offspring pancreas. The numbers of genes showing a significant increase or decrease in expression after the comparison between the groups. According to the analysis between the 90 CAF and 90 control groups, expression increased in only 384 genes; but expression decreased in 6 genes.

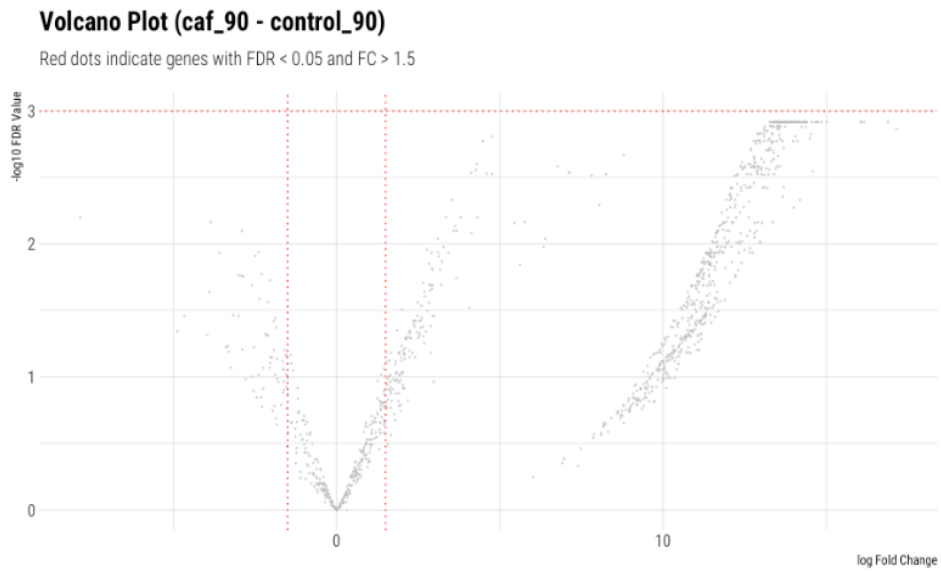


Figure 3.47 Volcano plot of 90 days old offspring pancreatic genes expressions. The graph showed the distribution of all genes according to their logFC and FDR values. Genes shown in red represent statistically significant genes between the two groups. The genes with statistically significant differences as a result of group comparison were listed according to their FDR values. The logFC value in the table shows how many fold changes the gene has in the second group compared to the first group; P Value refers to the P value after the statistical analysis, and FDR refers to the False Discovery Rate value. P and FDR values were rounded up to the 5th digit.

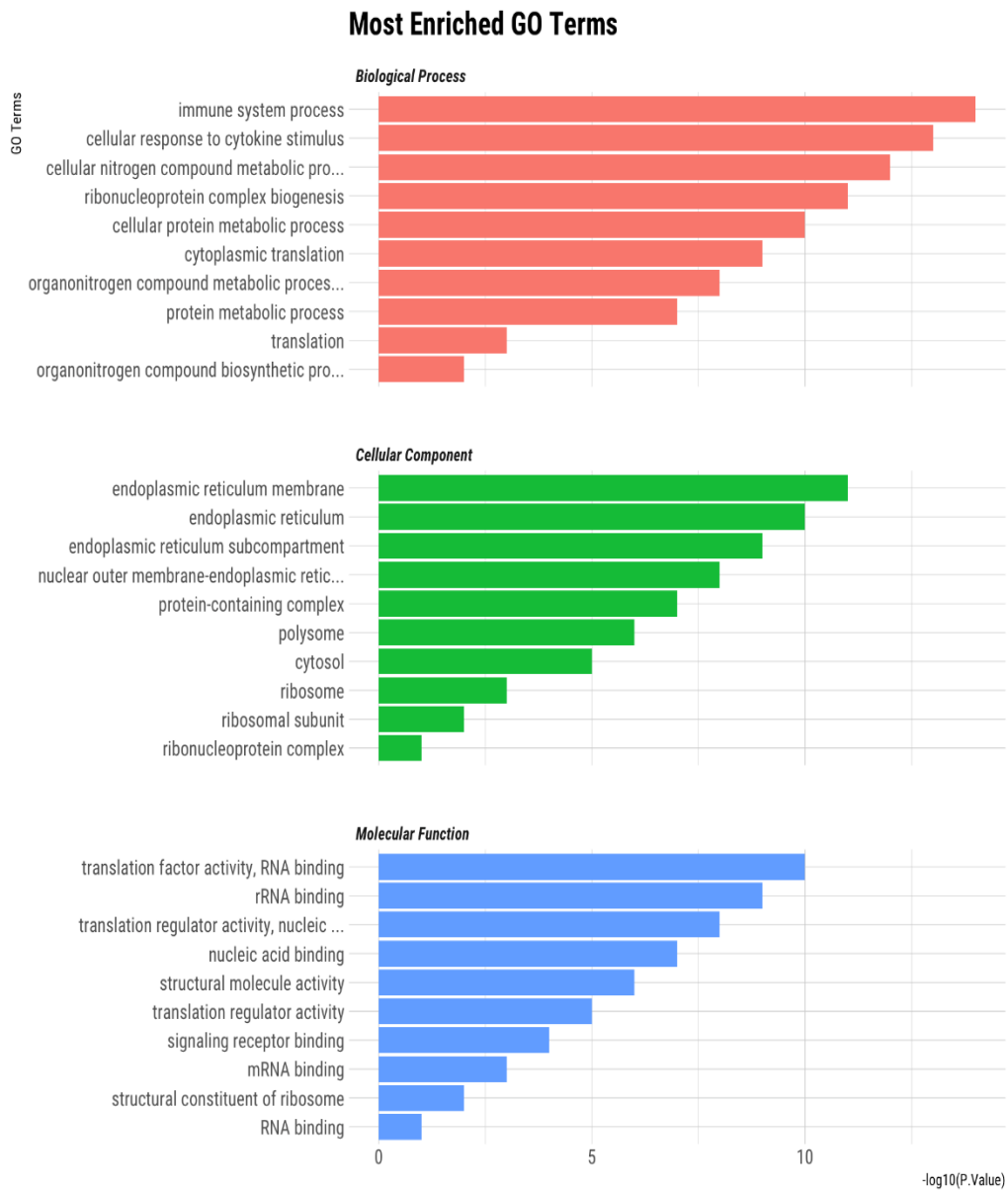


Figure 3.48 Gene Ontology (GO) enrichment analysis of the differentially expressed genes in 20 and 90 days old offspring. The numbers of enriched genes according to the (A) biological process, (B) cellular component and (C) molecular function categories.

3.11. Western Blot Analysis

In order to determine insulin protein content in the pancreatic tissues, Western blot analysis was performed using anti-insulin. Figure 3.49 showed a representative Western blot image and the densitometric analysis of insulin (12 kDa) protein levels in 20 days old offspring. The protein levels were normalized with beta actin (42 kDa) which was the internal control. The data were expressed as arbitrary units obtained by analyzing the bands using the software ImageJ. showed that there was no difference in the insulin levels in the pancreases of these groups ($p>0.05$).

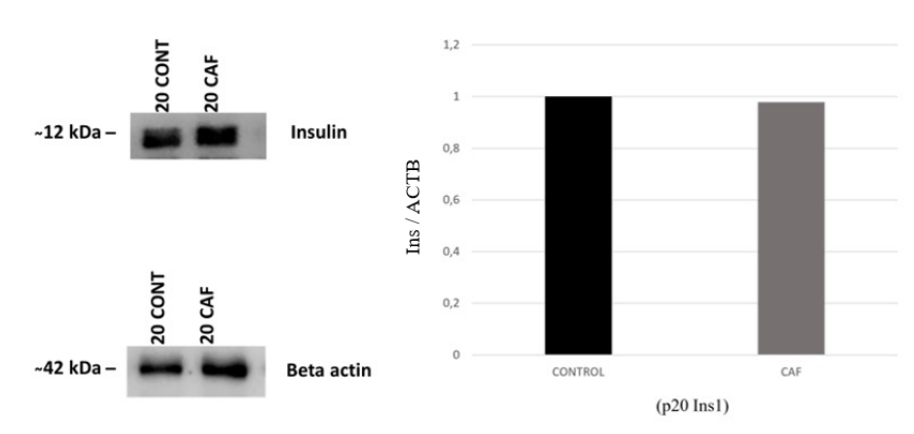


Figure 3.49. Representative image of Western blot for anti-insulin in 20 days old offspring pancreas. Thirty μg protein samples were loaded to each lane. Insulin protein levels in pancreatic tissues of 20 days old offspring control and CAF groups were obtained and anti-beta actin was used as an internal control. The quantification of immunoblots on the right (control group, $n=3$, CAF group, $n=3$, technical replicates) demonstrated that there was no statistically significant difference between the groups as data was analyzed with independent samples t-test ($p>0.05$). Values are the mean \pm SEM.

Figure 3.50 showed a representative Western blot image and the densitometric analysis of insulin protein levels in the mother and 90 days old offspring groups. The protein levels were normalized with beta actin content which was an internal control. The result is shown as arbitrary units after using ImageJ to analyze the bands. As the results indicated that both 90 days old offspring and the mother groups (n=3, technical replicates for both groups) insulin amount were significantly lowered in the CAF group vs. the control group pancreas tissues. (90 days old offspring **** $p < 0.0001$ and the mother group **** $p < 0.0001$).

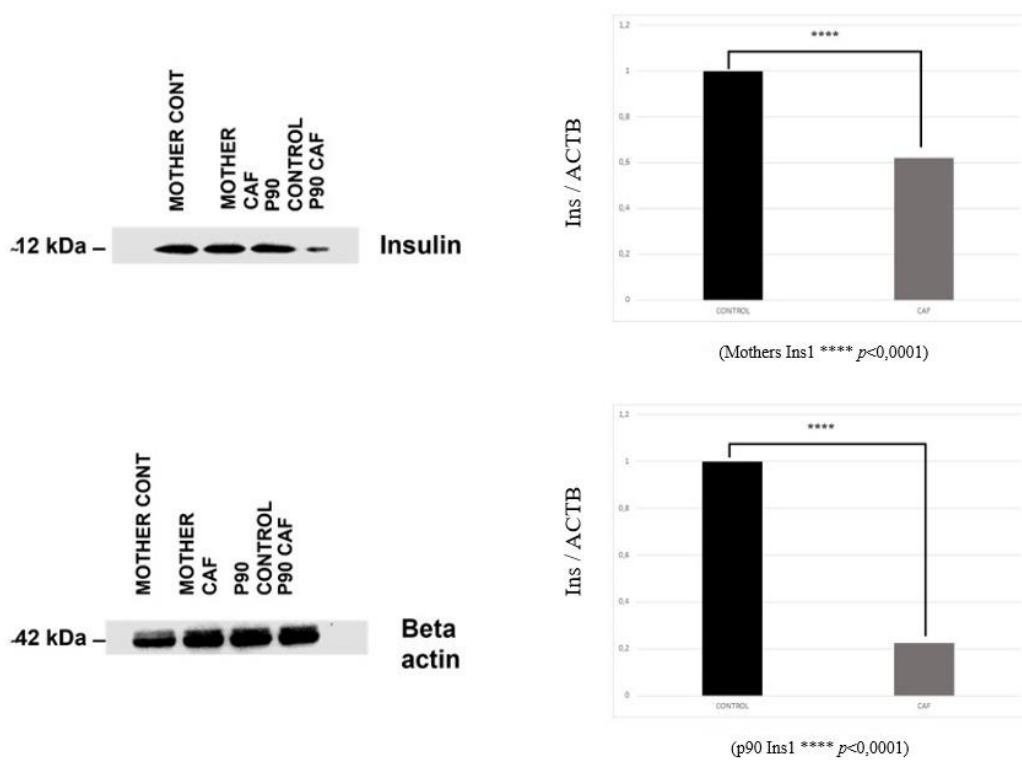


Figure 3.50 Representative image of Western blot of the mother and 90 days old offspring for anti-insulin. Thirty μg of protein was loaded onto the wells. Insulin protein levels in pancreatic tissue of the mother and 90 days old offspring control and CAF groups were measured. (Control group, n=3, CAF group, n=3 technical replicates). Data were analyzed with independent samples t-test (**** $p < 0.0001$). Each bar indicates the mean \pm SEM.

CHAPTER 4

DISCUSSION

Obesity is associated with elevated blood glucose levels and insulin resistance which is critical in defining the risk and development of T2D (Osborn & Olefsky 2012). In our study both excess weight increase as a marker of obesity and increased blood glucose levels as a marker of T2D were detected when a cafeteria diet was applied to the CAF group mothers.

Besides, the expression of glucagon hormone was assessed with IHC in mother groups, since T2D is a state of relative glucagon overproduction. As a result, more glucagon hormone expression was observed in the maternal CAF group compared to the maternal control group, thus reconfirming the diabetic status of the mother CAF group. However, it may also be an indicator of an increase in the alfa cell population which may indicate the increased beta cell dedifferentiation in T2D of these subjects.

The average body weight of 20 days old offspring of the control group was higher than the average body weight of the CAF group which was in accordance with the observations of the previous study, which reported that offspring of overweight mothers gained less weight and grew less than babies of normal-weight mothers from just after birth to three months (Ode *et al.* 2012). Also, the blood insulin levels of 20 days old offspring were higher in the control group in comparison with the CAF group which may indicate that maternal obesity influences offspring T2D susceptibility.

According to glucose stimulated insulin release test results performed with the isolated pancreatic islet cells from 20 days old and 90 days old offspring groups, it was revealed

that there was no significant difference between the control and the CAF groups of 0 and 90 days old offspring groups while 20 days offspring control group secreted insulin levels were higher in comparison with the CAF group. Likewise, these results confirm the negative effect of maternal obesity on metabolism, especially in the 20 days old offspring groups, since impaired glucose-stimulated insulin secretion is responsible for pancreatic beta cell failure and one of the major causes of developing T2D confirming the previous studies (Paul *et al.* 2022).

When morphology of islet cells` size and distributions were obtained there was a significant difference in islet size between the offspring groups. The relative frequencies of large islets ($\geq 60 \mu\text{m}$) were decreased in the CAF group consistent with previous studies done with T2D patients` samples (Clark *et al.* 1988, Deng *et al.* 2004) and our result may confirm that maternal obesity had diabetes predisposition effect on offspring from another aspect.

It was sought to determine whether decreased islet cell viability rate observed in offspring of the CAF group and decreased beta cell viability rate in 0 and 20 days old offspring groups in the CAF group would be associated with changes in islet cell composition or beta cell apoptosis. Besides, isolated islet cells of 90 days old offspring did not show a meaningful difference between the control and CAF groups in glucose stimulated insulin secretion assay. The functional stress overload on the remaining functional beta cells of the CAF group islet cells may compensate for the difference as seen in early periods of T2D (Prentki & Nolan 2006).

Beta-cell dedifferentiation to endocrine progenitor like cells under hyperglycemia induced metabolic stress conditions was an alternative proposed mechanism for diabetic loss of functional beta cell number and insulin content. To date, studies using animal experiments have found that pancreatic cells of mice exhibit a progenitor cell like character and undergo dedifferentiation in response to hyperglycemia (Talchai *et al.* 2012). In this study, according to the gene expression studies, it was observed that progenitor gene expressions like Neurogenin 3, Chromogranin A and Vimentin were up regulated in both mother and offspring CAF groups vs the control group in

accordance with previously mentioned studies (Roefs *et al.* 2017, Herold *et al.* 2018). It has also been shown in these studies that pancreatic endocrine cell subtypes, especially alpha cells, show progenitor cell characteristics in this transformation process (Cinti, *et al.* 2016) which can be also an explanatory finding for hyperglucagonemia in diabetes patients (Talchai *et al.* 2012). Therefore, pancreatic hormone gene expressions like insulin and glucagon showed that while insulin gene expression was lower in all the CAF group vs. the control group and glucagon gene expression was higher in the CAF group than the control group may explain our hypothesis. Apart from that, somatostatin gene expression level difference between the CAF and control groups may be an indicator for the cell transdifferentiation of pancreatic endocrine cells as indicated in the previous study (Piran *et al.* 2014).

In a previous study, pancreatic tissue sections of T2D patients showed a 3-fold increase in the number of Chromogranin A-positive endocrine cells (Broedbaek and Hilsted 2016). In this study, the gene expression data showed more increased levels for Chromogranin A in all ages of offspring in the CAF groups. Since Chga is a pancreatic endocrine progenitor marker like Neurog3 (Talchai *et al.* 2012), higher expression levels of Chga may indicate that offspring of the CAF group endocrine pancreatic cells may had more progenitor cell kind of character than the control group. Besides another functional pancreatic beta cell marker, Pdx1 gene expression was found higher in the mother control group than in the CAF group which may indicate the diabetic condition of the CAF group mothers. Additionally, it was also shown that mature functional pancreatic beta cell marker gene FoxO1 expression was significantly lower in the CAF groups than in the control group. FoxO1 as a transcription factor is functioning in beta cell signal integration and regulation (Kitamura *et al.* 2002; Okamoto *et al.* 2006). Since FoxO1 has been also found to determine cell fate under metabolic stress, there is an inverse relationship between FoxO1 and beta cell differentiation, and FoxO1 is required to maintain beta cell identity (Talchai *et al.* 2012). Our data indicated that FoxO1 plays a crucial role in the beta cell dedifferentiation process. According to our results, another finding was that these marker gene expression levels were significantly

different in all age groups of offspring showing that maternal obesity has a great effect on offspring's pancreas towards adulthood.

The overall transcription activity of the 20 and 90 days old offspring control and CAF groups was evaluated by next generation sequencing based on transcriptome analysis. When the genes that were expressed differently in the CAF group were examined functionally, it was shown that many genes related to metabolic stress, inflammation, and cellular dedifferentiation were differentially expressed.

When the genes showing the highest expression difference between the 20 and 90 days old offspring control and CAF groups were functionally evaluated; in mice, SPARC is necessary for maintaining glucose homeostasis and insulin secretion (Atorrasagasti *et al.* 2019), and it stimulates insulin production by reducing RGS4 protein levels in pancreatic beta cells (Hu *et al.* 2020). Bioinformatics analysis identifies TMSB4X expression as a potential T2D marker (Lu *et al.* 2020). Additionally, it has been shown that TMSB4X participates in tissue repair and inflammation, which appear to be related to the inflammatory process of metabolic syndrome (Lan *et al.* 2015). Diabetic nephropathy is aggravated by ATP5B down-regulation. In the renal tubular regions of db/db diabetic mice, ATP5B expression, histological abnormalities, and fibrosis were considerably elevated (Guan *et al.* 2005). In a mouse model of diabetes, RACK1 mRNA levels were reduced, and RACK1 is essential for controlling the IRE1alpha signaling pathway in pancreatic beta cells (Qui *et al.* 2010) FASN activity has been reported to have a considerable impact on rates of energy expenditure, fat mass, and insulin sensitivity (Menendez *et al.* 2009). Divergent protein expression with the progression of diabetes was revealed by the differential expression of Eef1a1 and Eef2 (Han *et al.* 2011). Early-stage type 2 diabetes in db/db mice exhibited as a reduction in eEF2 phosphorylation in the renal cortical homogenates (Sataranatarajan *et al.* 2007). Colla1 is the most significant gene in the extracellular matrix receptor interaction pathway and is linked to hypoglycemia. Thus, Colla1 is a new possible therapeutic target for treating T2D as a result (Lin *et al.* 2021). Under hyperglycemic/hyperinsulinemic conditions, the kidneys' mRNA expression of Col3A1 increased whereas it decreased in the heart (Gaikwad *et al.* 2010).

Besides, among the differentially expressed other genes HTT, GNAS, NCOR1, HMGN3, SIRT2, IGF1, SOX6, STAT3, SERPINH1, MVP, SIRT1, EEF1G, RPS2, Ldha, Hk1, Mylk, Igfbp4, Foxo1; in mice, the Huntington (HTT) gene has an influence on the pancreatic beta cell quality and was downregulated in dedifferentiated beta cells. (Neelankal John *et al.* 2018) In human pancreatic beta cells, the GNAS gene is a key regulator of insulin secretory ability (Taneera *et al.* 2019). An exciting therapeutic element to improve metabolic health in chronic disorders including type 2 diabetes and obesity is the NCOR-1, a transcription factor related to progenitor cell development (Jannapureddy *et al.* 2021). The pancreatic beta cells' transcriptional profile and insulin secretion are both influenced by the nucleosome binding protein HMGN3. At the Glut2 promoter, the interactions of HMGN3 and PDX1 with chromatin are strengthened by one another (Ueda *et al.* 2009). Adipocyte differentiation, fatty acid oxidation, gluconeogenesis, and insulin sensitivity are just a few of the physiological processes that the SIRT2 gene is crucial for. It also plays a role in inflammation, oxidative stress, mitochondrial function, and adipocyte differentiation. In metabolically-related tissues like skeletal muscle, SIRT2 has been found to have anti-inflammatory and anti-oxidative stress properties. It also enhances mitochondrial activity (Kitada *et al.* 2019). In mice, IGF1 increases insulin sensitivity and glucose tolerance. Impaired glucose homeostasis can result from reduced IGF1 signaling in mice caused by IGF1R gene inactivation (Hong *et al.* 2017). T2D drastically reduces the expression of Slc38a2 mRNA in human and rodent adipose tissue (Hatanaka *et al.* 2006) Both a long-term high-fat feeding in normal mice and a standard chow diet for genetically obese ob/ob mice resulted in a significant decrease in SOX6 mRNA levels (Iguchi *et al.* 2005). Through bioinformatics research coupled with validations, STAT3, SERPINH1, MVP, SIRT1, EEF1G, and RPS2 may be crucial genes in the development and prognosis of obesity (Joshi *et al.* 2021). Ldha, Hk1, Mylk, and Igfbp4 are beta cell-restricted genes, indicators of immature cells, and beta cell progenitors that do not express insulin (Nimkulrat *et al.* 2021). FoxO1 integrates insulin/hormone-dependent pathways in the pathogenesis of beta-cell stress, which is necessary to maintain beta cell identity and prevent beta cell conversion into non-beta pancreatic endocrine cells due to the same chronic metabolic stress, which

may help to explain why there is a particularly gradual loss of FoxO1 expression as diabetes progresses (Talchai *et al.*, 2012).

All those genes were down regulated in 20 days offspring CAF group respect to control group accordance with the progenitor endocrine cell character expected to observe with the effect of maternal obesity.

Similarly, SIRT2, Foxo1, EEF1G, Igfbp4, genes were down-regulated in the 90 days old offspring CAF group respected to the control group as resembling progenitor cell character while other genes like SPARC, FASN, RACK1, TMSB4X, Col1a1, Col3a1, Eef2, HTT, GNAS, NCOR1, Gnas, Stat3 are up-regulated may point out metabolic normalization with age. Since some genes were observed to have very low expression in transcriptome analysis in most of the 90 days old offspring samples, these samples may be needed to be repeated with new samples.

Western blot results for insulin protein expression showed that intracellular proinsulin levels in the mother and 90 days old offspring groups were lower in the CAF groups compared to the control groups. However, there was no difference between the CAF and control groups in the 20 days old offspring, where the effect of maternal obesity was observed more clearly according to the previous results in the study. Considering that insulin gene expression was lower in all mother and offspring CAF groups compared to the control group, and the normalization observed in the CAF group in the plasma insulin and glucose-stimulated insulin secretion levels of the 90 days old offspring, it may confirm that mature insulin secretion can occur at a certain level against insulin resistance that occurs in diabetes and prediabetes. The presence of more intracellular proinsulin in pancreatic tissue samples of the 20 days old offspring CAF group compared to the 90 days old offspring CAF group may be a sign of a defect in the insulin secretion mechanism demonstrated in T2D cases in different previous studies (Liew *et al.* 2014). Recent genome-wide association studies have discovered genes related to the processing of proinsulin, and carboxypeptidase E (CPE) plays a key role in this prohormone convertase activity. Studies on the production of insulin reveal that Cpe^{fat}/Cpe^{fat} mice had much higher levels of the insulin precursor,

proinsulin, indicating that a malfunctioning CPE impacts a proinsulin cleavage step that occurs earlier (Canaff *et al* 1999). Consistent with the results in these studies, CPE gene expression was significantly lower in the 20 days old offspring CAF group in this study compared to the control group. This showed us that a similar defect may have occurred in the intracellular insulin maturation and secretion mechanism of the 20 days old offspring group due to the intense metabolic stress caused by maternal obesity.

Epigenetic modifications presumably have a crucial role in the heritability of metabolic diseases like obesity and T2D. In particular, rodent studies showed that epigenetic mechanisms are responsible for linking maternal nutritional imbalances to the risk for T2D in adulthood (Lecoutre *et al.* 2021). Therefore, the maternal obesity effect that observed in the offspring groups in our study was most likely due to epigenetic changes such as different DNA methylation profiles and chromosome modifications passed from mother to offspring. To elucidate these inherited epigenetic mechanisms, more comprehensive studies on similar study models are required.

CHAPTER 5

CONCLUSIONS

The main aims of this study were dedifferentiation and beta cells reverting to a progenitor-like stage, and a certain part converting to other pancreatic endocrine cell types may be observed in T2D due to hyperglycemia induced chronic beta cell stress in offspring at different ages (0, 20 and 90 days old) whose mothers were obese and hyperglycemic and had never exposed to CAF diet. This could happen because stressed beta cells may lose functional beta cell markers and gain other endocrine cell markers like alpha cells. As a specific transcription factor, FoxO1 protects beta cell identity and prevents conversion into other pancreatic endocrine cells due to chronic pathophysiologic stress; hence dedifferentiation as a mechanism to protect beta cells from apoptosis by preserving them from redifferentiation under favorable metabolic conditions could be mentioned.

Besides, our study has some limitations that findings need to be interpreted carefully. Tissue samples were partially deformed due to disruptions in storage conditions and long waiting times. In addition, the inadequacy of tissue samples from offspring, especially 0 day old, showed that the size of the experimental groups should have been larger for the designed experiments.

Future studies may develop approaches to redifferentiation of dedifferentiated pancreatic beta cells into functional beta cells. This may be achieved with optimal drug therapies for T2D treatments as an effective treatment method.

REFERENCES

- Paul, A., Nath, D.P., Chatterjee, S. 2022. A minimal model of glucose-stimulated insulin secretion process explores factors responsible for the development of type 2 diabetes. *Applied Mathematical Modelling*, 108: 408-426. doi.org/10.1016/j.apm.2022.03.035
- Accili, D., Talchai, S.C., Kim-Muller, J.Y., Cinti, F., Ishida, E., Ordelheide, A.M., Kuo, T., Fan, J. & Son, J. 2016. When β -cells fail: lessons from dedifferentiation. *Diabetes, obesity & metabolism*, 18 Suppl 1(Suppl 1): 117-122. doi: 10.1111/dom.12723
- Afelik, S. & Rovira, M. 2017. Pancreatic β -cell regeneration: Facultative or dedicated progenitors? *Molecular and Cellular Endocrinology*, 445: 85-94. doi: 10.1016/j.mce.2016.11.008
- Al-Goblan, A.S., Al-Alfi, M.A. & Khan, M.Z. 2014. Mechanism linking diabetes mellitus and obesity. *Diabetes, metabolic syndrome and obesity: targets and therapy*, 7: 587-591. doi: 10.2147/DMSO.S67400
- Alvarez, M.L. & Doné, S.C. 2014. SYBR® Green and TaqMan® quantitative PCR arrays: expression profile of genes relevant to a pathway or a disease state. *Methods Mol Biol*, 1182: 321-359. doi: 10.1007/978-1-4939-1062-5_27
- Amo-Shiinoki, K., Tanabe, K., Hoshii, Y., Matsui, H., Harano, R., Fukuda, T., Takeuchi, T., Bouchi, R., Takagi, T. & Hatanaka, M. 2021. Islet cell dedifferentiation is a pathologic mechanism of long-standing progression of type 2 diabetes. *JCI insight*, 6(1). doi: 10.1172/jci.insight.143791
- Anderson, P.M. & Butcher, K.F. 2006. Childhood Obesity: Trends and Potential Causes. *The Future of children*, 16(1): 19-45. doi: 10.1353/foc.2006.0001
- Anna, V., van der Ploeg, H.P., Cheung, N.W., Huxley, R.R. & Bauman, A.E. 2008. Sociodemographic correlates of the increasing trend in prevalence of gestational diabetes mellitus in a large population of women between 1995 and 2005. *Diabetes care*, 31(12): 2288-2293. doi: 10.2337/dc08-1038
- Aronoff, S.L., Berkowitz, K., Shreiner, B. & Want, L. 2004. Glucose Metabolism and Regulation: Beyond Insulin and Glucagon. *Diabetes Spectrum*, 17(3): 183-190. doi: 10.2337/diaspect.17.3.183

- Atkinson, M.A., Bluestone, J.A., Eisenbarth, G.S., Hebrok, M., Herold, K.C., Accili, D., Pietropaolo, M., Arvan, P.R., Von Herrath, M., Markel, D.S. & Rhodes, C.J. 2011. How does type 1 diabetes develop?: the notion of homicide or β -cell suicide revisited. *Diabetes*, 60(5): 1370-1379. doi: 10.2337/db10-1797
- Back, S.H. & Kaufman, R.J. 2012. Endoplasmic reticulum stress and type 2 diabetes. *Annual review of biochemistry*, 81: 767-793.
- Bakhti, M., Böttcher, A. & Lickert, H. 2018. Modelling the endocrine pancreas in health and disease. *Nature Reviews Endocrinology*, 15(3): 155-171. doi: 10.1038/s41574-018-0132-z
- Basu, A., Dalla Man, C., Basu, R., Toffolo, G., Cobelli, C. & Rizza, R.A. 2009. Effects of type 2 diabetes on insulin secretion, insulin action, glucose effectiveness, and postprandial glucose metabolism. *Diabetes care*, 32(5): 866-872. doi: 10.2337/dc08-1826
- Benner, C., van der Meulen, T., Cacères, E., Tigyi, K., Donaldson, C.J. & Huising, M.O. 2014. The transcriptional landscape of mouse beta cells compared to human beta cells reveals notable species differences in long non-coding RNA and protein-coding gene expression. *BMC genomics*, 15(1): 620-620. doi: 10.1186/1471-2164-15-620
- Betts, J.G., Young, K.A., Wise, J.A., Johnson, E., Poe, B., Kruse, D.H., Korol, O., Johnson, J.E., Womble, M. & DeSaix, P. 2013. *Anatomy and physiology* pp.
- Brereton, M.F., Rohm, M. & Ashcroft, F.M. 2016. β -Cell dysfunction in diabetes: a crisis of identity? *Diabetes, obesity & metabolism*, 18 Suppl 1(Suppl 1): 102-109. doi: 10.1111/dom.12732
- Buettner, R., Schölmerich, J. & Bollheimer, L.C. 2007. High-fat Diets: Modeling the Metabolic Disorders of Human Obesity in Rodents*. *Obesity*, 15(4): 798-808. doi: 10.1038/oby.2007.608
- Butler, A.E., Janson, J., Bonner-Weir, S., Ritzel, R., Rizza, R.A. & Butler, P.C. 2003. β -Cell Deficit and Increased β -Cell Apoptosis in Humans with Type 2 Diabetes. *Diabetes*, 52(1): 102-110. doi: 10.2337/diabetes.52.1.102
- Cabrera, O., Berman, D.M., Kenyon, N.S., Ricordi, C., Berggren, P.-O. & Caicedo, A. 2006. The unique cytoarchitecture of human pancreatic islets has implications for islet cell function. *Proceedings of the National Academy of Sciences*, 103(7): 2334-2339.
- Campbell-Thompson, M., Fu, A., Kaddis, J.S., Wasserfall, C., Schatz, D.A., Pugliese, A. & Atkinson, M.A. 2016. Insulinitis and β -cell mass in the natural history of type 1 diabetes. *Diabetes*, 65(3): 719-731.

- Canaff, L., Bennett, H. P., & Hendy, G. N. (1999). Peptide hormone precursor processing: getting sorted? *Molecular and cellular endocrinology*, 156(1-2), 1–6. Doi: 10.1016/s0303-7207(99)00129-x
- Carter, J.D., Dula, S.B., Corbin, K.L., Wu, R. & Nunemaker, C.S. 2009. A practical guide to rodent islet isolation and assessment. *Biological procedures online*, 11: 3-31. doi: 10.1007/s12575-009-9021-0
- Chang-Chen, K.J., Mullur, R. & Bernal-Mizrachi, E. 2008. Beta-cell failure as a complication of diabetes. *Rev Endocr Metab Disord*, 9(4): 329-343. doi: 10.1007/s11154-008-9101-5
- Cinti, F., Bouchi, R., Kim-Muller, J.Y., Ohmura, Y., Sandoval, P.R., Masini, M., Marselli, L., Suleiman, M., Ratner, L.E., Marchetti, P. & Accili, D. 2016. Evidence of β -Cell Dedifferentiation in Human Type 2 Diabetes. *The Journal of clinical endocrinology and metabolism*, 101(3): 1044-1054. doi: 10.1210/jc.2015-2860
- Cito, M., Pellegrini, S., Piemonti, L. & Sordi, V. 2018. The potential and challenges of alternative sources of β cells for the cure of type 1 diabetes. *Endocrine connections*, 7(3): R114-R125. doi: 10.1530/EC-18-0012
- Clark, A., Wells, C., Buley, I., Cruickshank, J., Vanhegan, R., Matthews, D., Cooper, G., Holman, R. & Turner, R. 1988. Islet amyloid, increased A-cells, reduced B-cells and exocrine fibrosis: quantitative changes in the pancreas in type 2 diabetes. *Diabetes research (Edinburgh, Scotland)*, 9(4): 151-159.
- Clausen, T.D., Mathiesen, E.R., Hansen, T., Pedersen, O., Jensen, D.M., Lauenborg, J. & Damm, P. 2008. High Prevalence of Type 2 Diabetes and Pre-Diabetes in Adult Offspring of Women with Gestational Diabetes Mellitus or Type 1 Diabetes. *Diabetes care*, 31(2): 340-346. doi: 10.2337/dc07-1596
- Cordain, L., Eaton, S.B., Sebastian, A., Mann, N., Lindeberg, S., Watkins, B.A., O’Keefe, J.H. & Brand-Miller, J. 2005. Origins and evolution of the Western diet: health implications for the 21st century. *The American Journal of Clinical Nutrition*, 81(2): 341-354. doi: 10.1093/ajcn.81.2.341
- Costes, S., Bertrand, G. & Ravier, M.A. 2021. Mechanisms of beta-cell apoptosis in type 2 diabetes-prone situations and potential protection by GLP-1-based therapies. *International Journal of Molecular Sciences*, 22(10): 5303.
- Da Silva Xavier, G. 2018. The Cells of the Islets of Langerhans. *Journal of clinical medicine*, 7(3): 54. doi: 10.3390/jcm7030054

- Dabelea, D., Mayer-Davis, E.J., Saydah, S., Imperatore, G., Linder, B., Divers, J., Bell, R., Badaru, A., Talton, J.W., Crume, T., Liese, A.D., Merchant, A.T., Lawrence, J.M., Reynolds, K., Dolan, L., Liu, L.L., Hamman, R.F. & Study, S.f.D.i.Y. 2014. Prevalence of type 1 and type 2 diabetes among children and adolescents from 2001 to 2009. *JAMA*, 311(17): 1778-1786. doi: 10.1001/jama.2014.3201
- Davison, K.K. & Birch, L.L. 2001. Childhood overweight: a contextual model and recommendations for future research. *Obesity reviews: an official journal of the International Association for the Study of Obesity*, 2(3): 159-171. doi: 10.1046/j.1467-789x.2001.00036.x
- de Onis, M., Blössner, M. & Borghi, E. 2010. Global prevalence and trends of overweight and obesity among preschool children. *The American Journal of Clinical Nutrition*, 92(5): 1257-1264. doi: 10.3945/ajcn.2010.29786
- DeFronzo, R.A., Tripathy, D., Schwenke, D.C., Banerji, M., Bray, G.A., Buchanan, T.A., Clement, S.C., Gastaldelli, A., Henry, R.R., Kitabchi, A.E., Mudaliar, S., Ratner, R.E., Stentz, F.B., Musi, N., Reaven, P.D. & Study, A.N. 2013. Prevention of diabetes with pioglitazone in ACT NOW: physiologic correlates. *Diabetes*, 62(11): 3920-3926. doi: 10.2337/db13-0265
- Deng, S., Vatamaniuk, M., Huang, X., Doliba, N., Lian, M.-M., Frank, A., Velidedeoglu, E., Desai, N.M., Koeberlein, B. & Wolf, B. 2004. Structural and functional abnormalities in the islets isolated from type 2 diabetic subjects. *Diabetes*, 53(3): 624-632.
- Dunning, B.E. & Gerich, J.E. 2007. The Role of α -Cell Dysregulation in Fasting and Postprandial Hyperglycemia in Type 2 Diabetes and Therapeutic Implications. *Endocrine Reviews*, 28(3): 253-283. doi: 10.1210/er.2006-0026
- Eckel, R.H., Kahn, S.E., Ferrannini, E., Goldfine, A.B., Nathan, D.M., Schwartz, M.W., Smith, R.J. & Smith, S.R. 2011. Obesity and type 2 diabetes: what can be unified and what needs to be individualized? *The Journal of Clinical Endocrinology & Metabolism*, 96(6): 1654-1663.
- Evans-Molina, C., Hatanaka, M. & Mirmira, R.G. 2013. Lost in translation: endoplasmic reticulum stress and the decline of β -cell health in diabetes mellitus. *Diabetes, obesity & metabolism*, 15 Suppl 3(0 3): 159-169. doi: 10.1111/dom.12163
- Ferrannini, E. 2010. The Stunned β Cell: A Brief History. *Cell Metabolism*, 11(5): 349-352. doi: 10.1016/j.cmet.2010.04.009
- Ferrannini, E., Gastaldelli, A., Miyazaki, Y., Matsuda, M., Mari, A. & DeFronzo, R.A. 2005. β -Cell Function in Subjects Spanning the Range from Normal

Glucose Tolerance to Overt Diabetes: A New Analysis. *The Journal of Clinical Endocrinology & Metabolism*, 90(1): 493-500. doi: 10.1210/jc.2004-1133

- Flachs, P., Horakova, O., Brauner, P., Rossmeisl, M., Pecina, P., Franssen-van Hal, N., Ruzickova, J., Sponarova, J., Drahota, Z. & Vlcek, C. 2005. Polyunsaturated fatty acids of marine origin upregulate mitochondrial biogenesis and induce β -oxidation in white fat. *Diabetologia*, 48(11): 2365-2375.
- Gaikwad, A. B., Gupta, J., & Tikoo, K. 2010. Epigenetic changes and alteration of Fbn1 and Col3A1 gene expression under hyperglycaemic and hyperinsulinaemic conditions. *The Biochemical journal*, 432(2): 333–341. doi.org/10.1042/BJ20100414
- Gao, T., McKenna, B., Li, C., Reichert, M., Nguyen, J., Singh, T., Yang, C., Pannikar, A., Doliba, N., Zhang, T., Stoffers, D.A., Edlund, H., Matschinsky, F., Stein, R. & Stanger, B.Z. 2014. Pdx1 maintains β cell identity and function by repressing an α cell program. *Cell Metabolism*, 19(2): 259-271. doi: 10.1016/j.cmet.2013.12.002
- Gilbert, M. 2021. Role of skeletal muscle lipids in the pathogenesis of insulin resistance of obesity and type 2 diabetes. *Journal of Diabetes Investigation*, 12(11): 1934-1941.
- Gill, A., Kukreja, S., Malhotra, N. & Chhabra, N. 2013. Correlation of the serum insulin and the serum uric Acid levels with the glycated haemoglobin levels in the patients of type 2 diabetes mellitus. *Journal of clinical and diagnostic research: JCDR*, 7(7): 1295-1297. doi: 10.7860/JCDR/2013/6017.3121
- Guan, S. S., Sheu, M. L., Wu, C. T., Chiang, C. K., & Liu, S. H. 2015. ATP synthase subunit- β down-regulation aggravates diabetic nephropathy. *Scientific reports*, 5 :14561. doi.org/10.1038/srep14561
- Guo, S., Dai, C., Guo, M., Taylor, B., Harmon, J.S., Sander, M., Robertson, R.P., Powers, A.C. & Stein, R. 2013. Inactivation of specific β cell transcription factors in type 2 diabetes. *The Journal of clinical investigation*, 123(8): 3305-3316. doi: 10.1172/JCI65390
- Han, D., Moon, S., Kim, H., Choi, S. E., Lee, S. J., Park, K. S., Jun, H., Kang, Y., & Kim, Y. 2011) Detection of differential proteomes associated with the development of type 2 diabetes in the Zucker rat model using the iTRAQ technique. *Journal of proteome research*, 10(2): 564–577. doi.org/10.1021/pr100759a

- Haslam, D., Sattar, N. & Lean, M. 2006. ABC of obesity. Obesity--time to wake up. *BMJ (Clinical research ed.)*, 333(7569): 640-642. doi: 10.1136/bmj.333.7569.640
- Herold, Z., Doleschall, M., Kovcsdi, A., Patocs, A. & Somogyi, A. 2018. Chromogranin A and its role in the pathogenesis of diabetes mellitus. *Endokrynologia Polska*, 69(5): 598-610.
- Hong, H., Cui, Z.-Z., Zhu, L., Fu, S.-P., Rossi, M., Cui, Y.-H. & Zhu, B.-M. 2017. Central IGF1 improves glucose tolerance and insulin sensitivity in mice. *Nutrition & Diabetes*, 7(12): 2. doi: 10.1038/s41387-017-0002-0
- Hu, L., He, F., Huang, M., Zhao, Q., Cheng, L., Said, N., Zhou, Z., Liu, F., & Dai, Y. S. 2020. SPARC promotes insulin secretion through down-regulation of RGS4 protein in pancreatic β cells. *Scientific reports*, 10(1) :17581. doi.org/10.1038/s41598-020-74593-w
- Hunter, C.S. & Stein, R.W. 2017. Evidence for loss in identity, de-differentiation, and trans-differentiation of islet β -cells in type 2 diabetes. *Frontiers in genetics*, 8: 35.
- Hur, K.Y., Jung, H.S. & Lee, M.S. 2010. Role of autophagy in β -cell function and mass. *Diabetes, Obesity and Metabolism*, 12: 20-26. doi: 10.1111/j.1463-1326.2010.01278.x
- Ionescu-Tirgoviste, C., Gagniuc, P.A., Gubceac, E., Mardare, L., Popescu, I., Dima, S. & Militaru, M. 2015. A 3D map of the islet routes throughout the healthy human pancreas. *Scientific reports*, 5(1): 1-14.
- Izumi, T., Yokota-Hashimoto, H., Zhao, S., Wang, J., Halban, P.A. & Takeuchi, T. 2003. Dominant Negative Pathogenesis by Mutant Proinsulin in the Akita Diabetic Mouse. *Diabetes*, 52(2): 409-416. doi: 10.2337/diabetes.52.2.409
- Jannapureddy, S., Sharma, M., Yepuri, G., Schmidt, A.M. & Ramasamy, R. 2021. Aldose Reductase: An Emerging Target for Development of Interventions for Diabetic Cardiovascular Complications. *Frontiers in endocrinology*, 12. doi: 10.3389/fendo.2021.636267
- Jonas, J.-C., Sharma, A., Hasenkamp, W., Ilkova, H., Patanè, G., Laybutt, R., Bonner-Weir, S. & Weir, G.C. 1999. Chronic Hyperglycemia Triggers Loss of Pancreatic β Cell Differentiation in an Animal Model of Diabetes. *Journal of Biological Chemistry*, 274(20): 14112-14121. doi: 10.1074/jbc.274.20.14112
- Kahn, S.E., Haffner, S.M., Heise, M.A., Herman, W.H., Holman, R.R., Jones, N.P., Kravitz, B.G., Lachin, J.M., O'Neill, M.C., Zinman, B. & Viberti, G. 2006.

Glycemic durability of rosiglitazone, metformin, or glyburide monotherapy. *N Engl J Med*, 355(23): 2427-2443. doi: 10.1056/NEJMoa066224

Kitada, M., Ogura, Y., Monno, I. & Koya, D. 2019. Sirtuins and Type 2 Diabetes: Role in Inflammation, Oxidative Stress, and Mitochondrial Function. *Frontiers in endocrinology*, 10. doi: 10.3389/fendo.2019.00187

Kitamura, Y.I., Kitamura, T., Kruse, J.-P., Raum, J.C., Stein, R., Gu, W. & Accili, D. 2005. FoxO1 protects against pancreatic β cell failure through NeuroD and MafA induction. *Cell Metabolism*, 2(3): 153-163. doi: 10.1016/j.cmet.2005.08.004

Lan, X., Li, D., Zhong, B., Ren, J., Wang, X., Sun, Q., Li, Y., Liu, L., Liu, L., & Lu, S. 2015. Identification of differentially expressed genes related to metabolic syndrome induced with high-fat diet in E3 rats. *Experimental biology and medicine (Maywood, N.J.)*, 240(2): 235–241. doi.org/10.1177/1535370214554531

Lecoutre, S., Maqdasy, S. & Breton, C. 2021. Maternal obesity as a risk factor for developing diabetes in offspring: An epigenetic point of view. *World journal of diabetes*, 12(4): 366-382. doi: 10.4239/wjd.v12.i4.366

Lehmann, R., Zuellig, R.A., Kugelmeier, P., Baenninger, P.B., Moritz, W., Perren, A., Clavien, P.-A., Weber, M. & Spinass, G.A. 2007. Superiority of small islets in human islet transplantation. *Diabetes*, 56(3): 594-603.

Liew, C. W., Assmann, A., Templin, A. T., Raum, J. C., Lipson, K. L., Rajan, S., Qiang, G., Hu, J., Kawamori, D., Lindberg, I., Philipson, L. H., Sonenberg, N., Goldfine, A. B., Stoffers, D. A., Mirmira, R. G., Urano, F., & Kulkarni, R. N. 2014. Insulin regulates carboxypeptidase E by modulating translation initiation scaffolding protein eIF4G1 in pancreatic β cells. *Proceedings of the National Academy of Sciences of the United States of America*, 111(22): E2319–E2328. doi:10.1073/pnas.1323066111

Lin, G., Wan, X., Liu, D., Wen, Y., Yang, C., & Zhao, C. 2021. COL1A1 as a potential new biomarker and therapeutic target for type 2 diabetes. *Pharmacological research*, 165, 105436. doi.org/10.1016/j.phrs.2021.105436

Ling, C. & Rönn, T. 2019. Epigenetics in Human Obesity and Type 2 Diabetes. *Cell Metabolism*, 29(5): 1028-1044. doi:10.1016/j.cmet.2019.03.009

Lu, Y., Li, Y., Li, G., & Lu, H. 2020. Identification of potential markers for type 2 diabetes mellitus via bioinformatics analysis. *Molecular medicine reports*, 22(3), 1868–1882. doi.org/10.3892/mmr.2020.11281

- Makki, K., Froguel, P. & Wolowczuk, I. 2013. Adipose tissue in obesity-related inflammation and insulin resistance: cells, cytokines, and chemokines. *ISRN inflammation*, 2013: 139239-139239. doi: 10.1155/2013/139239
- Malterud, K. & Tonstad, S. 2009. Preventing obesity: Challenges and pitfalls for health promotion. *Patient Education and Counseling*, 76(2): 254-259. doi: 10.1016/j.pec.2008.12.012
- Marselli, L., Suleiman, M., Masini, M., Campani, D., Bugliani, M., Syed, F., Martino, L., Focosi, D., Scatena, F. & Olimpico, F. 2014. Are we overestimating the loss of beta cells in type 2 diabetes? *Diabetologia*, 57: 362-365. doi: 10.1007/s00125-013-3098-3
- Matsuda, T., Kido, Y., Asahara, S.-i., Kaisho, T., Tanaka, T., Hashimoto, N., Shigeyama, Y., Takeda, A., Inoue, T., Shibutani, Y., Koyanagi, M., Hosooka, T., Matsumoto, M., Inoue, H., Uchida, T., Koike, M., Uchiyama, Y., Akira, S. & Kasuga, M. 2010. Ablation of C/EBPbeta alleviates ER stress and pancreatic beta cell failure through the GRP78 chaperone in mice. *The Journal of clinical investigation*, 120(1): 115-126. doi: 10.1172/JCI39721
- Matveyenko, A.V. & Butler, P.C. 2008. Relationship between beta-cell mass and diabetes onset. *Diabetes, obesity & metabolism*, 10 Suppl 4(0 4): 23-31. doi: 10.1111/j.1463-1326.2008.00939.x
- Mealey, B.L. & Oates, T.W. 2006. Diabetes mellitus and periodontal diseases. *Journal of periodontology*, 77(8): 1289-1303.
- Menendez, J. A., Vazquez-Martin, A., Ortega, F. J., & Fernandez-Real, J. M. 2009. Fatty acid synthase: association with insulin resistance, type 2 diabetes, and cancer. *Clinical chemistry*, 55(3): 425-438. doi.org/10.1373/clinchem.2008.115352
- Misra, A., Gopalan, H., Jayawardena, R., Hills, A.P., Soares, M., Reza-Albarrán, A.A. & Ramaiya, K.L. 2019. Diabetes in developing countries. *Journal of diabetes*, 11(7): 522-539.
- Mitchell, N.S., Catenacci, V.A., Wyatt, H.R. & Hill, J.O. 2011. Obesity: overview of an epidemic. *The Psychiatric clinics of North America*, 34(4): 717-732. doi: 10.1016/j.psc.2011.08.005
- Morgan, D., Rebelato, E., Abdulkader, F., Graciano, M., Oliveira-Emilio, H., Hirata, A.E., Rocha, M., Bordin, S., Curi, R. & Carpinelli, A. 2009. Association of NAD (P) H oxidase with glucose-induced insulin secretion by pancreatic β -cells. *Endocrinology*, 150(5): 2197-2201.

- National Clinical Guideline, C. 2014. National Institute for Health and Care Excellence: Guidelines, Obesity: Identification, Assessment and Management of Overweight and Obesity in Children, Young People and Adults: Partial Update of CG43, National Institute for Health and Care Excellence (NICE) Copyright © National Clinical Guideline Centre, 2014., London, pp.
- Neeland, I.J., Turer, A.T., Ayers, C.R., Powell-Wiley, T.M., Vega, G.L., Farzaneh-Far, R., Grundy, S.M., Khera, A., McGuire, D.K. & de Lemos, J.A. 2012. Dysfunctional adiposity and the risk of prediabetes and type 2 diabetes in obese adults. *JAMA*, 308(11): 1150-1159.
- Neelankal John, A., Ram, R. & Jiang, F.-X. 2018. RNA-Seq Analysis of Islets to Characterise the Dedifferentiation in Type 2 Diabetes Model Mice db/db. *Endocrine Pathology*, 29(3): 207-221. doi: 10.1007/s12022-018-9523-x
- Niehoff, V. 2009. Childhood Obesity: A Call to Action. *Bariatric Nursing and Surgical Patient Care*, 4(1): 17-23. doi: 10.1089/bar.2009.9996
- Oakes, N.D., Cooney, G.J., Camilleri, S., Chisholm, D.J. & Kraegen, E.W. 1997. Mechanisms of liver and muscle insulin resistance induced by chronic high-fat feeding. *Diabetes*, 46(11): 1768-1774.
- Ode, K.L., Gray, H.L., Ramel, S.E., Georgieff, M.K. & Demerath, E.W. 2012. Decelerated early growth in infants of overweight and obese mothers. *The Journal of pediatrics*, 161(6): 1028-1034.
- Ogurtsova, K., Guariguata, L., Barengo, N.C., Ruiz, P.L.-D., Sacre, J.W., Karuranga, S., Sun, H., Boyko, E.J. & Magliano, D.J. 2022. IDF diabetes Atlas: Global estimates of undiagnosed diabetes in adults for 2021. *Diabetes research and clinical practice*, 183: 109118. doi: 10.1016/j.diabres.2021.109118
- Okamoto, H., Hribal, M.L., Lin, H.V., Bennett, W.R., Ward, A. & Accili, D. 2006. Role of the forkhead protein FoxO1 in beta cell compensation to insulin resistance. *The Journal of clinical investigation*, 116(3): 775-782. doi: 10.1172/JCI24967
- Osborn, O. & Olefsky, J.M. 2012. The cellular and signaling networks linking the immune system and metabolism in disease. *Nature medicine*, 18(3): 363-374.
- Ota, T. 2014. Obesity-induced inflammation and insulin resistance. *Frontiers in endocrinology*, 5: 204-204. doi: 10.3389/fendo.2014.00204
- Oyelade, J., Isewon, I., Oladipupo, F., Aromolaran, O., Uwoghiren, E., Ameh, F., Achas, M. & Adebisi, E. 2016. Clustering algorithms: their application to gene expression data. *Bioinformatics and Biology insights*, 10: BBI. S38316.

- Piran, R., Lee, S., Li, C., Charbono, A., Bradley, L. & Levine, F. 2014. Pharmacological induction of pancreatic islet cell transdifferentiation: relevance to type I diabetes. *Cell death & disease*, 5(7): e1357-e1357.
- Prentki, M., Matschinsky, Franz M. & Madiraju, S.R.M. 2013b. Metabolic Signaling in Fuel-Induced Insulin Secretion. *Cell Metabolism*, 18(2): 162-185. doi: 10.1016/j.cmet.2013.05.018
- Prentki, M. & Nolan, C.J. 2006. Islet beta cell failure in type 2 diabetes. *The Journal of clinical investigation*, 116(7): 1802-1812. doi: 10.1172/JCI29103
- Qiu, Y., Mao, T., Zhang, Y., Shao, M., You, J., Ding, Q., Chen, Y., Wu, D., Xie, D., Lin, X., Gao, X., Kaufman, R. J., Li, W., & Liu, Y. 2010. A crucial role for RACK1 in the regulation of glucose-stimulated IRE1alpha activation in pancreatic beta cells. *Science signaling*, 3(106): ra7. doi.org/10.1126/scisignal.2000514
- Qin, D. 2019. Next-generation sequencing and its clinical application. *Cancer biology & medicine*, 16(1): 4-10. doi: 10.20892/j.issn.2095-3941.2018.0055
- Rahier, J., Guiot, Y., Goebbels, R., Sempoux, C. & Henquin, J.-C. 2008. Pancreatic β -cell mass in European subjects with type 2 diabetes. *Diabetes, Obesity and Metabolism*, 10: 32-42.
- Rankin, M.M. & Kushner, J.A. 2010. Aging induces a distinct gene expression program in mouse islets. *Islets*, 2(6): 345-352. doi: 10.4161/isl.2.6.13376
- Rieck, S., White, P., Schug, J., Fox, A.J., Smirnova, O., Gao, N., Gupta, R.K., Wang, Z.V., Scherer, P.E., Keller, M.P., Attie, A.D. & Kaestner, K.H. 2009. The transcriptional response of the islet to pregnancy in mice. *Molecular endocrinology (Baltimore, Md.)*, 23(10): 1702-1712. doi: 10.1210/me.2009-0144
- Robertson, R.P. 2004. Chronic Oxidative Stress as a Central Mechanism for Glucose Toxicity in Pancreatic Islet Beta Cells in Diabetes. *Journal of Biological Chemistry*, 279(41): 42351-42354. doi: 10.1074/jbc.r400019200
- Roefs, M.M., Carlotti, F., Jones, K., Wills, H., Hamilton, A., Verschoor, M., Durkin, J.M.W., Garcia-Perez, L., Brereton, M.F. & McCulloch, L. 2017. Increased vimentin in human α - and β -cells in type 2 diabetes. *J Endocrinol*, 233(3): 217-227.
- Rokling-Andersen, M.H., Rustan, A.C., Wensaas, A.J., Kaalhus, O., Wergedahl, H., Røst, T.H., Jensen, J., Graff, B.A., Caesar, R. & Drevon, C.A. 2009. Marine n-3 fatty acids promote size reduction of visceral adipose depots, without

altering body weight and composition, in male Wistar rats fed a high-fat diet. *British Journal of Nutrition*, 102(7): 995-1006.

- Röder, P.V., Wu, B., Liu, Y. & Han, W. 2016. Pancreatic regulation of glucose homeostasis. *Experimental & molecular medicine*, 48(3): e219-e219. doi: 10.1038/emm.2016.6
- Sahoo, K., Sahoo, B., Choudhury, A.K., Sofi, N.Y., Kumar, R. & Bhadoria, A.S. 2015. Childhood obesity: causes and consequences. *Journal of family medicine and primary care*, 4(2): 187-192. doi: 10.4103/2249-4863.154628
- Sakata, M., Yasuda, H., Moriyama, H., Yamada, K., Kotani, R., Kurohara, M., Okumachi, Y., Kishi, M., Arai, T. & Hara, K. 2008. Prevention of recurrent but not spontaneous autoimmune diabetes by transplanted NOD islets adenovirally transduced with immunomodulating molecules. *Diabetes research and clinical practice*, 80(3): 352-359.
- Saleh, M., Gittes, G.K. & Prasad, K. 2021. Alpha-to-beta cell trans-differentiation for treatment of diabetes. *Biochem Soc Trans*, 49(6): 2539-2548. doi: 10.1042/bst20210244
- Sataranatarajan, K., Mariappan, M. M., Lee, M. J., Feliars, D., Choudhury, G. G., Barnes, J. L., & Kasinath, B. S. 2007. Regulation of elongation phase of mRNA translation in diabetic nephropathy: amelioration by rapamycin. *The American journal of pathology*, 171(6): 1733-1742. doi.org/10.2353/ajpath.2007.070412
- Satoh, T. 2014. Molecular mechanisms for the regulation of insulin-stimulated glucose uptake by small guanosine triphosphatases in skeletal muscle and adipocytes. *International Journal of Molecular Sciences*, 15(10): 18677-18692.
- Schaffer, A.E., Taylor, B.L., Benthuyzen, J.R., Liu, J., Thorel, F., Yuan, W., Jiao, Y., Kaestner, K.H., Herrera, P.L., Magnuson, M.A., May, C.L. & Sander, M. 2013. Nkx6.1 controls a gene regulatory network required for establishing and maintaining pancreatic Beta cell identity. *PLoS genetics*, 9(1): e1003274-e1003274. doi: 10.1371/journal.pgen.1003274
- Schwimmer, J.B. 2003. Health-Related Quality of Life of Severely Obese Children and Adolescents. *JAMA*, 289(14): 1813. doi: 10.1001/jama.289.14.1813
- Skyler, J.S., Bakris, G.L., Bonifacio, E., Darsow, T., Eckel, R.H., Groop, L., Groop, P.-H., Handelsman, Y., Insel, R.A., Mathieu, C., McElvaine, A.T., Palmer, J.P., Pugliese, A., Schatz, D.A., Sosenko, J.M., Wilding, J.P.H. & Ratner, R.E. 2017. Differentiation of Diabetes by Pathophysiology, Natural History, and Prognosis. *Diabetes*, 66(2): 241-255. doi: 10.2337/db16-0806

- Spijker, H.S., Song, H., Ellenbroek, J.H., Roefs, M.M., Engelse, M.A., Bos, E., Koster, A.J., Rabelink, T.J., Hansen, B.C., Clark, A., Carlotti, F. & de Koning, E.J.P. 2015. Loss of β -Cell Identity Occurs in Type 2 Diabetes and Is Associated with Islet Amyloid Deposits. *Diabetes*, 64(8): 2928-2938. doi: 10.2337/db14-1752
- Stanger, B.Z., Tanaka, A.J. & Melton, D.A. 2007. Organ size is limited by the number of embryonic progenitor cells in the pancreas but not the liver. *Nature*, 445(7130): 886-891.
- Steiner, D.J., Kim, A., Miller, K. & Hara, M. 2010. Pancreatic islet plasticity: interspecies comparison of islet architecture and composition. *Islets*, 2(3): 135-145.
- Stenström, G., Gottsäter, A., Bakhtadze, E., Berger, B. & Sundkvist, G.r. 2005. Latent Autoimmune Diabetes in Adults. *Diabetes*, 54(suppl_2): S68-S72. doi: 10.2337/diabetes.54.suppl_2.s68
- Swisa, A., Glaser, B. & Dor, Y. 2017b. Metabolic Stress and Compromised Identity of Pancreatic Beta Cells. *Frontiers in genetics*, 8: 21-21. doi:10.3389/fgene.2017.00021
- Talchai, C., Xuan, S., Lin, H.V., Sussel, L. & Accili, D. 2012. Pancreatic β cell dedifferentiation as a mechanism of diabetic β cell failure. *Cell*, 150(6): 1223-1234. doi: 10.1016/j.cell.2012.07.029
- Taneera, J., Dhaiban, S., Mohammed, A.K., Mukhopadhyay, D., Aljaibeji, H., Sulaiman, N., Fadista, J. & Salehi, A. 2019. GNAS gene is an important regulator of insulin secretory capacity in pancreatic β -cells. *Gene*, 715: 144028.
- Teker, H.T. 2014. Effect of maternal high fat diet on hypothalamus vacuolization of their offspring. MSc Thesis, Department of Biological Sciences, Middle East Technical University.
- Teta, M., Rankin, M.M., Long, S.Y., Stein, G.M. & Kushner, J.A. 2007. Growth and regeneration of adult β cells does not involve specialized progenitors. *Developmental cell*, 12(5): 817-826.
- Ueda, T., Furusawa, T., Kurahashi, T., Tessarollo, L. & Bustin, M. 2009. The nucleosome binding protein HMGN3 modulates the transcription profile of pancreatic beta cells and affects insulin secretion. *Molecular and cellular biology*, 29(19): 5264-5276. doi: 10.1128/MCB.00526-09

- van der Meulen, T. & Huising, M.O. 2015. Role of transcription factors in the transdifferentiation of pancreatic islet cells. *Journal of Molecular Endocrinology*, 54(2): R103-R117. doi: 10.1530/JME-14-0290
- van Haeften, T.W., Pimenta, W., Mitrakou, A., Korytkowski, M., Jenssen, T., Yki-Jarvinen, H. & Gerich, J.E. 2000. Relative contributions of β -cell function and tissue insulin sensitivity to fasting and postglucose-load glycemia. *Metabolism*, 49(10): 1318-1325. doi: 10.1053/meta.2000.9526
- Wajchenberg, B.L. 2007. β -Cell Failure in Diabetes and Preservation by Clinical Treatment. *Endocrine Reviews*, 28(2): 187-218. doi: 10.1210/10.1210/er.2006-0038
- Wali, J.A., Jarzebska, N., Raubenheimer, D., Simpson, S.J., Rodionov, R.N. & O'Sullivan, J.F. 2020. Cardio-metabolic effects of high-fat diets and their underlying mechanisms—A narrative review. *Nutrients*, 12(5): 1505.
- Wang, Z., York, N.W., Nichols, C.G. & Remedi, M.S. 2014. Pancreatic β cell dedifferentiation in diabetes and redifferentiation following insulin therapy. *Cell Metabolism*, 19(5): 872-882. doi: 10.1016/j.cmet.2014.03.010
- Weinberg, N., Ouziel-Yahalom, L., Knoller, S., Efrat, S. & Dor, Y. 2007. Lineage Tracing Evidence for In Vitro Dedifferentiation but Rare Proliferation of Mouse Pancreatic β -Cells. *Diabetes*, 56(5): 1299-1304. doi: 10.2337/db06-1654
- Weyer, C., Bogardus, C., Mott, D.M. & Pratley, R.E. 1999. The natural history of insulin secretory dysfunction and insulin resistance in the pathogenesis of type 2 diabetes mellitus. *The Journal of clinical investigation*, 104(6): 787-794. doi: 10.1172/JCI7231
- White, M.G., Marshall, H.L., Rigby, R., Huang, G.C., Amer, A., Booth, T., White, S. & Shaw, J.A.M. 2013. Expression of mesenchymal and α -cell phenotypic markers in islet β -cells in recently diagnosed diabetes. *Diabetes care*, 36(11): 3818-3820. doi: 10.2337/dc13-0705
- WHO, W.H.O. 2016. Consideration of the evidence on childhood obesity for the Commission on Ending Childhood Obesity: report of the ad hoc working group on science and evidence for ending childhood obesity, Geneva, Switzerland.
- WHO, W.H.O. 2022. (Web page: www.who.int/en/news-room/factsheets/detail/obesity-and-overweight) (Date accessed: 4 June).

- Wu, H., Patterson, C.C., Zhang, X., Ghani, R.B.A., Magliano, D.J., Boyko, E.J., Ogle, G.D. & Luk, A.O. 2022. Worldwide estimates of incidence of type 2 diabetes in children and adolescents in 2021. *Diabetes research and clinical practice*, 185: 109785.
- Yoon, K.H., Ko, S.H., Cho, J.H., Lee, J.M., Ahn, Y.B., Song, K.H., Yoo, S.J., Kang, M.I., Cha, B.Y., Lee, K.W., Son, H.Y., Kang, S.K., Kim, H.S., Lee, I.K. & Bonner-Weir, S. 2003. Selective β -Cell Loss and α -Cell Expansion in Patients with Type 2 Diabetes Mellitus in Korea. *The Journal of Clinical Endocrinology & Metabolism*, 88(5): 2300-2308. doi: 10.1210/jc.2002-020735
- Zimmermann, E., Gamborg, M., Sørensen, T.I.A. & Baker, J.L. 2015. Sex Differences in the Association Between Birth Weight and Adult Type 2 Diabetes. *Diabetes*, 64(12): 4220-4225. doi: 10.2337/db15-0494

APPENDICES

APPENDIX A

PRIMERS, TaqMan™ PROBES, RT-PCR CURVES and GENE EXPRESSION DATA TABLES

Figure A.1. Primers and TaqMan probes used in qRT-PCR (RP: reverse primer, FP: forward primer)

Primer - Probe Code	Nucleotide sequence (5'-3')	Base Range	T_m	GenBank Number
NeuroG3 F	GACCTCTAAGTCAGAGACTGTCACA	405-429	54,8°C	NM_021700
NeuroG3 S	CATTTTTTCCCAACCTCAGGA	439-459	57,0°C	NM_021700
NeuroG3 A	TTCGTGGTCCGAGGCTC	542-526	56,9°C	NM_021700
NeuroG3 R	GTGGGGTGGAATTGGA ACT	567-549	56,3°C	NM_021700
NeuroG3 TM (FAM)	F-CCCAAGAGACCCAGCAACCCTTT-Q	499-521	65,6°C	NM_021700
Pdx1 F	TCACGCGTGGAAAAGCCA	481-498	60,9°C	NM_022852

Pdx1 S	GCCAGTGGGCAGGAGGT	495-511	59,7°C	NM_022852
Pdx1 A	CCAGATTTTGATGTGTCTCTCAGTCAA	679-653	59,5°C	NM_022852
Pdx1 R	TTTCTTCCACTTCATGCGACG	709-689	59,0°C	NM_022852
Pdx1 TM (FAM)	F- TACGCAGCAGAACCGGAGGAGAATAAG AG-Q	515-543	67,6°C	NM_022852
Ins2 F	GACCCACAAGTGGCACA	235-251	54,3°C	NM_019130
Ins2 S	ACCCACAAGTGGCACAAC	236-253	55,8°C	NM_019130
Ins2 A	AGAGCAGATGCTGGTGCAG	360-342	56,9°C	NM_019130
Ins2 R	GCAGAGGGGTGGACAGG	419-403	57,1°C	NM_019130
Ins2 TM (FAM)	F-CACGATGCCGCGTTCTGC-Q	333-315	66,8°C	NM_019130
Sst F	CCACCGGGAAACAGGAAC	275-292	58,1°C	NM_012659
Sst S	CCACCGGGAAACAGGAA	275-291	56,8°C	NM_012659
Sst A	CTCCAGGGCATCGTTCTCT	357-339	56,6°C	NM_012659
Sst R	CATCTCGTCCTGCTCAGCT	396-378	55,5°C	NM_012659
Sst TR (FAM)	F-AACTGCTGTCCGAGCCCAACC-Q	314-334	65,0°C	NM_012659
GcG F	CTCAGTCCCACAAGGCAGA	38-56	56,3°C	NM_012707
GcG S	CAGTCCCACAAGGCAGAATAA	40-60	56,2°C	NM_012707

GcG A	CGTTCTCCTCCGTGTCTTGA	152-133	57,3°C	NM_012707
GcG R	CTGGAAGCTGGGAATGAT	175-157	55,8°C	NM_012707
GcG TM (FAM)	F- AATGAAGACCGTTTACATCGTGGCTGG- Q	64-90	66,6°C	NM_012707
Foxo1 F	GGAGAAGAGGCTCACCCCTG	618-636	56,4°C	AF114258
Foxo1 S	GATCTACGAGTGGATGGTGAAGAG	642-665	56,6°C	AF114258
Foxo1 A	GGGACAGATTGTGGCGAA	742-725	56,2°C	AF114258
Foxo1 R	GTTCCTTCATTCTGTA CTGAATAAACT	779-752	56,9°C	AF114258
Foxo1 TM (FAM)	F-ACAGCAACAGCTCGGCGGG-Q	692-710	66,4°C	AF114258
Vim F	CAGAGGGAGGAAGCCGAG	663-680	57,4°C	NM_031140
Vim S	CACCCTGCAGTCATTCAGAC	683-702	55,3°C	NM_031140
Vim A	GATTCCACTTTACGTTCAAGGTC	757-735	55,3°C	NM_031140
Vim R	GATCTCTTCATCGTGCAGCT	806-787	53,6°C	NM_031140
Vim TM (HEX)	ATGTTGACAATGCTTCTCTGGCACG	730-706	64,3°C	NM_031140
18S F	CGGCTACCACATCCAAGGAA	453-472	59,2°C	ratK01593
18S R	GCTGGAATTACCGCGGCT	639-622	60,1°C	ratK01593

18S TM (FAM)	F-CGCAAATTACCCACTCCCGACCC-Q	484-506	68,2°C	ratK01593
---------------------	-----------------------------	---------	--------	-----------

991159	18s rRNA		ratK01593	Tm
18S F	CggCTACCACATCCAaggAA	S	453-472	59,2°C
18S R	gCTggAATTACCgCggCT	A	639-622	60,1°C
18S_TM	F-CgCAAATTACCCACTCCCGACCC--Q	S	484-506	68,2°C

Figure A.2. 18s rRNA primer and probe sequences

991159	rat Foxo1, cDNA		AF114258	Tm
Foxo1 F	ggAgAAgAggCTCACCCCTg	S	618-636	56,4°C
Foxo1 S	gATCTACgAgTggATggTgAAgAg	S	642-665	56,6°C
Foxo1 A	gggACAgATTgTggCgAA	A	742-725	56,2°C
Foxo1 R	gTTCCTTCATTCTgTACTCgAATAAACT	A	779-752	56,9°C
Foxo1 TM	F-ACAgCAACAgCTCggCggg--Q	S	692-710	66,4°C

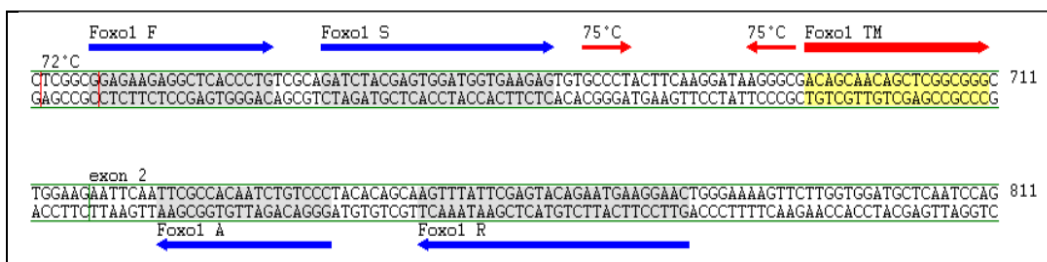


Figure A.3. Foxo1 primer and probe sequences

991159	rat Glucagon, cDNA		NM_012707	Tm
Gcg F	CTCAgTCCCACAAGgCAgA	S	38-56	56,3°C
Gcg S	CAgTCCCACAAGgCAgAATAA	S	40-60	56,2°C
Gcg A	CgTTCTCCTCCgTgTCTTgA	A	152-133	57,3°C
Gcg R	CTgggAAgCTgggAAgAT	A	175-157	55,8°C
Gcg TM	F-AATgAAgACCgTTTACATCgTggCTgg--Q	S	64-90	66,6°C

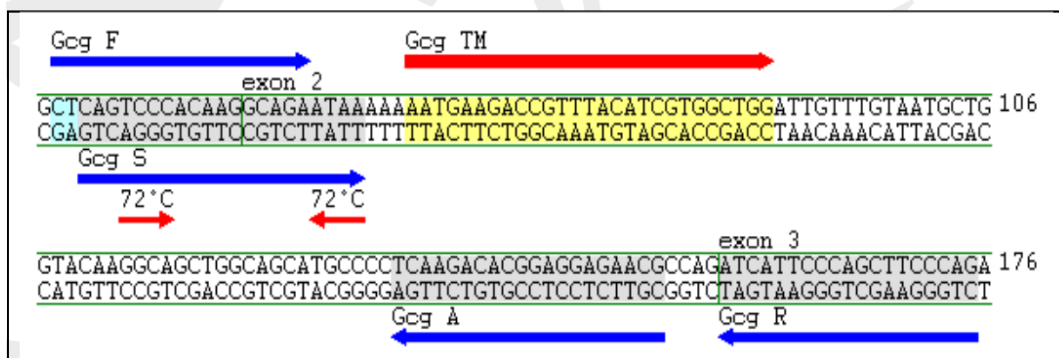


Figure A.4. Gcg primer and probe sequences

991159	rat Insulin II cDNA		NM_019130	Tm
Ins2 F	gACCCACAAGTggCACA	S	235-251	54,3°C
Ins2 S	ACCCACAAGTggCACAAC	S	236-253	55,8°C
Ins2 A	AgAgCAgATgCTggTgCAg	A	360-342	56,9°C
Ins2 R	gCAgAggggTggACAgg	A	419-403	57,1°C
Ins2 TM	F-CACgATgCCgCgCTTCTgC--Q	A	333-315	66,8°C

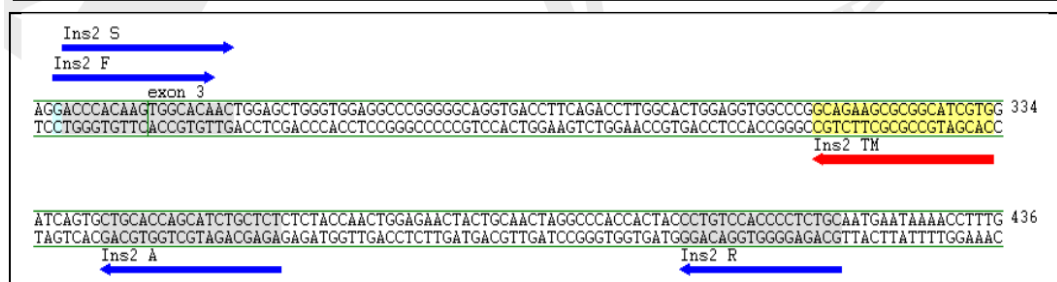
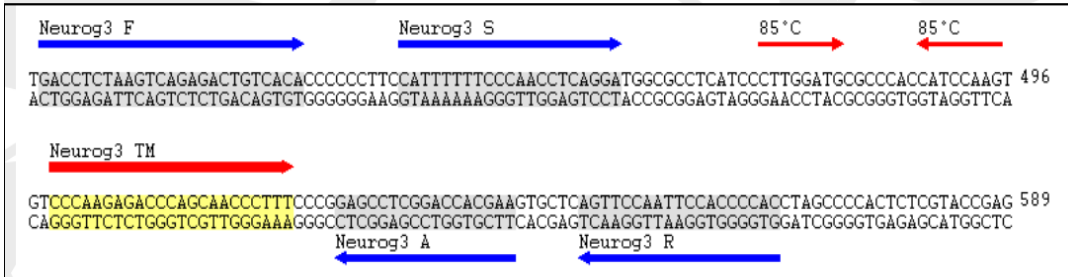


Figure A.5. Ins2 primer and probe sequences

991159	Neurogenin 3, mRNA-gDNA		NM_021700	Tm
Neurog3 F	gACCTCTAAgTCAGAgACTgTCACA	S	405-429	54,8°C
Neurog3 S	CATTTTTTCCCAACCTCaggA	S	439-459	57,0°C
Neurog3 A	TTCgTggTCCgAggCTC	A	542-526	56,9°C
Neurog3 R	gTgggggTggAATTggAACT	A	567-549	56,3°C
Neurog3 TM	F-CCCAgAgACCCAgCAACCCTTT--Q	S	499-521	65,6°C



Legend for figures with sequences :

- | | | | |
|-------------------------------|----------------------|--|-------------------|
| Deep blue arrows, grey shaded | primers | Red arrows, yellow shaded or red boxed | TaqMan probes |
| Orange arrows, yellow shaded | 3'-FL labeled probes | Green boxes / Blue boxes | Exons / Introns |
| Blue arrows, blue shaded | 5'-LC labeled probes | Red or pink boxes | possible conflict |
| | | Red arrows or red boxes | stem-loops |

Figure A.6. Neurog3 primer and probe sequences

991159	Pdx1, mRNA		NM_022852	Tm
Pdx1_F	TCACgCgTggAAAAgCCA	S	481-498	60,9°C
Pdx1_S	gCCAgTgggCaggAggT	S	495-511	59,7°C
Pdx1_A	CCAgATTTTgATgTgTCTCTCAgTCAA	A	679-653	59,5°C
Pdx1_R	TTTCTTCCAATTTCATgCgACg	A	709-689	59,0°C
Pdx1_TM	F-TACgCAGCAgAACCggAggAgAATAAgAg--Q	S	515-543	67,6°C

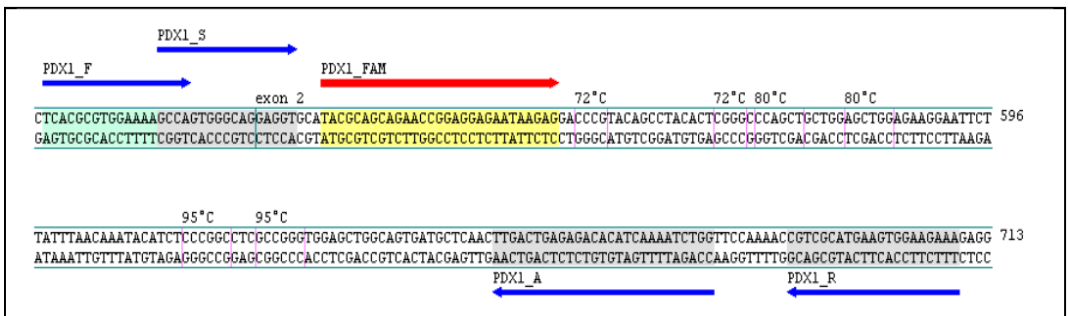


Figure A.7. Pdx1 primer and probe sequences

991159	rat Somatostatin cDNA		NM_012659	Tm
Sst F	CCACCgggAAACAggAAC	S	275-292	58,1°C
Sst S	CCACCgggAAACAggAA	S	275-291	56,8°C
Sst A	CTCCAgggCATCgTTCTCT	A	357-339	56,6°C
Sst R	CATCTCgTCCTgCTCAgCT	A	396-378	55,5°C
Sst TM	F-AACTgCTgTCCgAgCCCAACC--Q	S	314-334	65,0°C



Figure A.8. Sst primer and probe sequences

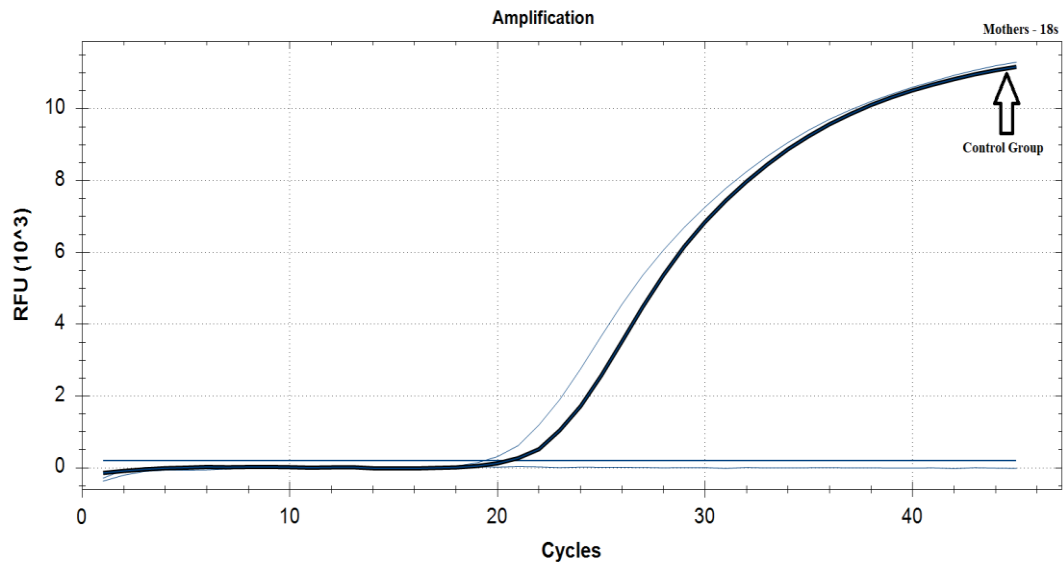


Figure A.9. Mothers 18s region RT- qPCR graphic.

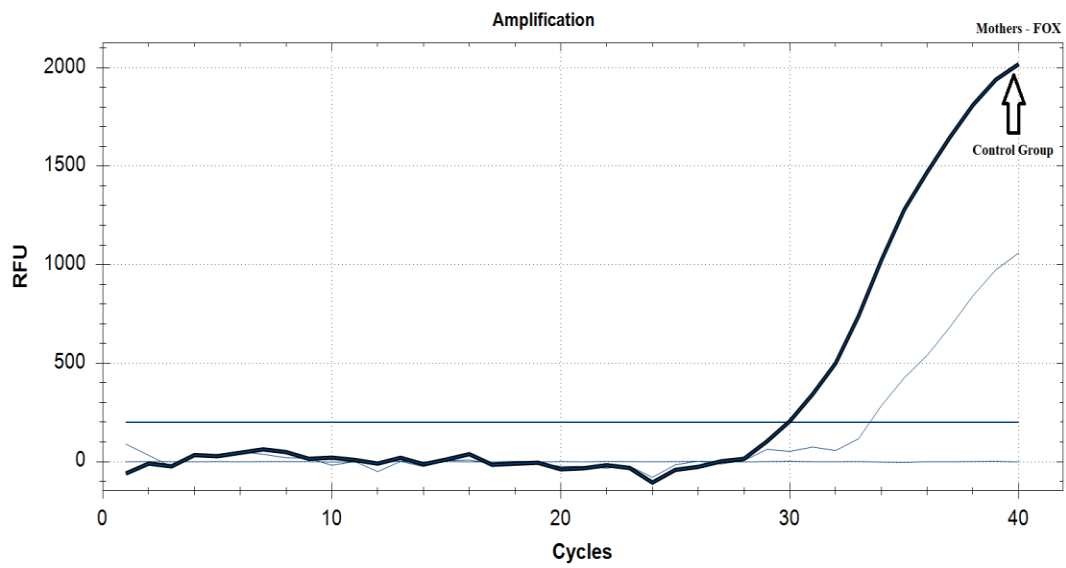


Figure A.10. Mothers FOX gene RT- qPCR graphic.

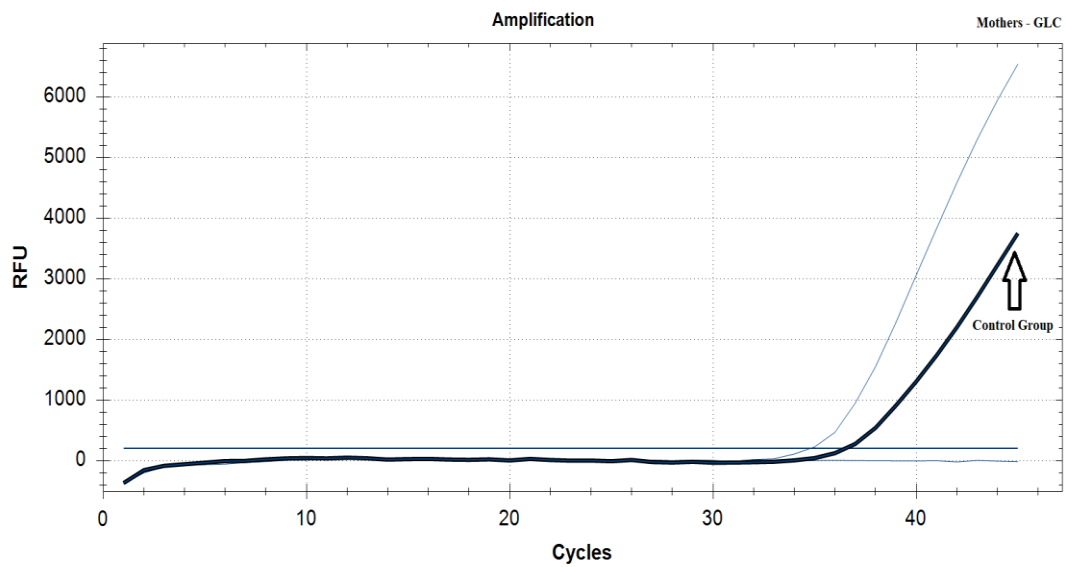


Figure A.11. Mothers GLC gene RT- qPCR graphic.

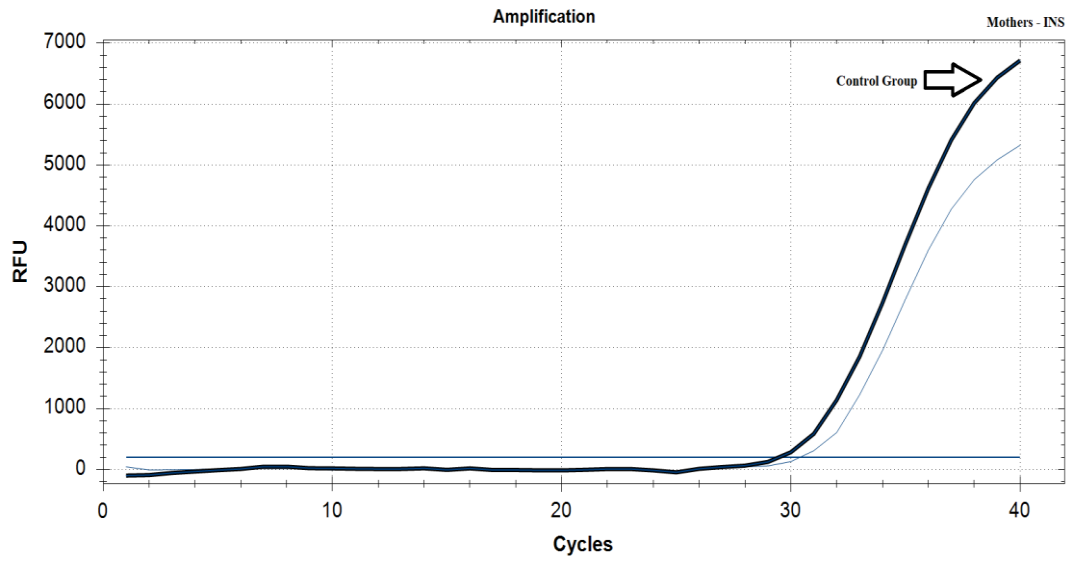


Figure A.12. Mothers **INS** gene RT- qPCR graphic.,

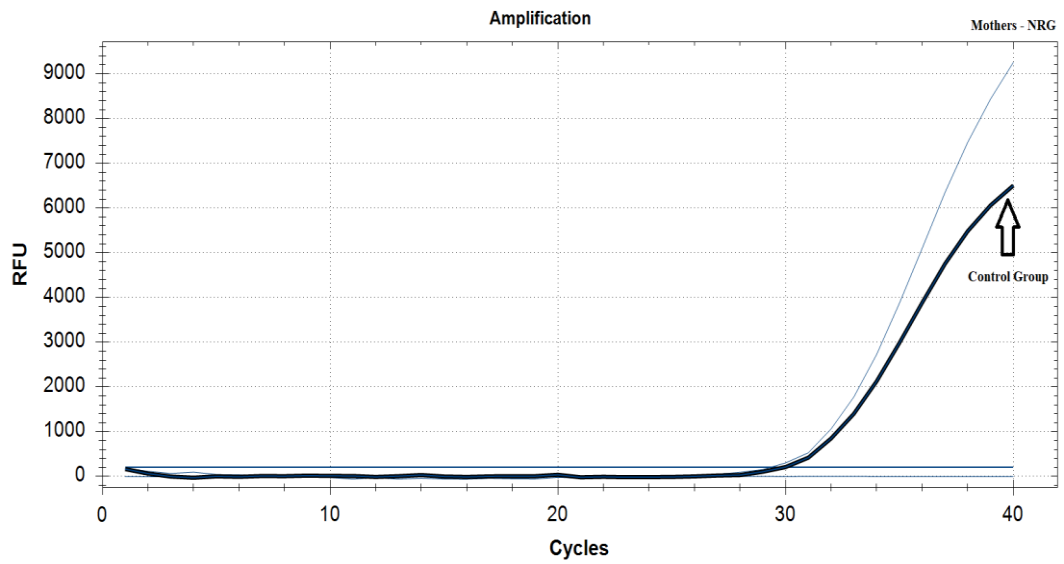


Figure A.13. Mothers **NRG** gene RT- qPCR graphic.

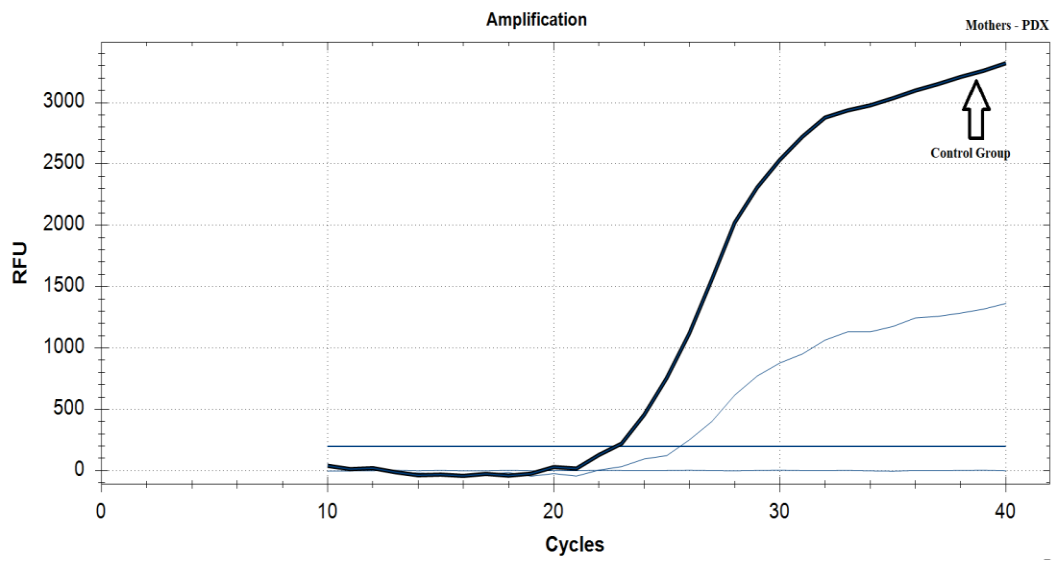


Figure A.14. Mothers **PDX** gene RT- qPCR graphic.,

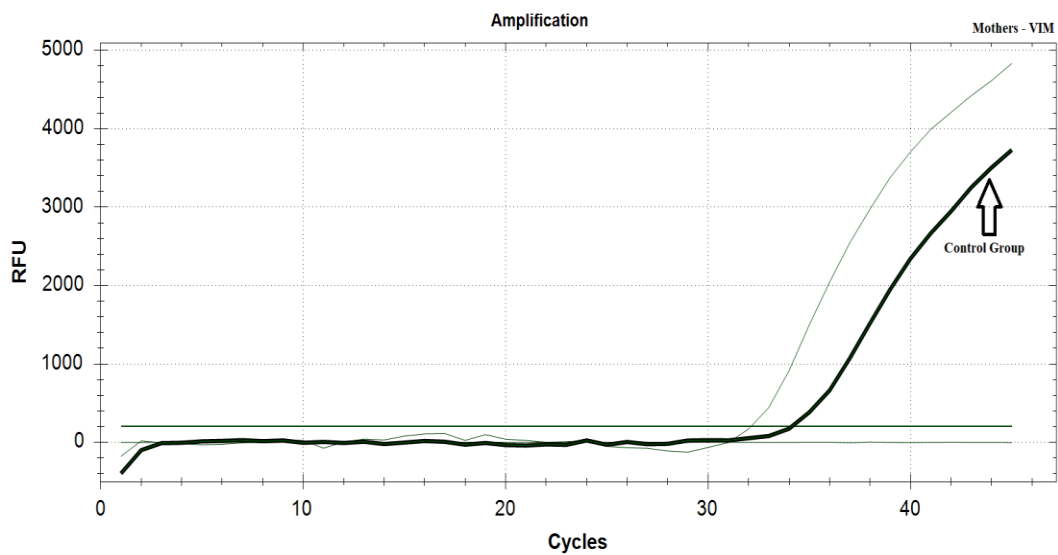


Figure A.15. Mothers **VIM** gene RT- qPCR graphic.

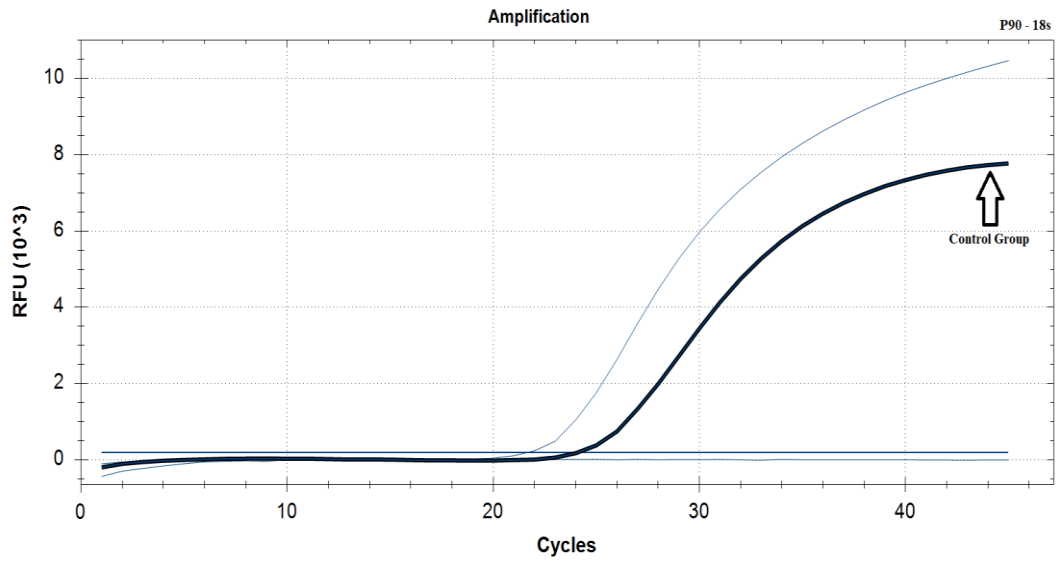


Figure A.16. P90 18s region RT- qPCR graphic.

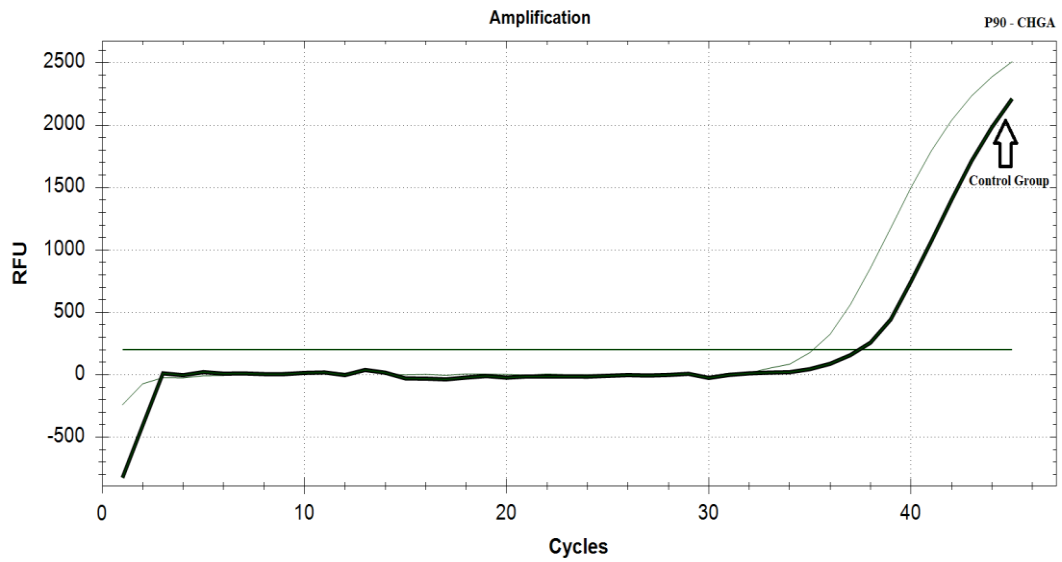


Figure A.17. P90 CHGA gene RT- qPCR graphic.

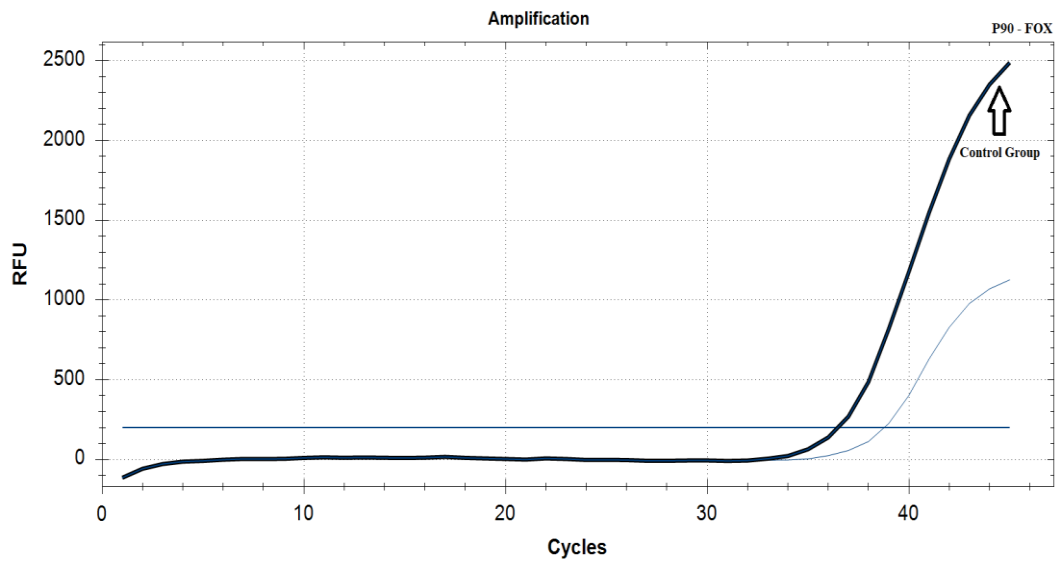


Figure A.18. P90 FOX gene RT- qPCR graphic.

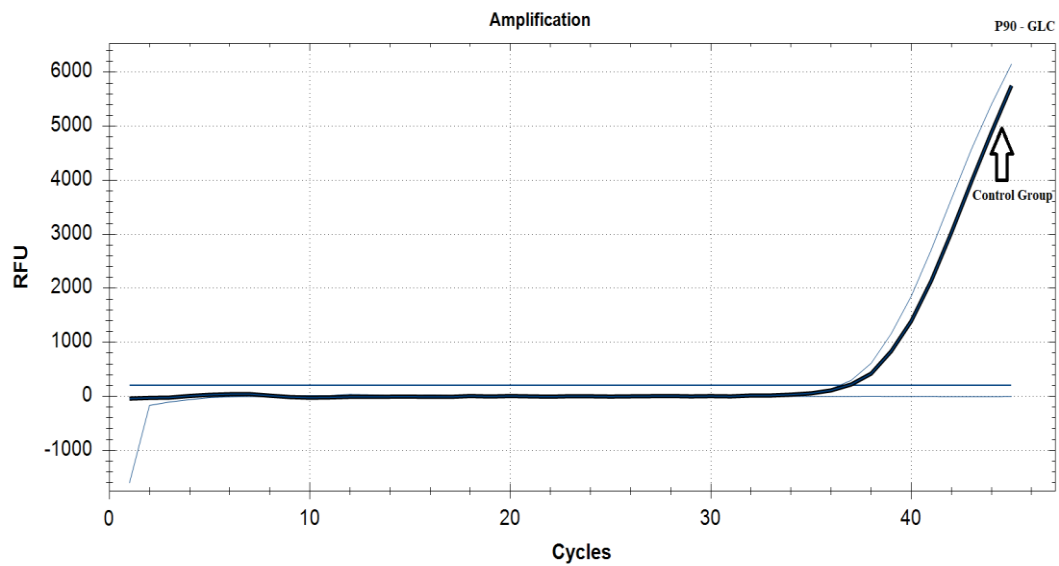


Figure A.19. P90 GLC gene RT- qPCR graphic.

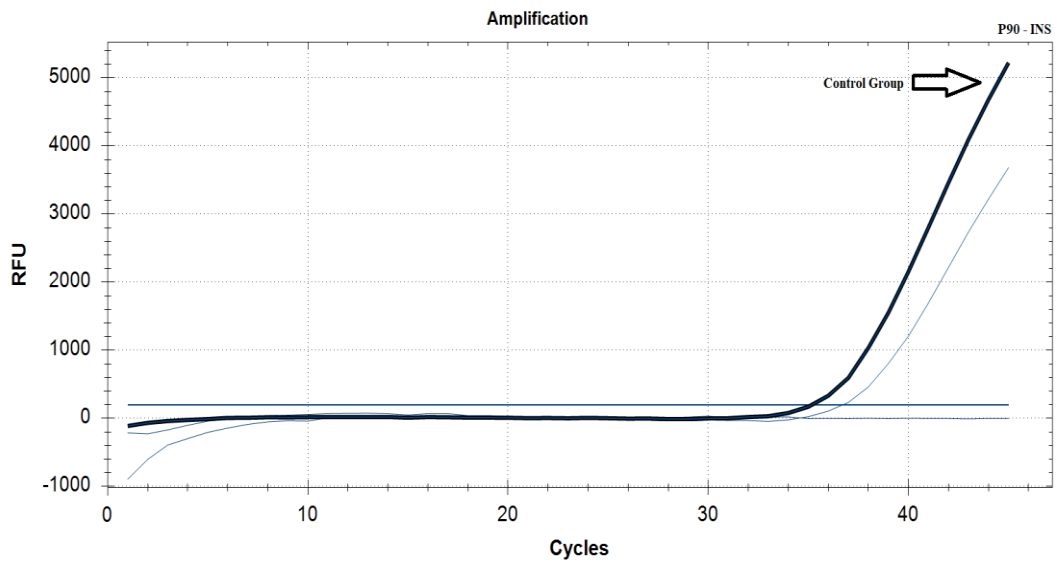


Figure A.20. P90 INS gene RT- qPCR graphic.

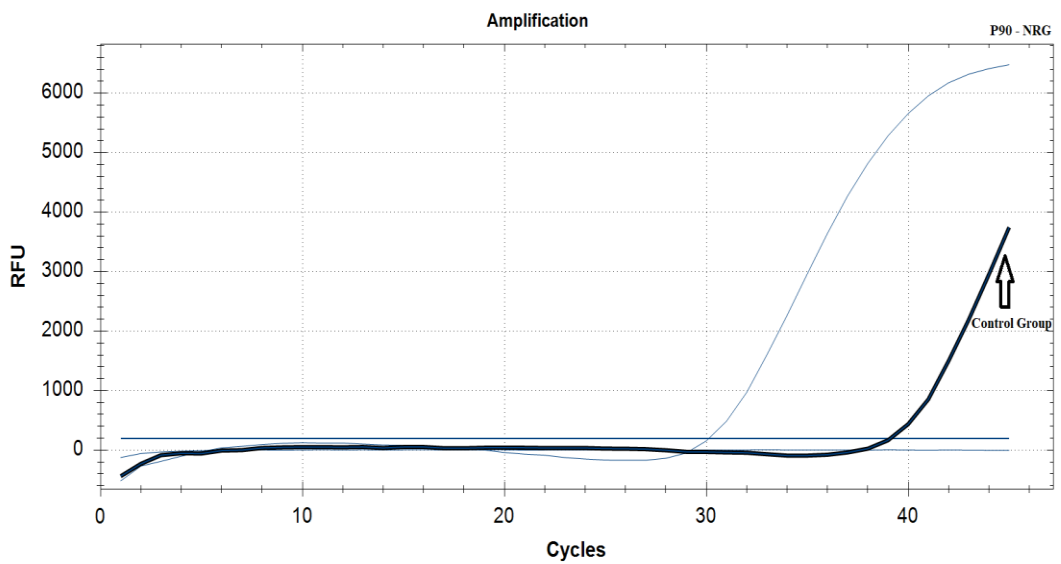


Figure A.21. P90 NRG gene RT- qPCR graphic.

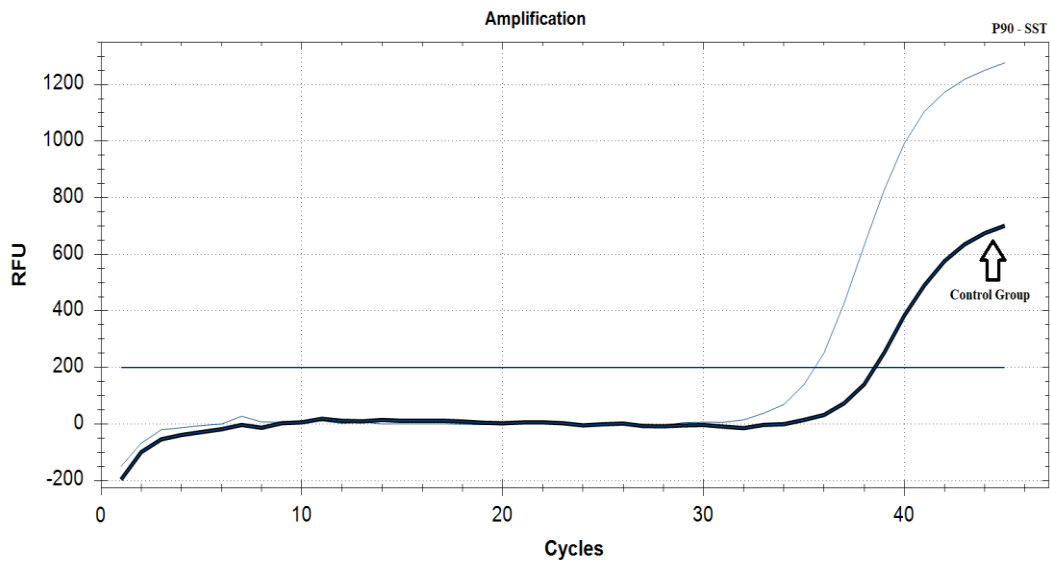


Figure A.22. P90 SST gene RT- qPCR graphic.

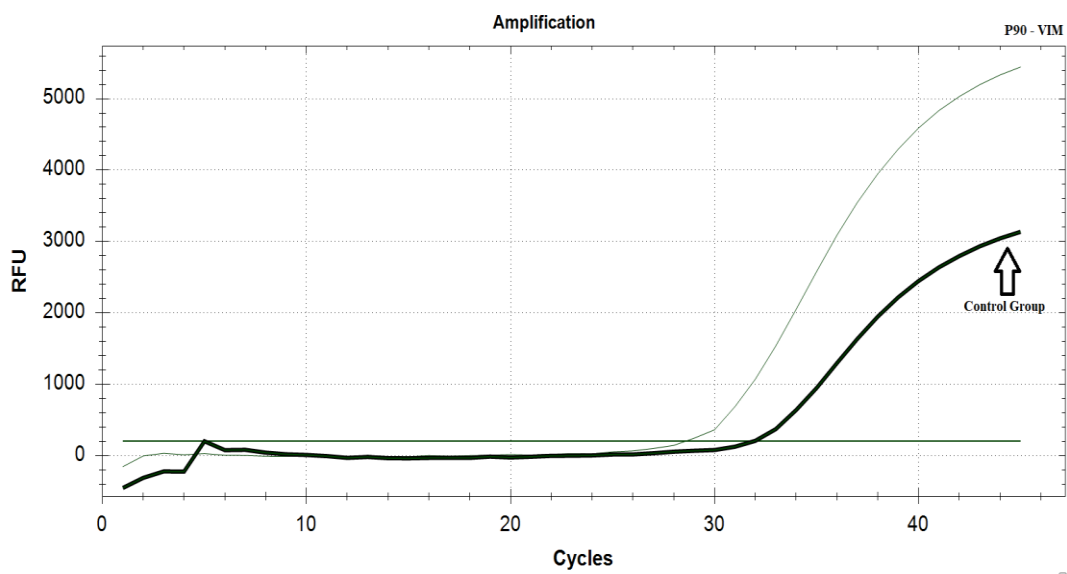


Figure A.23. P90 VIM gene RT- qPCR graphic.

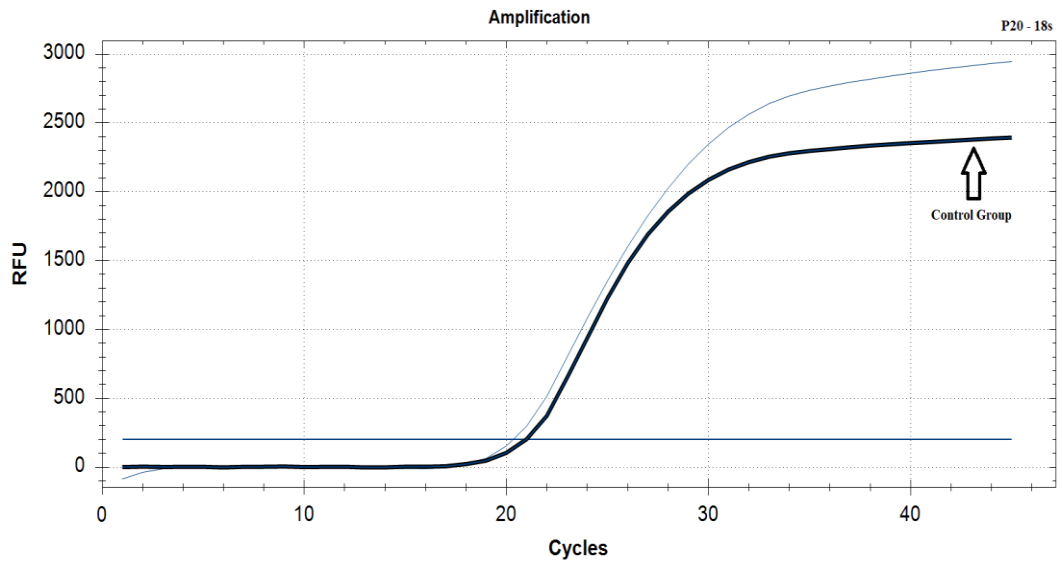


Figure A.24. P20 18s region RT- qPCR graphic.

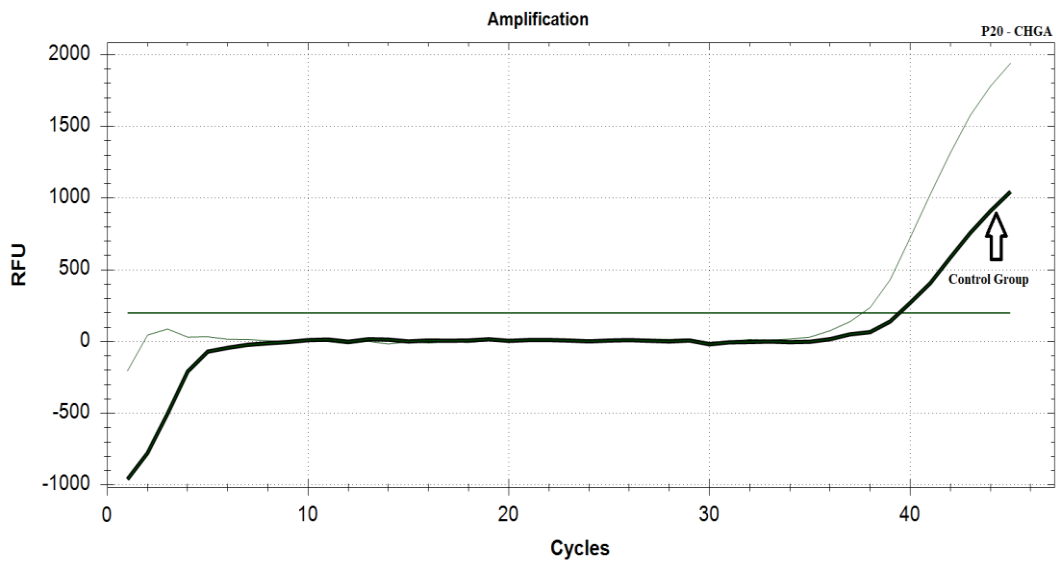


Figure A.25. P20 CHGA gene RT- qPCR graphic.

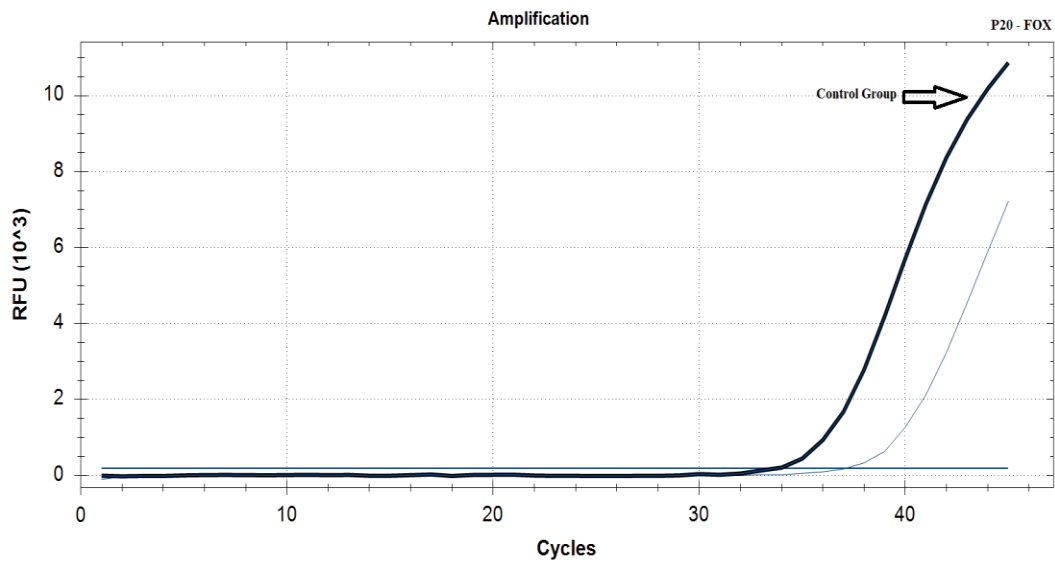


Figure A.26. P20 FOX gene RT- qPCR graphic.

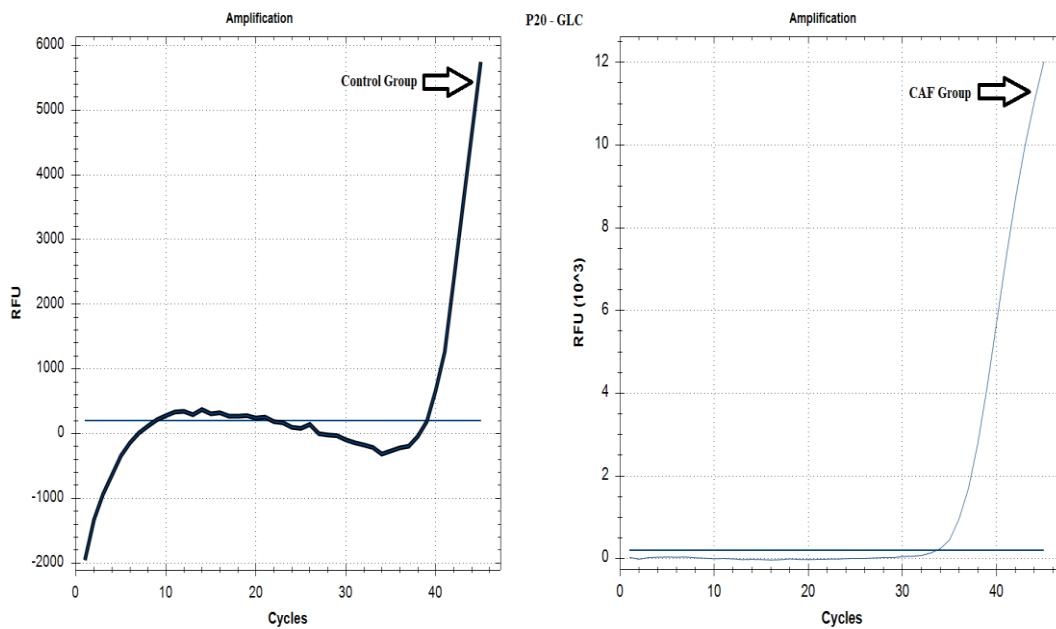


Figure A.27. P20 GLC gene RT- qPCR graphic.

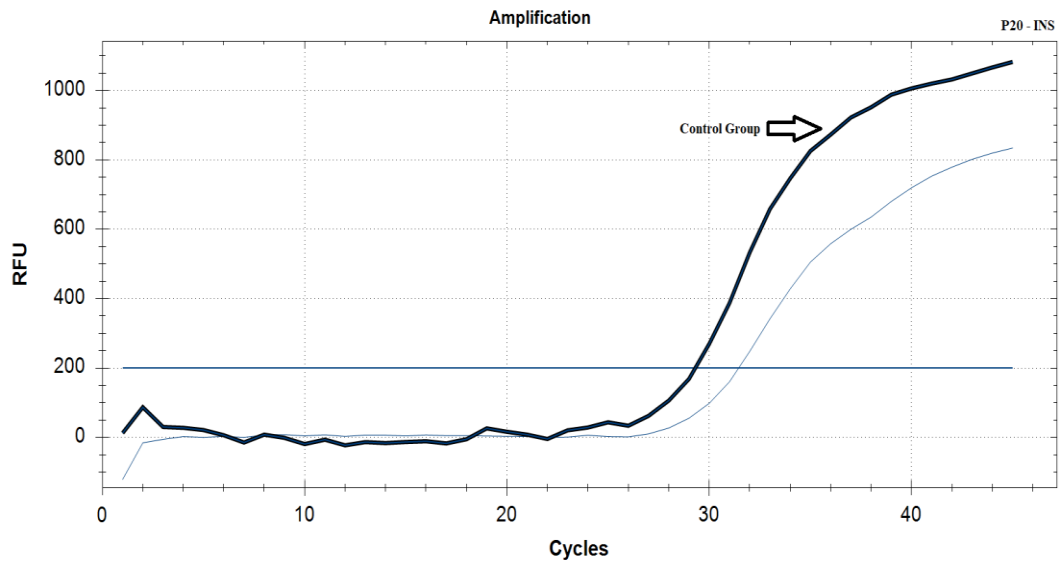


Figure A.28. P20 INS gene RT- qPCR graphic.

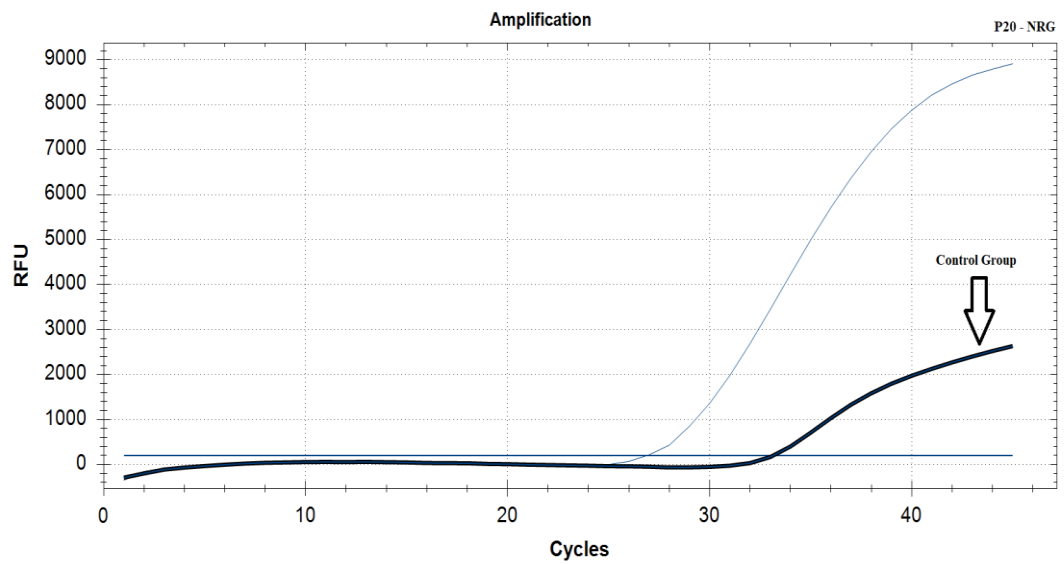


Figure A.29. P20 NRG gene RT- qPCR graphic.

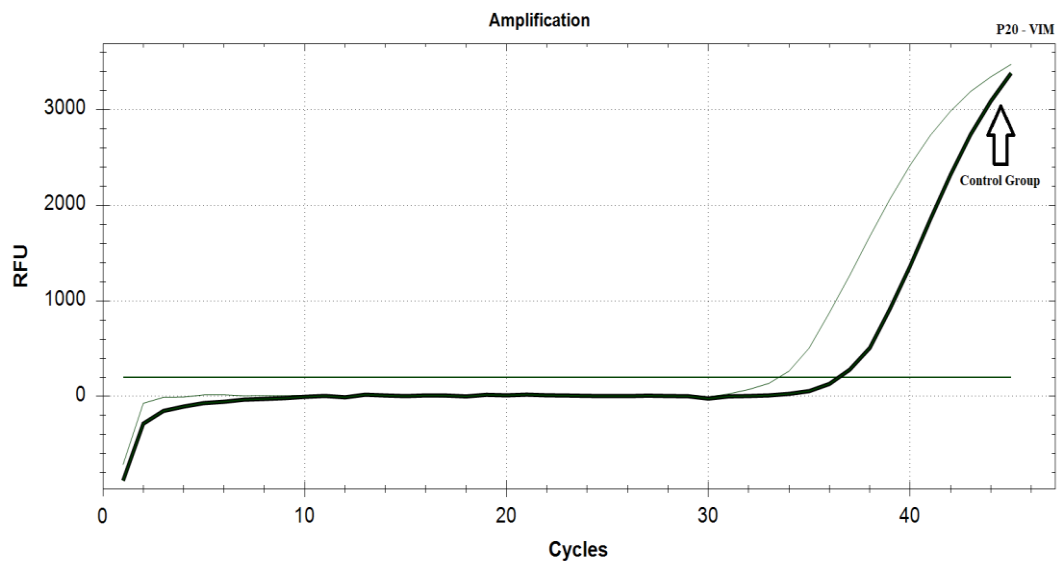


Figure A.30. P20 VIM gene RT- qPCR graphic.

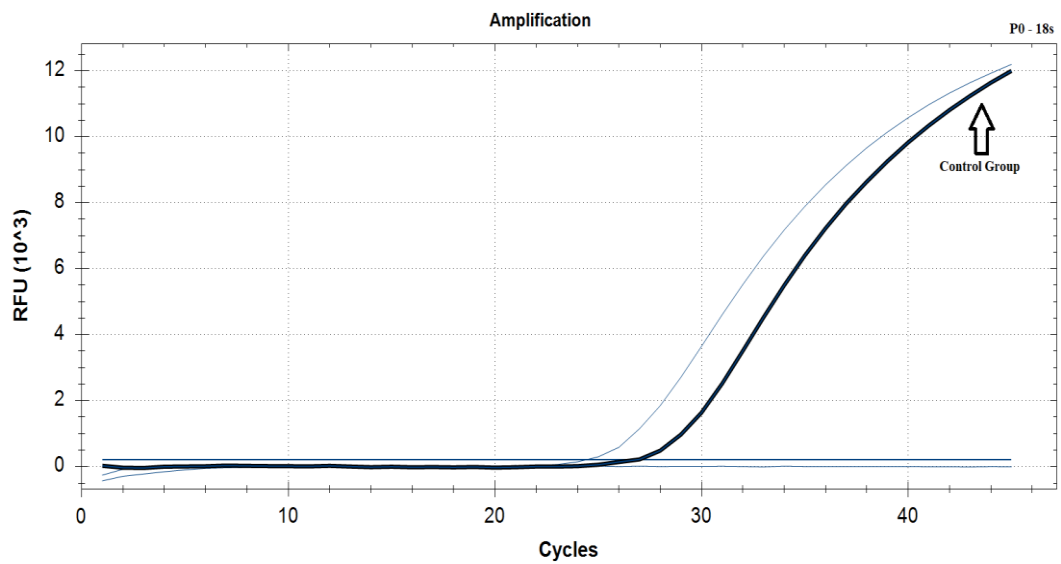


Figure A.31. P0 18s region RT- qPCR graphic.

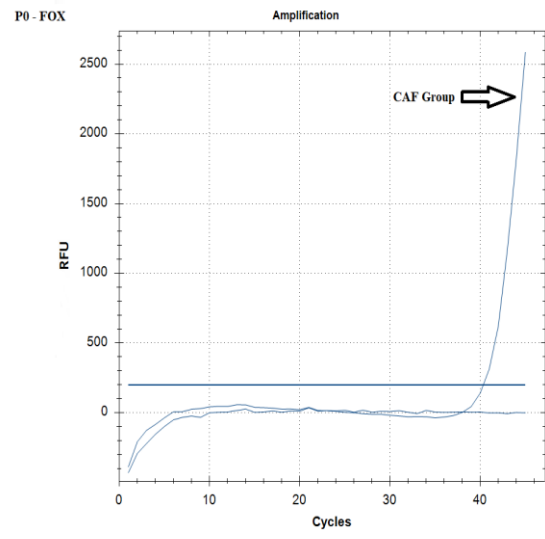
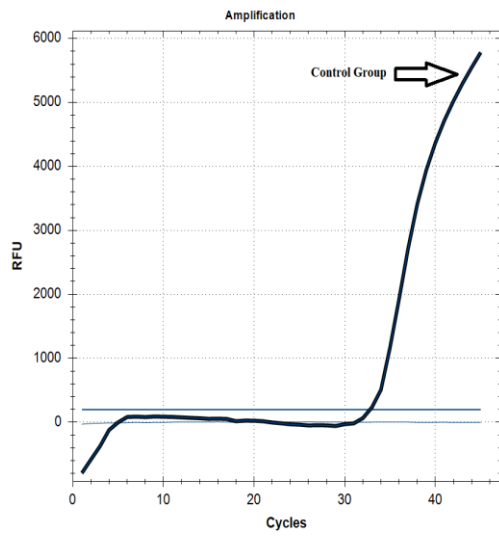


Figure A.32. P0 FOX gene RT- qPCR graphic.

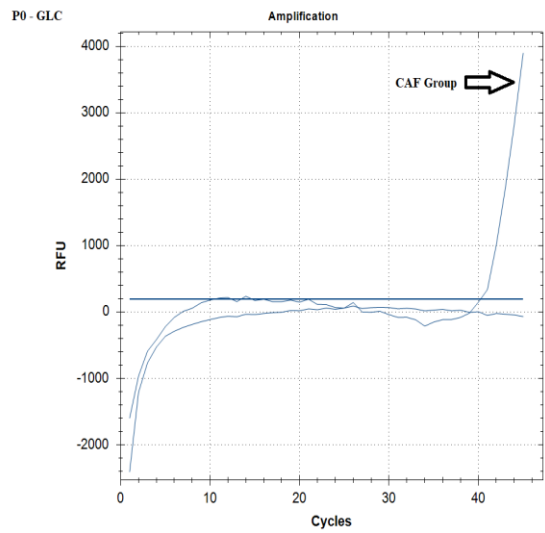
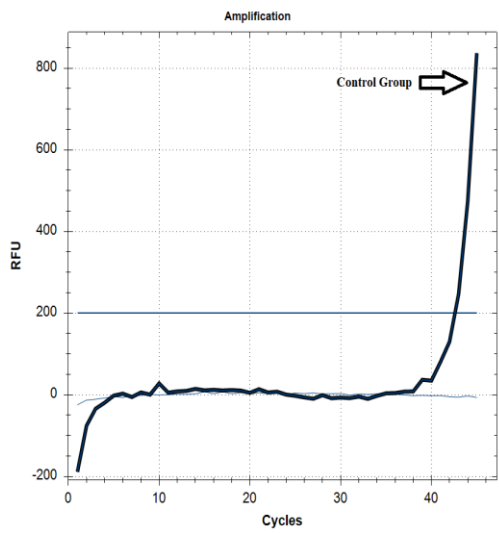


Figure A.33. P0 GLC gene RT- qPCR graphic.

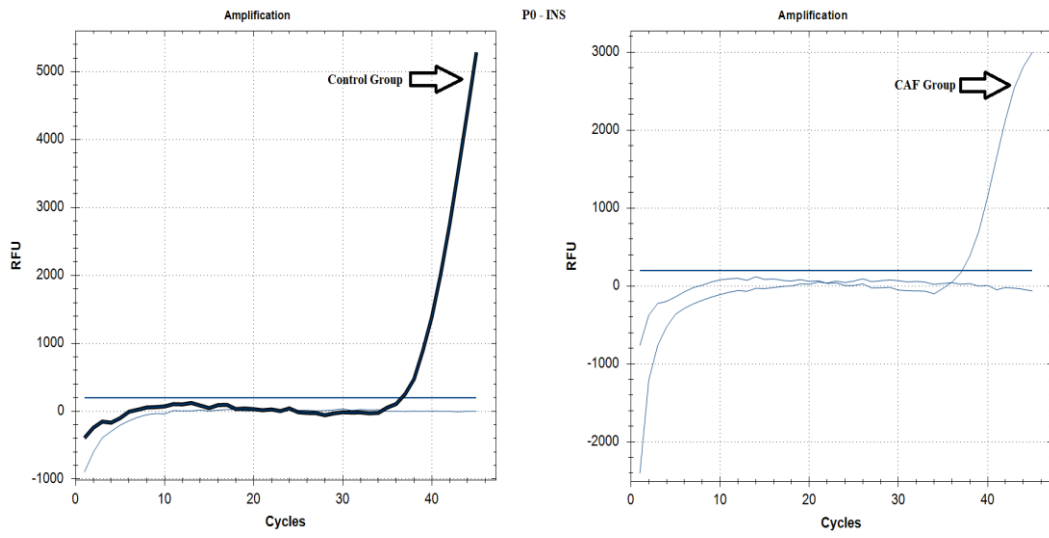


Figure A.34. P0 INS gene RT- qPCR graphic.

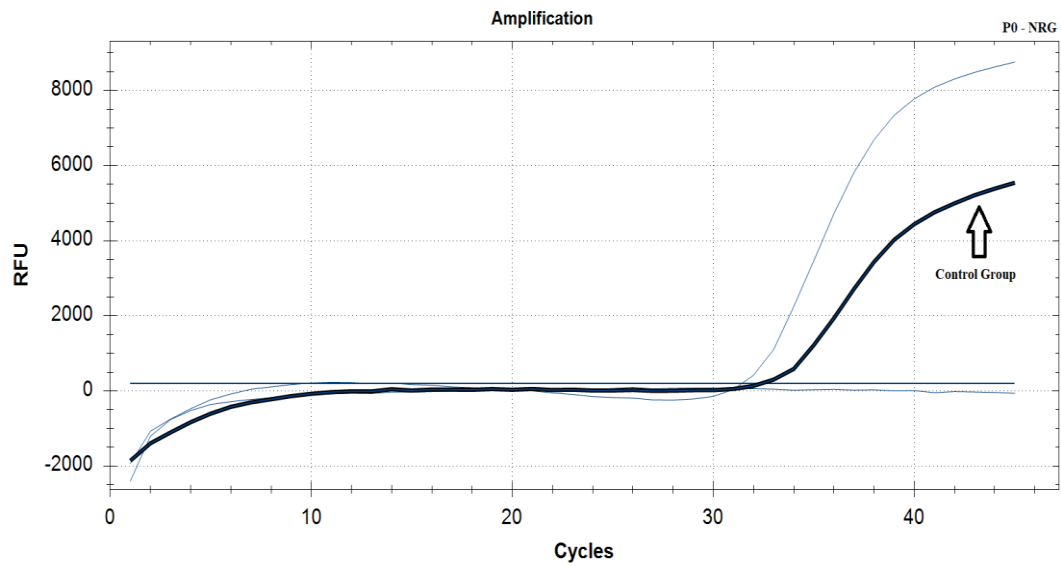


Figure A.35. P0 NRG gene RT- qPCR graphic.

Table A.1. Gene expression data table for mothers ($\Delta\Delta Cq$)


Target	Sample	Expression	Expression SEM	Corrected Expression SEM	Mean $C_{q\downarrow}$	$C_{q\downarrow}$ SEM	P-Value
FoxO1	CAF	0,02199	0,01488	0,01488	40,73	0,97665	0,00000
 FoxO1	CONTROL	2,22883	1,50884	1,50884	35,22	0,97665	
Gcg	CAF	1,00000	1,14201	1,14201	34,36	1,64757	0,00973
Gcg	CONTROL	0,57138	0,73169	0,73169	36,32	1,84746	
Ins2	CAF	0,30398	0,09943	0,09943	26,48	0,47193	0,00001
Ins2	CONTROL	2,22883	0,72909	0,72909	24,77	0,47193	
Neurog3	CAF	1,00000	0,50059	0,50059	29,22	0,72220	0,00001
Neurog3	CONTROL	0,05831	0,03031	0,03031	34,47	0,75000	
Pdx1	CAF	0,00136	0,00000	0,00000	31,36	0,00000	0,00001
Pdx1	CONTROL	2,22883	0,00000	0,00000	21,84	0,00000	
VIM	CAF	1,00000	0,00000	0,00000	32,11	0,00000	0,00001
VIM	CONTROL	0,55036	0,00000	0,00000	34,12	0,00000	

Table A.2. Gene expression data table for 0 days old offspring ($\Delta\Delta Cq$)

Target	Sample	Expression	Expression SEM	Corrected Expression SEM	Mean Cq	Cq SEM	P-Value
FoxO1	CAF	0,01323	0,00000	0,00000	40,34	0,00000	0,00001
FoxO1	CONTROL	2,29623	0,00000	0,00000	32,80	0,00000	
Gcg	CAF	2,46204	0,00000	0,00000	40,25	0,00000	0,00001
Gcg	CONTROL	0,45220	0,00000	0,00000	42,60	0,00000	
Ins2	CAF	1,73656	0,00000	0,00000	37,14	0,00000	0,00001
Ins2	CONTROL	2,29623	0,00000	0,00000	36,64	0,00000	
Neurog3	CAF	2,46204	0,00000	0,00000	31,42	0,00000	0,00001
Neurog3	CONTROL	1,17108	0,00000	0,00000	32,40	0,00000	

Table A.3. Gene expression data table for 20 days old offspring ($\Delta\Delta Cq$)

Target	Sample	Expression	Expression SEM	Corrected Expression SEM	Mean Cq	Cq SEM	P-Value
FoxO1	CAF	0,10939	0,01392	0,01392	37,22	0,00000	0,00001
FoxO1	CONTROL	1,30977	0,90357	0,90357	34,02	0,99188	
Gcg	CAF	1,00000	0,12727	0,12727	33,60	0,00000	0,00001
Gcg	CONTROL	0,03040	0,00387	0,00387	39,03	0,00000	
Ins2	CAF	0,44158	0,08054	0,08054	32,29	0,25501	0,00001

Table A.4. Gene expression data table for 90 days old offspring ($\Delta\Delta Cq$)

Target	Sample	Expression	Expression SEM	Mean Cq	Cq SEM	P-Value
FoxO1	CAF	0,42087	0,19194	37,63	0,65794	0,00000
FoxO1	CONTROL	5,39031	1,81156	36,38	0,48486	
Gcg	CAF	1,00000	0,07789	36,51	0,11237	0,34375
Gcg	CONTROL	0,94437	0,00000	39,03	0,00000	
Ins2	CAF	0,88266	0,33189	35,17	0,54247	0,03594
Ins2	CONTROL	5,39031	1,35924	34,99	0,36379	
Neurog3	CAF	1,00000	0,44894	30,63	0,64768	0,00000
Neurog3	CONTROL	0,04452	0,01999	37,55	0,64768	
Sst	CAF	1,00000	0,34464	36,33	0,49722	0,01722
Sst	CONTROL	1,16978	0,34869	38,53	0,43004	
VIM	CAF	1,00000	0,37758	35,18	0,54473	0,02411
VIM	CONTROL	0,68952	0,35384	38,15	0,74035	

Table A.5. Gene expression data table of Chga

Group	CONTROL	CAF	P-VALUE
0	1,89211529	2,80889	0,0001
20	1,68797621	2,710769	0,0001
90	1,23714264	2,245402	0,0001

APPENDIX B

PROTEIN ASSAY and WESTERN BLOT

	Bradford Standard (ug/ml)	OD Values 1. Repeat	OD Values 2. Repeat	OD Values 3. <u>Tekrar</u>	Median	CV Values
	0	0,3876	0,3797	0,3843	0,38	1,03
	200	0,5164	0,5207	0,5152	0,52	0,56
	400	0,6655	0,6679	0,6685	0,67	0,24
	600	0,7957	0,8203	0,826	0,81	1,98
	800	0,9031	0,9031	0,8755	0,89	1,78
	1000	0,9826	0,9489	0,9739	0,97	1,81
Mother Cont.	Y values	0,5969	0,5739	0,585	0,59	1,97
Mother CAF		0,4819	0,5114	0,5025	0,5	3,03
<u>0 day</u> Cont.		0,5095	0,5378	0,5099	0,52	3,13
<u>0 day</u> CAF		0,4844	0,4761	0,4846	0,48	1,01
<u>20 day</u> Cont.		0,6394	0,6236	0,6425	0,64	1,6
<u>20 day</u> CAF		0,5166	0,5178	0,5169	0,52	0,12
<u>90 day</u> Cont.		0,6999	0,6666	0,703	0,69	2,93
<u>90 day</u> CAF		0,7672	0,7722	0,8163	0,79	3,44

Table B.1. Od values and protein amounts in samples

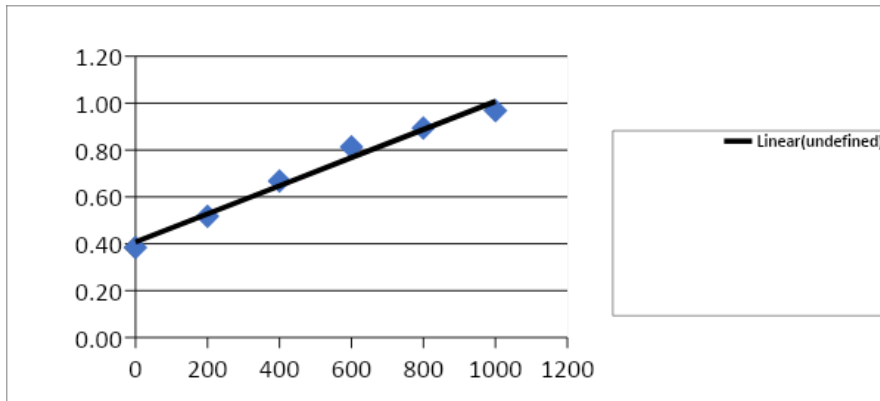


Figure B.1. BSA calibration curve. This standard curve of Protein concentration (mg/ml) (X axis) vs. absorbance (595nm) (Y axis) was used to estimate protein concentrations of the samples. $R^2 = 0.9814$; coefficient of the slope $b = 0.4076$, and intercept = 0.0006 was used to calculate protein concentration in mg/ml from absorbance readings of pancreatic samples. Below, it represents that how the sample concentrations were then calculated.

			$y = Ax + B$				
Groups	y (Y value in graphic = OD value)	A (slope)	x (Unknown conc.)	B	*dilution*	Final concentration	$\mu\text{g}/1\mu\text{L}$
Mother CAF	0,585	0,0006	291,78	0,4102	40	11671,11	11,67
0 day Cont.	0,499	0,0006	147,33	0,4102	40	5893,33	5,89
0 day CAF	0,519	0,0006	181,44	0,4102	20	3628,89	3,63
20 day Cont.	0,482	0,0006	119,17	0,4102	30	3575	3,58
20 day CAF	0,635	0,0006	374,94	0,4102	30	11248,33	11,25
90 day Cont.	0,517	0,0006	178,17	0,4102	30	5345	5,35
90 day CAF	0,69	0,0006	466,06	0,4102	40	18642,22	18,64
Mother CAF	0,785	0,0006	625,06	0,4102	40	25002,22	25

Table B.2. BSA calibration values for each group.

Groups	Loading Volume	Loading Protein	5x loading	20x dtt	Protein concentration	Protein volume	dH ₂ O
1 Mother Cont.	15	30,00	3	0,75	11,67	2,57	8,68
2 Mother CAF	15	30,00	3	0,75	5,89	5,09	6,16
3 0 day Cont.	15	30,00	3	0,75	3,63	8,27	2,98
4 0 day CAF	15	30,00	3	0,75	3,58	8,39	2,86
5 20 day Cont.	15	30,00	3	0,75	11,25	2,67	8,58
6 20 day CAF	15	30,00	3	0,75	5,35	5,61	5,64
7 90 day Cont.	15	30,00	3	0,75	18,64	1,61	9,64
8 90 day CAF	15	30,00	3	0,75	25,00	1,20	10,05

Table B.3. Protein loading amounts for the groups.

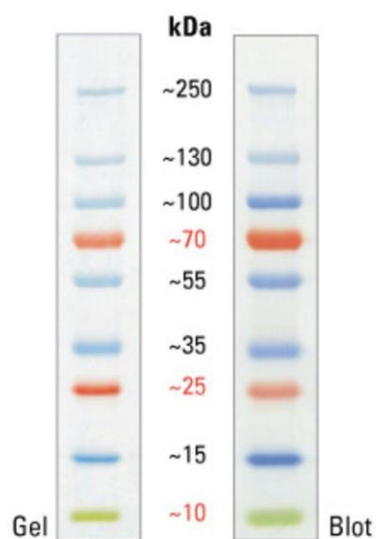


Figure B.2. PageRuler™ Plus Prestained Protein Ladder, 10 to 250 kDa

APPENDIX C

TRANSCRIPTOME

Raw Data Statistics

Sample ID	Total read bases (bp)	Total reads	<u>GC</u> (%)	<u>AT</u> (%)	Q20(%)	Q30(%)
0CONT	6,651,075,230	65,852,230	48.35	51.65	98.54	95.94
20CONTROL1	9,856,000 	89,422,560	50.39	49.61	98.29	95.26
20CONTROL2	7,208,770,364	71,373,964	47.84	52.16	98.27	95.42
20CAF1	8,553,567,992	84,688,792	74.72	25.28	92.47	85.81
20CAF2	8,022,746,130	79,433,130	72.94	27.06	92.95	86.57
90CAF1	6,781,751,858	67,146,058	65.73	34.27	91.74	85.74
90CAF2	6,816,539,288	67,490,488	51.35	48.65	95.81	90.97
90CONT1	8,558,009,164	84,732,764	65.63	34.37	92.31	85.94
90CONT2	7,812,788,340	77,354,340	65.48	34.52	93.04	87.01
MOTHERCAF1	6,653,867,880	65,879,880	51.69	48.31	95.66	90.62
MOTHERCONT1	8,785,133,924	86,981,524	63.0	37.0	92.95	86.42

Table C.1. Raw data stats

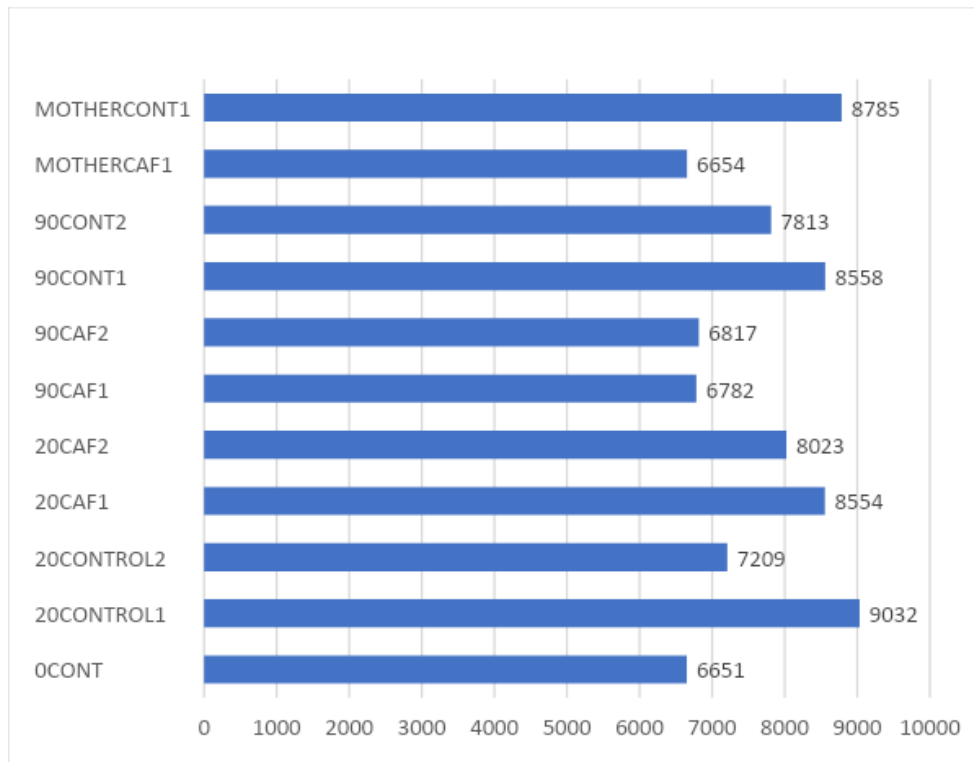


Figure C.1. Throughput of Raw data

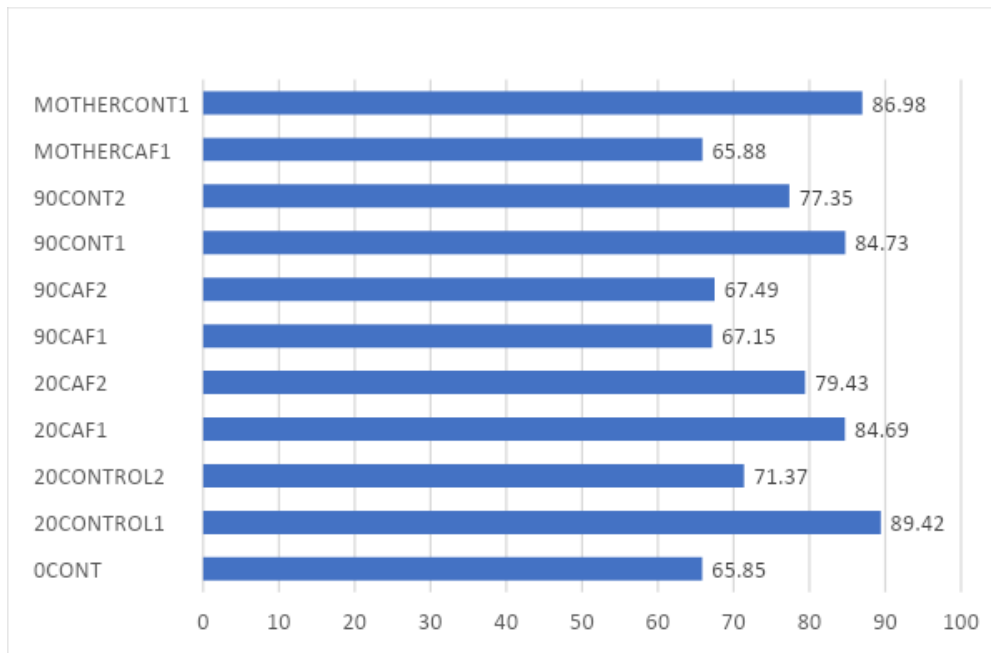


Figure C.2. Total read count of Raw data

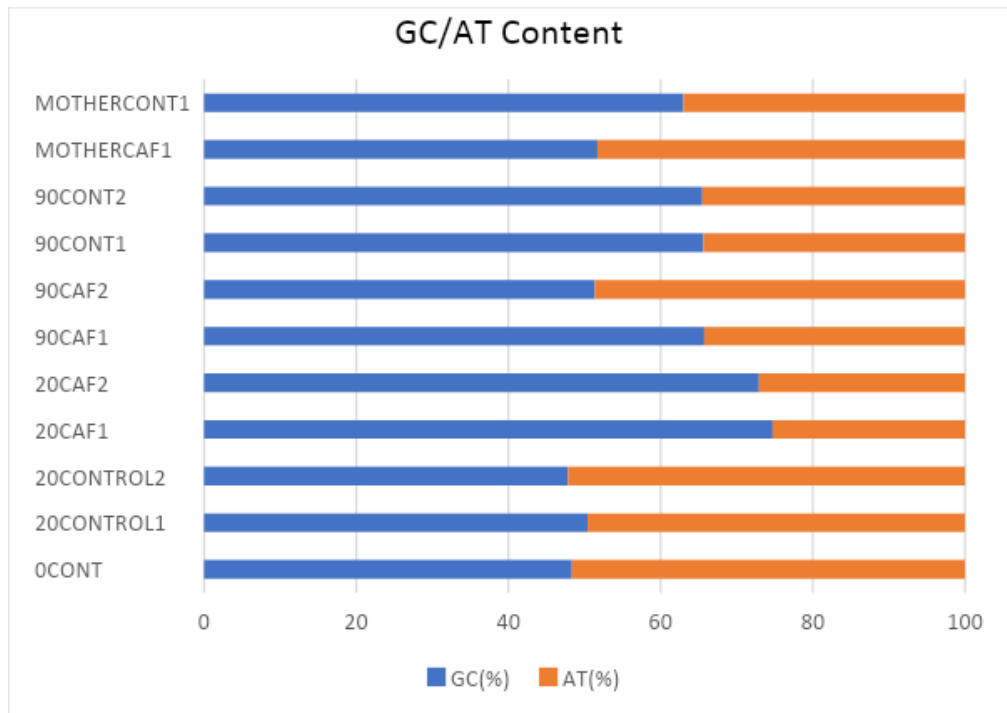


Figure C.3. GC/AT content of Raw data

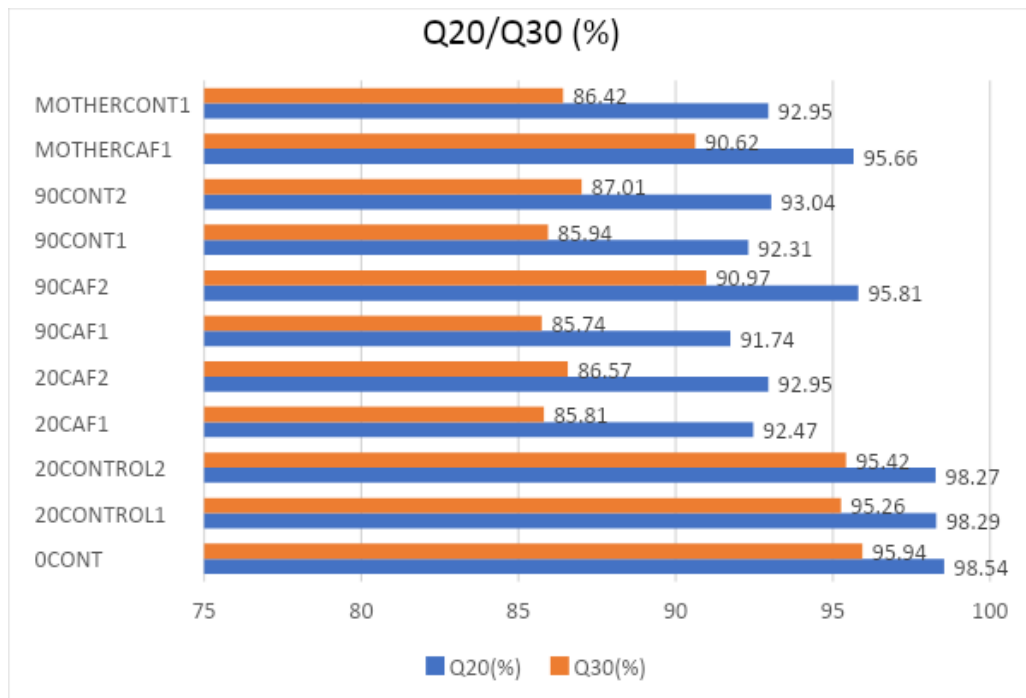


Figure C.4. Q20/Q30 scores of Raw data

CURRICULUM VITAE

PERSONAL INFORMATION

Surname, Name: Feyat, Mehmet Sedat

Nationality: Turkish (T.C.)

Date and Place of Birth: 26 August 1980, Van

Phone: +90 532 257 60 87

Email: mehmet.sedat.feyat@gmail.com, sedat.feyat@metu.edu.tr

EDUCATION

Degree	Institution	Year of Graduation
BS	Hacettepe University Biology	2004
High School	Atatürk Foreign Language Intensive High School, Van	1998

WORK EXPERIENCE

Year	Place	Enrollment
2004	HÜ MBG Labs, Hacettepe Üniv., Ankara, Turkey	Special Study Student
2012-2016	Adacell Research Center, DEAH, Ankara, Turkey	Research Assistant
2016	Aziz Sancar Research Center	R&D Specialist
2020-2022	TUSEB	Project Staff
2022-Present	HBB Biotech	Founder R&D

FOREIGN LANGUAGES

Advanced English

PUBLICATIONS

1. M. S. Feyat, M. S. Feyat, S. Mercan, S. Mercan, E. Calisir, E. Calisir, G. Boyuk, G. Boyuk, F. A. Pinarli, F. A. Pinarli, E. Fadillioglu, E. Fadillioglu, T. Delibasi & T. Delibasi (2015). The Modified Rat Pancreatic Beta Cell Purification Method with Flow Cytometer. *Acta Physiologica*, 215: 32-33
2. S. Mercan, S. Mercan, G. Boyuk, G. Boyuk, M. S. Feyat, M. S. Feyat, M. Caliskan, M. Caliskan, S. Boyuk, S. Boyuk, C. Sucularli, C. Sucularli, E. Fadillioglu, E. Fadillioglu, T. Delibasi & T. Delibasi (2015). Results Of Islet Cell Isolations From The Tail Section Of The Human Pancreas. *Acta Physiologica*, 215: 32-32

POSTERS AND PRESENTATIONS

1. M. S. Feyat, M. S. Feyat, S. Mercan, S. Mercan, E. Calisir, E. Calisir, G. Boyuk, G. Boyuk, F. A. Pinarli, F. A. Pinarli, E. Fadillioglu, E. Fadillioglu, T. Delibasi & T. Delibasi . The Modified Rat Pancreatic Beta Cell Purification Method with Flow Cytometer (Poster Presentation in 41st National Physiology Congress Venue 2015)

STUDENT SCHOLARSHIPS AND AWARDS

Basic Sciences Undergraduate Scholarship (Scientific and Technology Research Council of Turkey-TUBITAK)

PATENTS

A Method and Detection Kit for Quantitative Detection of Sars-Cov-2 with Real-Time PCR. Patent Application No. TR 2021/008133, filed May 05 2021. Patent Pending.

ACADEMIC SERVICE

Reviewed for Journal: Turkish Journal of Biology